Charles University

Faculty of Science

Study programme:

Experimental Plant Biology

Mgr. Miloš Duchoslav

Function of PsbO isoforms

Funkce izoforem PsbO

Doctoral thesis

Supervisor: RNDr. Lukáš Fischer, Ph.D.

Prague, 2022

Author's declaration

I hereby declare that this doctoral thesis documents my own work and I wrote it independently. This work or any substantial part of the text is not a subject to any other defending procedure. I declare that all sources were cited and acknowledged properly.

Prohlášení autora

Prohlašuji, že jsem tuto dizertační práci vypracoval samostatně. Tato práce nebo její podstatná část nebyla předložena k získání jiného nebo obdobného akademického titulu. Dále prohlašuji, že všechny použité zdroje byly správně citovány.

Prague/V Praze 2022-01-27

Miloš Duchoslav

Supervisor's declaration

I hereby confirm that contribution of Miloš Duchoslav to the published and unpublished work included in this thesis corresponds to what he declares here.

Prohlášení školitele

Prohlašuji, že podíl Miloše Duchoslava na publikacích a nepublikovaných výsledcích, zahrnutých v této dizertační práci, odpovídá tomu, co deklaruje.

Prague/V Praze 2022-01-27

Lukáš Fischer

Mým dětem, které se mne opakovaně ptaly: „Tati, a už jsi zjistil, jak to v těch kytkách funguje?“

To my children, who repeatedly asked me: “Dad, did you already find out how the things are working in the plants?”

Táta zkoumá kytky.

Dad is investigating plants.

(Anna Duchoslavová, 01/2022)

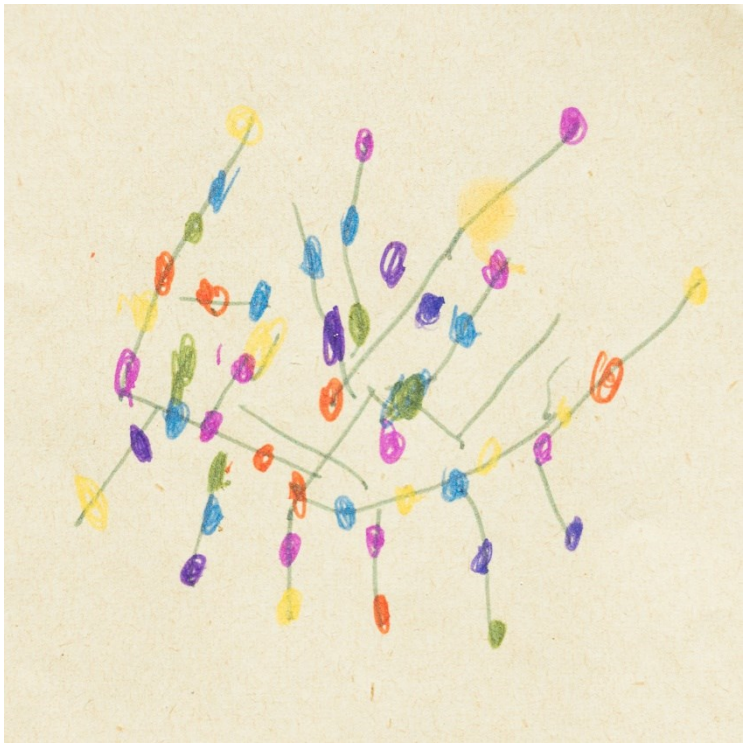

Protein

(Anna Duchoslavová, 01/2022)

Acknowledgement – Poděkování

Lukášovi, svému školiteli, bych chtěl poděkovat především za přátelský přístup, podporu a pochopení pro mé další aktivity, ať už se jednalo o čas věnovaný rodině nebo třeba organizaci biologických soustředění pro středoškoláky Arachne.

Všem současným i bývalým členům Lab 210, jakož i mnohým dalším lidem z Katedry experimentální biologie rostlin, bych chtěl poděkovat za velmi příjemné a přátelské prostředí a mnohé rady a pomoc.

Mým studentům – Katce Hlavsové, Vaškovi Svobodovi a Ondrovi Nyklesovi – děkuji za pomoc s některými experimenty a za to, že mne nutili lépe práci rozmýšlet.

Hance Šanderové děkuji za pomoc s měřením GTPázové aktivity a Radkovi Fišerovi za měření fluorescence tryptofanu v PsbO, ač se nakonec většina těchto výsledků v dizertaci neobjevila.

Martině Pichrtové děkuji za možnost využívat FluorCam na Katedře botaniky.

Louskáčkovi (Martinovi Weiserovi) děkuji za konzultace statistických metod. Společně s Tomášem Koubkem mi také umožnili využívat LED světla Katedry botaniky, za což jsem vděčný.

Markovi Romáškovi děkuji za jazykovou korekuturu.

I would like to thank Slim (Göran Samuelsson) for the opportunity to repeatedly come to his lab and for his overall support. I would also like to thank Tatyana Shutova and Anke Carius, thanks to whom the joint paper was written. Many thanks also to other friends from Umeå, who made my stays there more pleasing.

I would like to also thank all other people who helped me, advised me or supported me during my research and work on this thesis.

Nakonec bych rád poděkoval své rodině, především rodičům a své ženě, za velkou podporu a za to, že nikdy nezpochybňovali smysl mé práce (aspoň ne nahlas).

Financial support

Experiments presented in this work were done at the Department of Experimental Plant Biology, Faculty of Science, Charles University, Czech Republic and at Umeå Plant Science Centre, Department of Plant Physiology, Umeå University, Sweden. The work was financially supported by Charles University (projects GA UK No. 362211 and No. 1472314) and by Ministry of Education, Youth and Sports of Czech Republic (project No. LO1417).

Contents

Abstract (English version)

Oxygenic photosynthesis is crucial for most forms of the life on the Earth. The splitting of water and evolution of oxygen is conducted by photosystem II (PSII), a multi-subunit pigment-protein complex embedded in the thylakoid membrane. PsbO is an indispensable subunit of PSII, bound to its transmembrane subunits from the luminal side. The main function of PsbO is to stabilise and protect Mn_4CaO_5 cluster where the water splitting occurs. However, it has probably also some auxiliary functions. These additional functions might be different for isoforms of PsbO proteins, as suggested for *Arabidopsis thaliana*, which expresses two genes encoding protein isoforms PsbO1 and PsbO2. This thesis studies auxiliary functions of PsbO with a focus on functional differences between PsbO isoforms.

We found that besides *Arabidopsis thaliana*, also many other plant species express two *psbO* genes. Interestingly, the duplication of *psbO* gene occurred many times independently, generally at the roots of modern angiosperm families. In spite of this, the PsbO isoforms differ at similar sites in the protein structure, suggesting that similar subfunctionalisation of PsbO isoforms occurred parallelly in various lineages.

Biochemical characterisation of PsbO from green alga *Chlamydomonas reinhardtii* and PsbO1 and PsbO2 from potato (*Solanum tuberosum*) showed that the PsbO proteins from evolutionary distant photosynthetic organisms are very similar regarding the secondary structure and that conformation of the β-barrel part of PsbO is influenced by pH changes.

Investigation of *Arabidopsis thaliana* mutants with various amounts of PsbO1 and PsbO2 revealed that the total level of PsbO in a plant has a major effect on the function of PSII and phenotype of the plant. However, contrary to a general opinion, we show that the particular isoform present in a plant has rather marginal effect on the photosynthetic performance, both under normal conditions and under high light. Analysis of proteome changes in mutants with low level of PsbO1 or PsbO2 confirmed this result and unravelled some unexpected consequences of the low amount of PsbO in the plants.

Based on our results, we propose that PsbO isoforms does not have fundamentally different function, but rather differ in fine modulation of some process. We hypothesise that the frequent aspartate – glutamate substitutions between isoforms might tune the pH-dependent conformational changes of PsbO that might participate in regulation of PSII activity or repair.

Abstrakt (česká verze)

Oxygenní fotosyntéza je zásadní pro většinu forem života na Zemi. Rozklad vody, při kterém se uvolňuje kyslík, je zajišťován fotosystémem II (PSII), pigment-proteinovým komplexem nacházejícím se v tylakoidní membráně chloroplastů. PsbO je jeho nepostradatelná podjednotka, která se váže na transmembránové podjednotky PSII z luminální strany. Hlavní funkcí PsbO je stabilizovat a chránit manganový klastr (Mn_4CaO_5), na kterém probíhá rozklad vody. Pravděpodobně má však i další, doplňkové funkce. Tyto doplňkové funkce mohou být rozdílné u izoforem proteinu PsbO, což bylo navrženo pro huseníček (*Arabidopsis thaliana*), který exprimuje dva geny kódující proteinové izoformy PsbO1 a PsbO2. Tato dizertační práce je zaměřena na doplňkové funkce PsbO s důrazem na rozdíly mezi izoformami.

Analýzou sekvencí *psbO* jsme zjistili, že kromě huseníčku exprimuje dva geny *psbO* i mnoho dalších druhů rostlin. Zajímavé je, že duplikace genu *psbO* proběhla mnohokrát nezávisle, typicky ve společném předkovi současných čeledí krytosemenných rostlin. Nicméně izoformy PsbO se přesto liší na podobných místech struktury. To naznačuje, že u PsbO mohlo proběhnout paralelně u různých linií podobné rozrůznění funkcí.

Biochemická charakterizace PsbO ze zelené řasy *Chlamydomonas reinhardtii* a dvou izoforem PsbO z bramboru (*Solanum tuberosum*) ukázala, že proteiny PsbO z evolučně vzdálených fotosyntetizujících organismů mají velmi podobnou sekundární strukturu a že konformace β-soudkové části PsbO je ovlivňována změnami pH.

Charakterizací mutantů huseníčku s různými množstvími PsbO1 a PsbO2 jsme potvrdili, že celkové množství PsbO v rostlině má zásadní vliv na fenotyp. V kontrastu s převažujícím názorem je však naše zjištění, že na rostlinu a její fotosyntetický aparát má minimální vliv, která izoforma PsbO je v ní přítomná, a to jak za normálních podmínek, tak při vysoké ozářenosti. Analýza proteomu mutantů s nízkou hladinou PsbO1 nebo PsbO2 potvrdila tyto výsledky a ukázala některé nečekané efekty nízkého množství PsbO v rostlinách.

Na základě našich výsledků jsme navrhli hypotézu, že izoformy PsbO nemají zásadně odlišnou funkci, ale spíše jemně modulují nějaký proces. Spekulujeme, že časté záměny aspartát – glutamát mezi izoformami PsbO by mohly ladit konformační změny závislé na pH, které by se mohly podílet na regulaci aktivity nebo funkce PSII.

Abbreviations

A. thaliana	*Arabidopsis thaliana*
ATP	adenosine triphosphate
CRISPR-Cas9	clustered regularly interspaced short palindromic repeats – CRISPR associated 9
DNA	deoxyribonucleic acid
EPR	electron paramagnetic resonance
F_V/F_M	maximum quantum yield of photosystem II
GL	growth light (normal light conditions, around 120 µmol photons m^{-2} s^{-1})
GTP	guanosine triphosphate
HL	high light
LHC	light harvesting complex
LCHII	light harvesting complex of photosystem II
NPQ	non-photochemical quenching
OEC	oxygen evolving centre
PAGE	polyacrylamide gel electrophoresis
PAR	photosynthetically active radiation
PCA	principal component analysis
PCR	polymerase chain reaction
PQ	plastoquinone
PQH_2	plastoquinol
PSI	photosystem I
PSII	photosystem II
rETR	relative electron transport rate
$rETR_{max}$	maximum of relative electron transport rate
RLC	rapid light curve
RNA	ribonucleic acid
RNAi	RNA interference
RNAseq	RNA sequencing
SDS	sodium dodecyl sulphate
T-DNA	transfer DNA (of *Agrobacterium tumefaciens*)
UTR	untranslated region
WT	wild type

Symbols used for genes, proteins and mutants

psbO1, *psbO2*	genes
PsbO1, PsbO2	proteins
psbo1	mutant with impaired *psbO1* gene (producing only PsbO2 protein)
psbo2	mutant with impaired *psbO2* gene (producing only PsbO1 protein)
*psbo1*psbo2*	double mutant with impaired *psbO2* gene and partially restored expression of *psbO1* (producing only low amount of PsbO1 protein)
*psbo1*oc*	*psbo1* mutant with partially restored expression of *psbO1* (out-crossed from the crossing with *psbo2* mutant)
psbo2oc	*psbo2* mutant out-crossed from the crossing with *psbo1* mutant
psbo1bc	*psbo1* mutant after back-cross to WT

1 Introduction

The origin of oxygenic photosynthesis more than 2.3 billion years ago caused major changes in the history of the Earth. Allowing to generate energy and reducing power directly from sunlight and water, it greatly increased global primary productivity and led to a rise of oxygen in Earth's atmosphere. This allowed the evolution of organisms and their metabolic processes as we know them today (Fischer *et al.* 2016).

Nowadays, detailed understanding of photosynthesis is not only a challenge for primary science. It might also show ways how to improve photosynthesis for today's people's needs. Higher crop yields and an increased tolerance of photosynthesis to stressful conditions are required to satisfy increasing food demands (Long *et al.* 2015). Moreover, artificial photosynthesis inspired by the natural one might help to decrease our dependence on fossil fuels (Zhang & Sun 2019).

1.1 Photosystem II

1.1.1 Function of photosystem II

Photosystem II (PSII) is a multi-subunit pigment-protein complex embedded in a thylakoid membrane. PSII functions as water:plastoquinone oxidoreductase, pumping electrons from water to plastoquinone (PQ) using energy from light. A quantum of light is absorbed by pigments embedded in antenna proteins and the energy is transferred to the reaction centre of PSII, to a special pair of chlorophylls P_{D1} and P_{D2}, often called by the spectroscopic term P680 (Renger & Renger 2008). This is where a charge separation occurs. An electron is released from P680 and transferred quickly through several cofactors to PQ in Q_B site. The electron hole left by the charge separation is highly oxidative and it drives water splitting. It extracts an electron from a tyrosine residue Y_Z, which subsequently extracts an electron from the Mn_4CaO_5 cluster. The Mn_4CaO_5 cluster binds two water molecules that are oxidised by four photochemical turnovers to dioxygen. The Mn_4CaO_5 cluster together with the parts of the proteins surrounding it are called the oxygen evolving centre (OEC). On the other side of the PSII, two electrons are used to reduce PQ, which is protonated to form plastoquinol (PQH_2). The water:plastoquinone oxidoreductase function of PSII is summarised in Eq. 1 (Renger & Renger 2008; Barber 2016).

Eq. 1 $$2H_2O \xrightarrow{4h\nu} O_2 + 2PQH_2$$

It is important to note that the protons from the water are released into the thylakoid lumen, whereas the protons used to form PQH_2 are taken from the stroma. In this manner, PSII contributes to the proton gradient across the thylakoid membrane (Renger & Renger 2008). The function of PSII is summarised in Fig. 1.1.

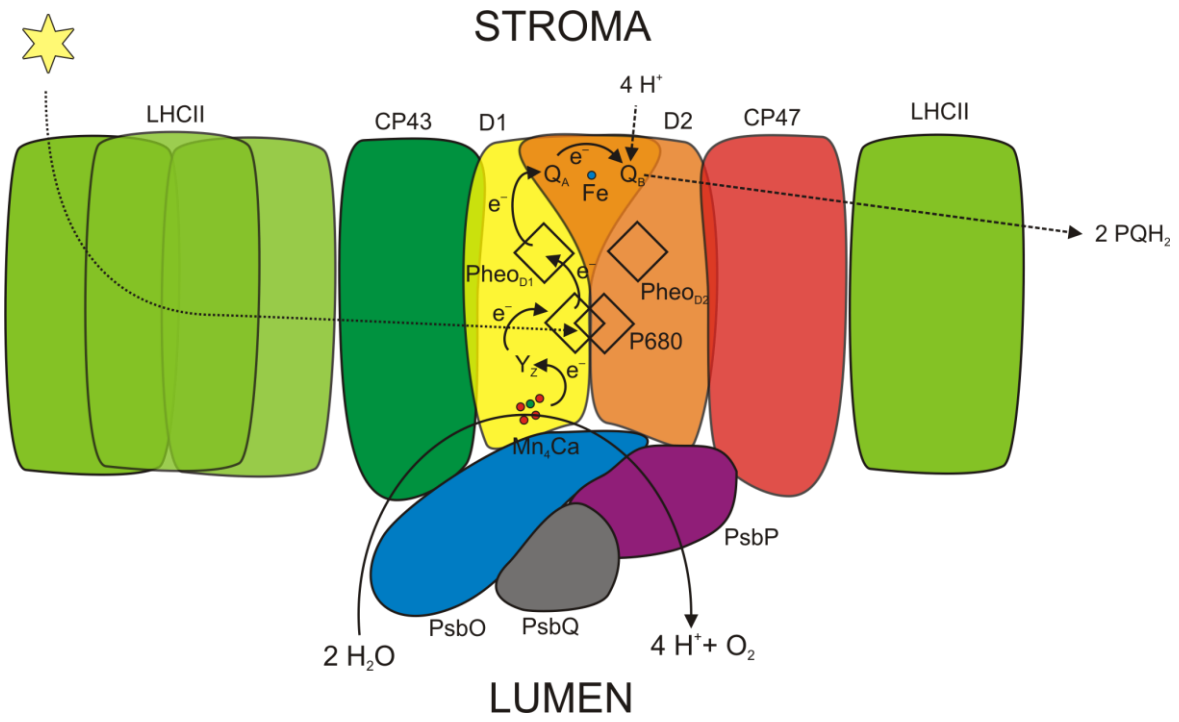

Fig. 1.1: A simplified scheme of PSII function: Charge separation, driven by energy from light absorbed by antenna complexes, takes place at a special pair of chlorophylls (P680). Electrons (e^-) are transferred through several cofactors to PQ in QB site. Electrons are replenished to P680 through the tyrosine residue YZ from the Mn_4CaO_5 cluster, where the water splitting occurs. The rest of the split water, protons (H^+) and molecular oxygen (O_2), is released into the lumen.

1.1.2 Structure of photosystem II

The first resolved structures of PSII were obtained by X-ray crystallography of PSII from thermophilic cyanobacteria, *Thermosynechococcus elongatus* and *Thermosynechococcus vulcanus* (Zouni *et al.* 2001; Kamiya & Shen 2003; Biesiadka *et al.* 2004; Ferreira *et al.* 2004; Loll *et al.* 2005; Guskov *et al.* 2009; Umena *et al.* 2011; Tanaka *et al.* 2017). The resolution improved during the years from 3.8 Å (Zouni *et al.* 2001) to 1.85 Å (Tanaka *et al.* 2017).

In recent years, the state-of-the-art crystallography of cyanobacterial PSII was focused mainly on elucidating the mechanism of photosynthetic water oxidation using femtosecond pulses of X-ray free-electron laser. This technique allowed to obtain structures of PSII and its Mn_4CaO_5 cluster at various stages of the Kok cycle with resolution close to 2 Å (Kern *et al.* 2018; Suga *et al.* 2019; reviewed in Cox *et al.* 2020).

Since the reaction centre of the PSII is similar in cyanobacteria and plants, much information from the crystal structures of the cyanobacterial PSII could be used also for the plant PSII. However, some of the smaller subunits differ between cyanobacteria and plants, especially regarding the extrinsic subunits bound from the luminal side (Pagliano *et al.* 2013). Thus, the structure of the plant PSII was needed to elucidate these structural specifics.

In 2016, structure of PSII from spinach (*Spinacia oleracea*) with resolution 3.2 Å obtained by single-particle cryo-electron microscopy was published (Wei *et al.* 2016). The same technique allowed to solve also structures of PSII from pea (*Pisum sativum*) at 2.7 Å resolution (Su *et al.* 2017) and from pea under high light conditions at 3.8 Å resolution (Grinzato *et al.* 2020). The structure from *Arabidopsis thaliana* was available first at 5.3 Å resolution (Bezouwen *et al.* 2017) and recently at 2.8 Å resolution (Graça *et al.* 2021). The structures of PSII from the red alga *Cyanidium caldarium* and the green alga *Chlamydomonas reinhardtii* are also available (Ago *et al.* 2016; Shen *et al.* 2019; Sheng *et al.* 2019). The structures of PSII from pea and spinach are shown in Fig. 1.2 and Fig. 1.5.

The reaction centre of PSII is formed by 6 proteins: D1 and D2, binding most of the redox cofactors forming the electron transport chain between water and PQ, intrinsic antenna proteins CP47 and CP43 and α and β subunits of cytochrome *b*559 (PsbE and PsbF). Around this highly conserved reaction centre are positioned several integral membrane subunits with a low molecular mass and only 1 or 2 transmembrane helices (Shi *et al.* 2012; Pagliano *et al.* 2013).

Extrinsic subunits that do not have any transmembrane domains and are bound to the luminal side of membrane subunits differ between cyanobacteria and plants. The only conserved subunit is PsbO, which is also the biggest one (molecular weight around 27 kDa). PsbV (cytochrome *c*550) and PsbU are present in cyanobacteria but missing in plants. PsbP, PsbQ and PsbTn are present in plants (De Las Rivas *et al.* 2004; Pagliano *et al.* 2013). It is important to note that cyanobacteria contain homologues of PsbP and PsbQ called CyanoP and CyanoQ (De Las Rivas *et al.* 2004; Thornton *et al.* 2004; Sato 2010). While CyanoP is not stably associated with PSII, CyanoQ is probably a part of an active cyanobacterial PSII (Thornton *et al.* 2004; Roose *et al.* 2007), although it is missing in available structures.

Some proteins associated with PSII are not found in structures of PSII, either because of a too weak binding or because of being bound only in special situations such as stress, assembly or degradation (Shi *et al.* 2012). One of such proteins is PsbR, which is needed for optimal oxygen evolution and the binding of PsbP (Suorsa *et al.* 2006). PsbR probably has a C-terminal transmembrane α-helix and N-terminal luminal domain; however, its position within PSII is unclear (Roose *et al.* 2016; Bezouwen *et al.* 2017).

1.1.3 Structure of PSII-LHCII supercomplex from plants

Both in cyanobacteria and plants, a large fraction of PSII forms dimers. In plants, the homodimer of PSII core complex (C_2) is surrounded by light-harvesting complexes (LHC) embedded in the thylakoid membrane (Kouřil *et al.* 2012; Rantala *et al.* 2020). This contrasts with cyanobacteria that use other types of antenna complexes, phycobilisomes, which reside on the PSII outside of the thylakoid membrane (Blankenship 2014).

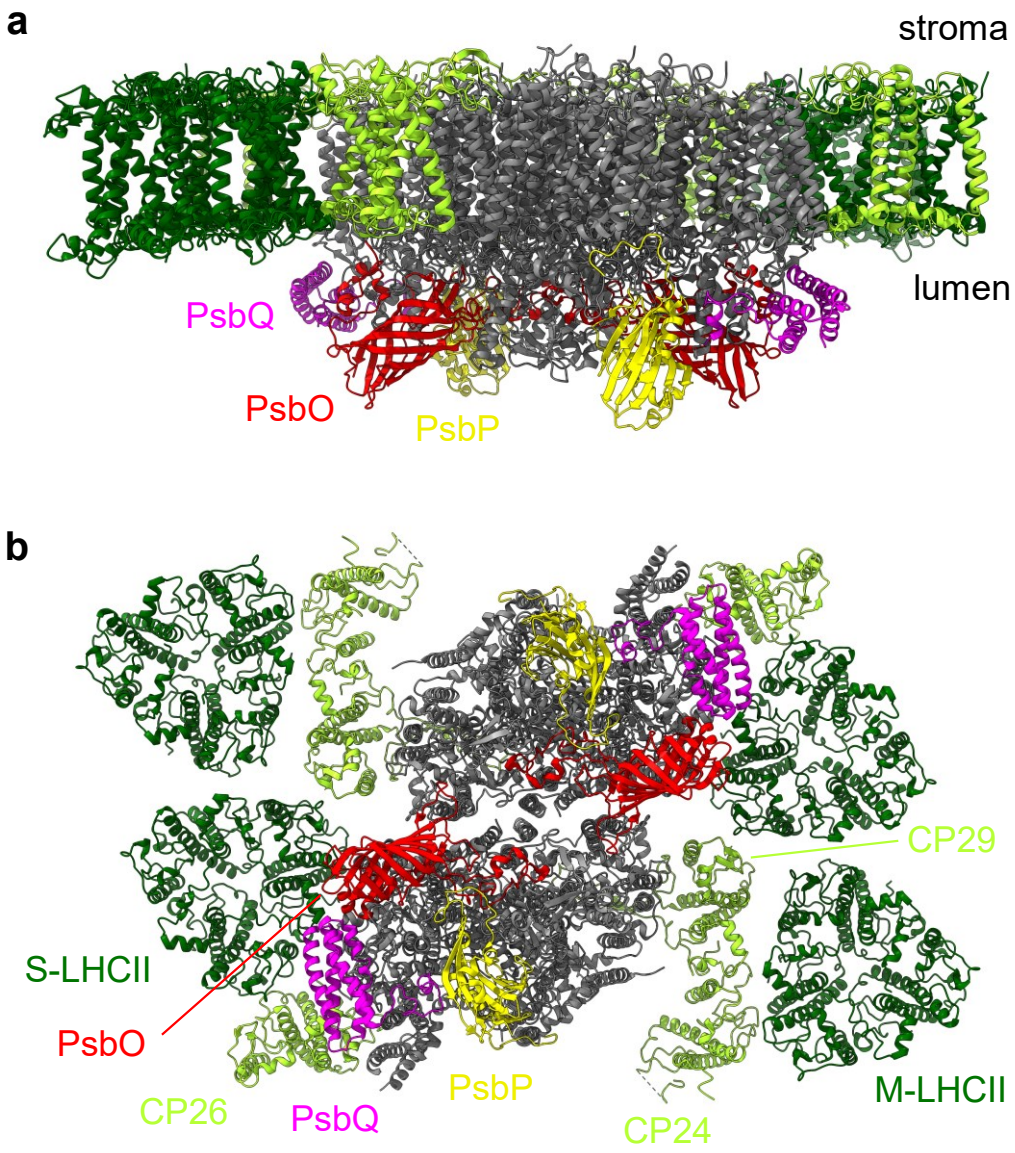

Fig. 1.2: Structure of PSII-LHCII supercomplex (type $C_2S_2M_2$) from pea. **a** Side view (view parallel with membrane plane). **b** View from lumen (view perpendicular to membrane plane). PSII core subunits are shown in grey, LHCII trimers in dark green, minor Lhcb subunits (CP29, CP26 and CP24) in light green, PsbO in red, PsbP in yellow and PsbQ in magenta. Based on the structure of stacked PSII-LHCII supercomplex from pea (PDB: 5XNL; Su *et al.* 2017). Visualised with UCSF ChimeraX, version 1.2 (Pettersen *et al.* 2021).

The light-harvesting complex II (LHCII), the antenna system of plant PSII, is formed by 6 different Lhcb proteins (Lhcb1-6). Various combinations of Lhcb1, Lhcb2 and Lhcb3 form so-called LHCII trimers. Lhcb4 (CP29), Lhcb5 (CP26) and Lhcb6 (CP24) occur in monomeric states. The dimeric core of PSII (C_2) can be surrounded by several LHCII trimers and monomers. In the most abundant PSII-LHCII supercomplex, $C_2S_2M_2$, both core monomers (C) are associated with a strongly bound LHCII trimer (S) and a moderately bound LHCII trimer (M). Loosely bound LHCII trimers (L) can be also bound in the supercomplex, giving rare $C_2S_2M_2L_{1\text{-}2}$ supercomplexes. The monomeric Lhcb proteins are positioned between PSII core and LHCII trimers (Kouřil *et al.* 2012; Rantala *et al.* 2020).

Single-particle cryo-electron microscopy allowed to solve the structure of the whole PSII-LHCII supercomplex, thus the structure of PSII from spinach is available as C_2S_2 supercomplex (Wei *et al.* 2016), while the structures of PSII from pea and *A. thaliana* are available as $C_2S_2M_2$ supercomplexes (Bezouwen *et al.* 2017; Su *et al.* 2017; Graça *et al.* 2021). Structure of $C_2S_2M_2$ supercomplex is shown in Fig. 1.2.

1.2 PsbO

PsbO protein, also named manganese-stabilising protein (MSP), oxygen-evolving enhancer 1 (OEE1), oxygen-evolving centre (OEC) 33 kDa subunit (OE33) or 33 kDa extrinsic protein, is the biggest extrinsic subunit of PSII. PsbO is probably present in all oxyphototrophs, organisms performing oxygenic photosynthesis, both prokaryotic and eukaryotic (De Las Rivas *et al.* 2004).

In eukaryotes, some of the subunits of PSII are encoded by the chloroplast genome and some by the nuclear genome. PsbO, as other extrinsic subunits, is encoded by the nuclear genome (Seidler 1996; De Las Rivas *et al.* 2004). Thus, it is synthesized at soluble ribosomes in cytoplasm. The transport into the chloroplast and then into the thylakoid lumen is directed by an N-terminal transit peptide, which consists of two parts, chloroplast-targeting and thylakoid-targeting. Each part of the transit peptide is cleaved by a peptidase during the translocation, giving the final mature protein in the thylakoid lumen. PsbO is transported by the SEC translocation pathway from the chloroplast stroma into the thylakoid lumen (Yuan *et al.* 1994; Seidler 1996; Jiang *et al.* 2020).

Molecular weight of PsbO from spinach calculated from amino acid sequence (26.53 kDa) is a in agreement with the mass measured by mass spectrometry, suggesting that there is no posttranslational modification other than the transit peptide cleavage (Svensson *et al.* 2002). However, when subjected to SDS-PAGE, the apparent molecular mass of PsbO is 33 kDa, which is the source of the alternative name “OEC 33 kDa subunit”. This anomalous migration might be caused by reduced SDS binding (Zubrzycki *et al.* 1998).

1.2.1 Structure of PsbO

The main part of PsbO consists of β-barrel composed of eight antiparallel β-strands (Fig. 1.3). The central part of the β-barrel is full of bulky hydrophobic residues. The longest loops extending from the β-barrel are β5-β6 loop, inserted between β-strands 5 and 6, and N-terminal loop. Short α-helices are located in the N-terminal loop and β5-β6 loop. The axis of the β-barrel is orientated at about 40° to the membrane plane (De Las Rivas & Barber 2004; Wei *et al.* 2016; Su *et al.* 2017). While the β-barrel part of PsbO is rigid, the loops become disordered in solution, when PsbO is not bound to PSII (Nowaczyk *et al.* 2004; Bommer *et al.* 2016). The N-terminus, β1-β2 loop and β5-β6 loop can become flexible under some conditions also when PsbO is bound to PSII (Su *et al.* 2017; Graça *et al.* 2021).

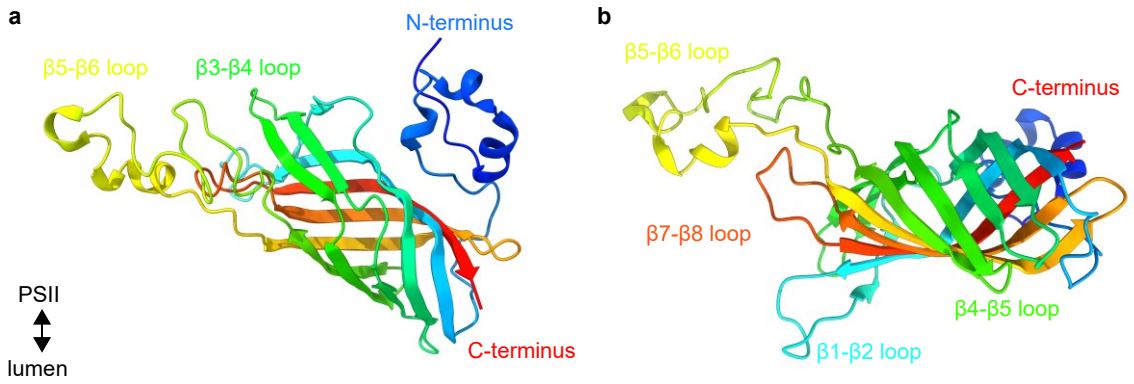

Fig. 1.3: Structure of PsbO. **a** Side view of PsbO (view parallel with membrane plane). The PSII-binding part of PsbO is facing upward. **b** PsbO viewed from lumen (view perpendicular to the membrane plane). Based on structure of stacked PSII-LHCII supercomplex from pea (PDB: 5XNL; Su *et al.* 2017). Visualised with UCSF ChimeraX, version 1.2 (Pettersen *et al.* 2021).

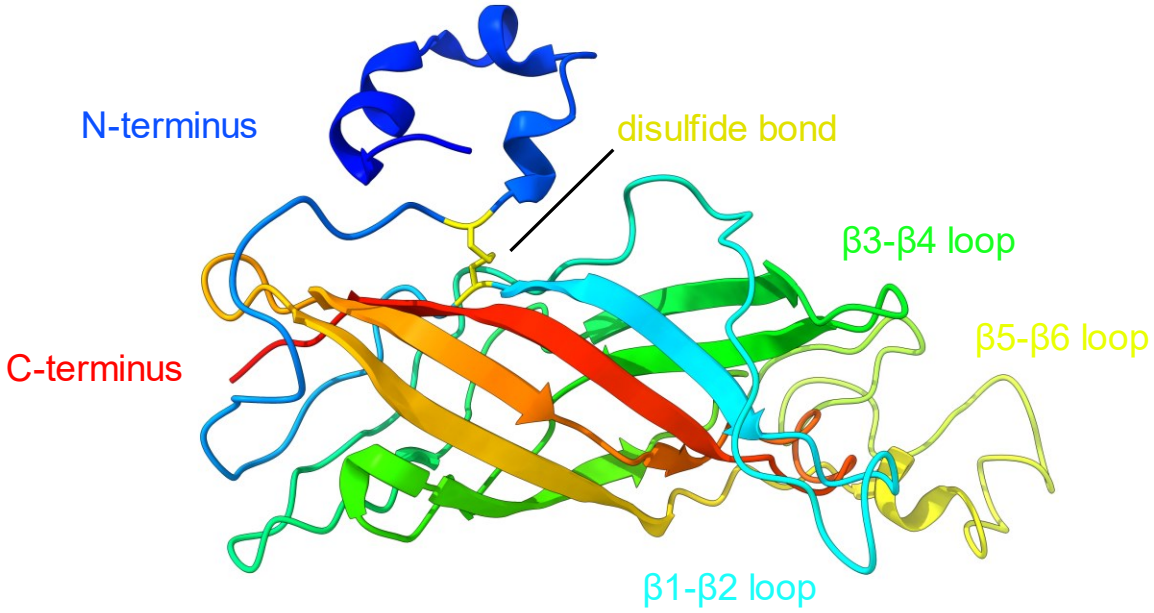

Fig. 1.4: PsbO with disulfide bond (shown in yellow) between the N-terminal loop and the β1 strand. Based on the structure of PSII-LHCII supercomplex from spinach (PDB: 3JCU, Wei *et al.* 2016). Note that four N-terminal amino acid residues were not resolved in this structure and are missing in the figure compared to the structure of pea PsbO in Fig. 1.3. Visualised with UCSF ChimeraX, version 1.2 (Pettersen *et al.* 2021).

PsbO has two conserved cysteine residues that form a disulfide bond between the N-terminal loop and the β1 strand (Fig. 1.4). This disulfide bond stabilises the structure of PsbO. Reduction of this disulfide bond in spinach leads to unfolding of the protein (Tanaka *et al.* 1989; Nikitina *et al.* 2008). Mutated PsbO with cysteine residues exchanged for alanine residues has also disordered structure in solution. However, under *in vitro* conditions, this mutated PsbO was able to bind to PSII and support oxygen evolution (Betts *et al.* 1996; Wyman & Yocum 2005).

1.2.2 Interactions of PsbO on PSII

PsbO is bound to membrane subunits of PSII from the luminal side of the membrane (Fig. 1.2 and Fig. 1.5). The binding region on PsbO is comprised of one end of the β-barrel, the loops extending from this end (loops β1-β2, β3-β4, β5-β6 and β7-β8) and the N-terminal loop. The main interactions are with subunits D1, D2, CP43 and CP47. The N-terminal loop interacts also with one-helix membrane subunit PsbW. The β1-β2 and β3-β4 loops of PsbO interact also with CP47 subunit of the other monomer of PSII (De Las Rivas & Barber 2004; Wei *et al.* 2016; Su *et al.* 2017).

PsbO also interacts with other extrinsic subunits. According to PSII structures from spinach (Wei *et al.* 2016) and pea (Su *et al.* 2017), PsbQ interacts with the N-terminal loop of PsbO, while PsbP interacts with the β5-β6 loop. However, the contact surfaces are small. There is no interaction between PsbO and the smallest extrinsic subunit of PSII, the PsbTn protein (Wei *et al.* 2016; Su *et al.* 2017).

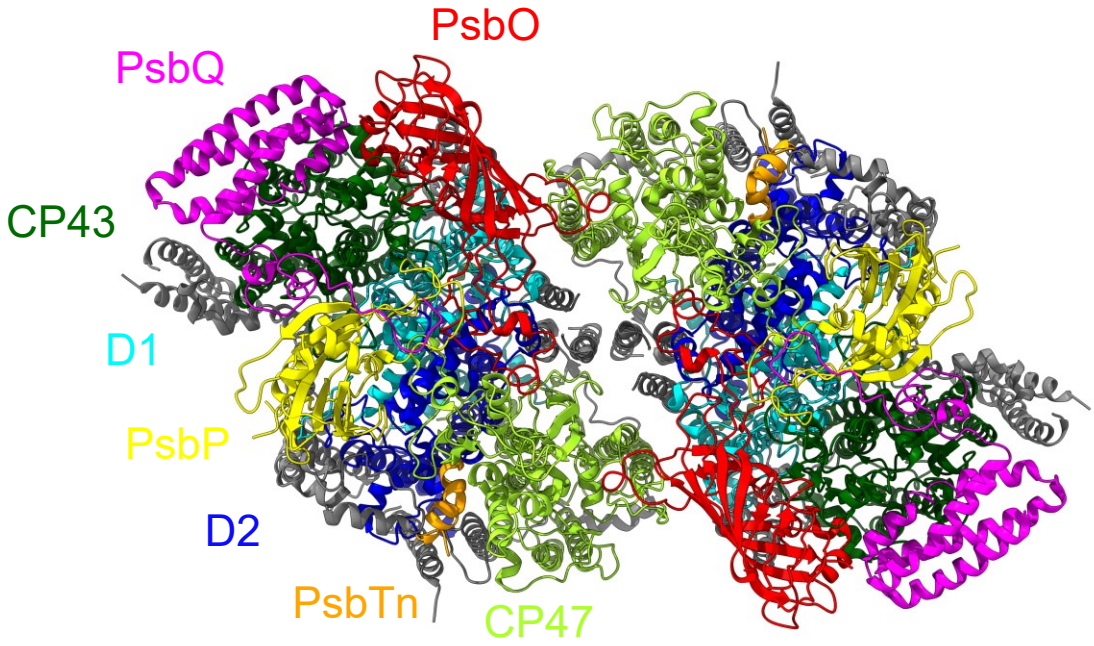

Fig. 1.5: Structure of PSII dimer from spinach viewed from lumen (view perpendicular to membrane plane). Membrane subunits: D1 is shown in cyan, D2 in blue, CP47 in light green, CP43 in dark green and other membrane subunits in grey. Extrinsic subunits: PsbO is shown in red, PsbP in yellow, PsbQ in magenta and PsbTn in orange. Based on structure of PSII-LHCII supercomplex from spinach (PDB: 3JCU, Wei *et al.* 2016). Lhcb proteins are not shown. Visualised with UCSF ChimeraX, version 1.2 (Pettersen *et al.* 2021).

1.2.3 Functions of PsbO

1.2.3.1 Stabilisation of Mn_4CaO_5 cluster

Cyanobacterium *Synechocystis* sp. PCC 6803 with deleted *psbO* gene is able to grow photoautotrophically, but it grows at slower rate (Burnap & Sherman 1991). In contrast, neither the mutant of green alga *Chlamydomonas reinhardtii* lacking PsbO, nor *Arabidopsis thaliana* (*A. thaliana*) with silenced expression of both *psbO* paralogs is able to assemble PSII and grow photoautotrophically (Mayfield *et al.* 1987; Yi *et al.* 2005).

The main function of PsbO is probably maintaining structural integrity of oxygen-evolving centre (OEC). PsbO does not provide any ligands directly to the Mn_4CaO_5 cluster, which is bound between D1 and CP43 proteins, however, it is bound close to this site (De Las Rivas & Barber 2004; Wei *et al.* 2016; Su *et al.* 2017). When isolated PSII membranes are depleted of the PsbO, they are able to evolve oxygen, albeit at very low rates. High Cl^- and Ca^{2+} concetrations are needed to maintain the intactness of Mn_4CaO_5 cluster without PsbO (Bricker 1992). The effect of PsbO depletion on the Mn_4CaO_5 cluster is similar to the effect of Cl^- and Ca^{2+} depletion and the oxygen evolution requirements for these ions are lowered in the presence of PsbO (reviewed in Bricker *et al.* 2012). This suggests that PsbO maintains the right conformation around Mn_4CaO_5 cluster, and that this conformation involves also Cl^- and Ca^{2+} ions bound in right positions. This function is shared with PsbP and PsbQ, whose presence also influence requirements of oxygen evolution for Cl^- and Ca^{2+} (Bricker *et al.* 2012).

There is nowadays no doubt that the Mn_4CaO_5 cluster contains Ca^{2+} cation. However, it is not clear whether there is also an additional Ca^{2+} binding site in the PSII structure. Murray and Barber (2006) identified Ca^{2+} bound to PsbO in PSII structure from cyanobacteria (PDB: 1S5L, Ferreira *et al.* 2004). The same Ca^{2+} binding site was identified also in other cyanobacterial PSII structure (Guskov *et al.* 2009). In another PSII structures, Ca^{2+} was identified at different site of PsbO (Umena *et al.* 2011; Suga *et al.* 2015). No Ca^{2+} binding site that would involve residues from PsbO was found in PSII structures from plants (Wei *et al.* 2016; Su *et al.* 2017; Graça *et al.* 2021). It is unclear whether the Ca^{2+} was lost in some preparations of PSII, or whether it is a crystallisation artefact in other (Bricker *et al.* 2012).

Guskov *et al*. (2009) found one Cl^- ion in PSII structure from cyanobacteria and Umena *et al.* (2011) found also a second one. The same binding sites are visible also in the PSII structures from plants (Wei *et al.* 2016; Su *et al.* 2017). Both of the Cl^- ions are bound near the Mn_4CaO_5 cluster. They may have a role in maintaining the coordination environment of the Mn_4CaO_5 cluster or in arrangement of water inlet or proton outlet channels (Umena *et al.* 2011).

The importance of PsbO and PsbP for stabilisation of PSII structure around Mn_4CaO_5 cluster was demonstrated also by Tokano *et al.* (2020) using high-speed atomic force microscopy. After dissociation of extrinsic proteins from PSII, luminal domain of CP43 shows conformational fluctuations. These fluctuations are delayed in the presence of $CaCl_2$ and induced by light, suggesting that the start of the fluctuations is related to a destruction of the Mn_4CaO_5 cluster (Tokano *et al.* 2020)[1].

1.2.3.2 Channels connecting Mn_4CaO_5 cluster and lumen

OEC needs for its function inlet of water and outlet of oxygen and protons. Several channels that would allow transport of water, oxygen and protons between Mn_4CaO_5 cluster and bulk solution in lumen were identified in the PSII structure (Murray & Barber 2007; Ho & Styring 2008; Gabdulkhakov *et al.* 2009; Vassiliev *et al.* 2010). The channels should not only allow efficient transport of substrate and products but might also protect the Mn_4CaO_5 cluster from exogenous reductants.

PsbO is participating in formation of some of the predicted channels (Murray & Barber 2007; Gabdulkhakov *et al.* 2009; Vassiliev *et al.* 2010). As PsbO contains many polar groups, especially carboxylic groups (aspartic and glutamic acid residues), it might be important especially for proton removal from the OEC. Carboxylic groups on PsbO connected by hydrogen-bond networks to Mn_4CaO_5 cluster can provide buffering capacity, ensure rapid transport of protons and act as a "proton antenna" (Shutova *et al.* 2007; Bondar & Dau 2012; Lorch *et al.* 2015; Barry *et al.* 2017; Guerra *et al.* 2018; Gerland *et al.* 2020). Various protonation states of PsbO have an impact on its structure. This suggests that there might be some feedback regulation of PSII activity by PsbO (Shutova *et al.* 2005; Gerland *et al.* 2020).

1.2.3.3 Stabilisation of PSII dimers and bigger assemblies

PsbO participates on the interaction between monomers of PSII in PSII dimer, interacting with CP47 subunit from the other monomer (De Las Rivas & Barber 2004; Wei *et al.* 2016; Su *et al.* 2017). Cyanobacterial mutants without PsbO do not have almost any dimers of PSII (Bentley & Eaton-Rye 2008). Electron microscopy analysis of spinach PSII-LHCII complexes after removal of PsbO showed conformation changes, which were also interpreted as destabilisation of monomer-monomer interactions (Boekema *et al.* 2000).

In cyanobacteria, PsbO might be involved in formation of bigger assemblies of PSII. Hellmich *et al.* (2014) obtained structure of row of PSII dimers, where one of the dimer-dimer contacts is between PsbOs. The site of the contact is a "cyano loop", a β4-β5 loop,

[1] Supplementary data of Tokano *et al.* (2020) contain movies of PSII captured by high-speed atomic force microscopy (https://pubs.acs.org/doi/10.1021/acs.jpcb.0c03892).

which is about 8 amino acid residues longer in cyanobacteria than in eukaryotes. It is probable that such interaction does not occur in plants, because of the missing cyano loop and because the PSII dimer is usually surrounded by LHCII.

1.2.3.4 GTPase activity and PSII repair

It was shown that PsbO from spinach is able to bind (Spetea *et al.* 2004) and also hydrolyse GTP, although at very slow rates (Lundin *et al.* 2007b). The putative GTP-binding site is conserved in plants, but not in green alga *Chlamydomonas reinhardtii* or cyanobacteria *Thermosynechococcus* (Lundin *et al.* 2007b). This is in line with observation that PsbO from these species does not bind GTP (Lundin *et al.* 2007b; Spetea & Lundin 2012).

GTPase activity of PsbO was higher when the PsbO was bound to PSII rather than free in solution. Also, GTP stimulated release of PsbO from PSII in some experiments (Lundin *et al.* 2007b).

GTP was found to be important for degradation of photodamaged D1 subunit of PSII (Spetea *et al.* 1999). Thus, it suggests that PsbO might be involved in the process of replacement of D1 protein (Lundin *et al.* 2007b).

D1 is the most frequently damaged subunit of PSII. Thus, photosynthetic organisms have a specialised repair cycle for PSII with damaged D1 protein. After the photodamage of D1, PSII core subunits are phosphorylated (on the stromal side) and the PSII dimer monomerise. The PSII migrates from appressed grana membranes, where functional PSII complexes are mostly localised, to non-appressed stroma-exposed thylakoids. The phosphorylated core subunits are again dephosphorylated, probably on the way to stroma-exposed thylakoids. PSII is partially disassembled, CP43 and extrinsic proteins PsbO, PsbP and PsbQ and maybe also some other subunits are released. The damaged D1 is digested by proteases. New D1 protein is cotranslationally inserted into PSII. Released subunits are again assembled to PSII, which migrates back to appressed grana membranes, dimerise and form PSII-LHCII complexes (reviewed in Järvi *et al.* 2015).

However, there are still many doubts if and how PsbO could be involved the process of PSII repair (Bricker & Frankel 2011).

1.2.4 PsbO isoforms in *Arabidopsis thaliana*

A. thaliana expresses two *psbO* genes, *psbO1* (At5g66570) and *psbO2* (At3g50820), encoding for PsbO1 and PsbO2 proteins (The Arabidopsis Genome Initiative 2000; Murakami *et al.* 2002). The mature forms of the proteins (without transit peptide) differ in only 11 amino acid residues (Murakami *et al.* 2002, 2005).

PsbO1 is the major isoform with higher amounts in the *A. thaliana* plants. However, the exact ratio of isoforms varies in the literature. The PsbO2 isoform was reported to account for 10% (Murakami *et al.* 2005), 20% (Lundin *et al.* 2007a) or 41% (Dwyer *et al.* 2012) of total PsbO. The expression of the isoforms stays similar during plant development and during various short time stresses (Lundin *et al.* 2008).

1.2.4.1 Biochemical characteristics of PsbO isoforms

The only biochemical characterisation of pure PsbO isoforms from *A. thaliana* was done by Murakami *et al.* (2005). The authors produced recombinant PsbOs and PsbO-depleted PSII particles to show that both PsbOs bind PSII with similar affinity, while the oxygen evolution activity of PSII was better restored by PsbO1. The maximum oxygen-evolving activity with PsbO2 was about 80% of that with PsbO1 (Murakami *et al.* 2005). It is important to note that the authors used PSII particles isolated from spinach, which might function slightly different with *A. thaliana* PsbOs, and they did not show any data about quality of the recombinant proteins (proper folding etc.).

Similar experiments, measurements of oxygen evolution by PSII with either PsbO1 or PsbO2, were done by Lundin *et al.* (2007a). The authors used isolated PSII-LHCII supercomplexes from *psbo1* and *psbo2* mutants. The oxygen evolution rates were not significantly different, however, the relative difference between means was similar as reported by Murakami *et al.* (Murakami *et al.* 2005; Lundin *et al.* 2007a).

PSII membranes isolated from *psbo1* and *psbo2* mutants were used to measure GTPase activity. The GTPase activity per mg of chlorophyll was slightly higher for *psbo1* mutant. When expressed per mol of PsbO, the activity was threefold higher for PsbO2 in *psbo1* mutant than for PsbO1 in *psbo2* mutant (Lundin *et al.* 2008). The calculated activities were very low, as the highest reported was around 12 mmol GTP (mol PsbO)$^{-1}$ min^{-1}, meaning that one PsbO cleaves one GTP in about 1 h 20 min. Similar results were obtained by Wang *et al.* (2015)[2].

1.2.4.2 *Arabidopsis thaliana psbo1* and *psbo2* mutants

A. thaliana plants with both *psbO* genes inactivated by mutation were reported to be seedling lethal (Suorsa *et al.* 2016). Plants with both *psbO* genes strongly silenced by RNA interference are able to grow only *in vitro* on medium with sucrose. The loss of PsbOs in these plants led to a concomitant loss of PSII reaction centre subunits and inability to grow photoautotrophically (Yi *et al.* 2005). However, mutants in single *psbO* gene are viable and able to grow photoautotrophically.

[2] These authors did not report absolute values of GTPase activity, just values relative to WT.

1.2.4.2.1 Mutant *psbo1*

Two different *psbo1* mutants, which lack PsbO1 protein and produce only PsbO2 protein, were described. Both point mutant in Landsberg *erecta* background (Murakami *et al.* 2002, 2005; Liu *et al.* 2007, 2009; Bricker & Frankel 2008) and T-DNA insertional mutant in Col-0 background (Lundin *et al.* 2007a, 2008; Allahverdiyeva *et al.* 2009; Suorsa *et al.* 2016) have similar phenotypes.

The *psbo1* mutant grows significantly slower than wild type (WT) plants (Murakami *et al.* 2002; Lundin *et al.* 2007a; Suorsa *et al.* 2016). It has lower amount of chlorophyll and other pigments (Suorsa *et al.* 2016), resulting in pale green leaves (Lundin *et al.* 2007a; Suorsa *et al.* 2016). The expression of *psbO2* gene was activated in compensatory manner, the PsbO2 level in *psbo1* was reported to be 40% and 70% (young and mature plants, Murakami *et al.* 2005) or 75% (Lundin *et al.* 2007a) of total PsbO level in WT when normalised for the same amount of chlorophyll. Suorsa et al. (2016) reported only 17% of total PsbO level in WT when normalised for the same amount of proteins. The reduction of the total ammount of PsbO in the *psbo1* mutant is accompanied by reduction of other PSII subunits (Murakami *et al.* 2005; Lundin *et al.* 2007a; Suorsa *et al.* 2016). The reported reduction is mostly similar to the reduction of total PsbO, suggesting that the ratio of PsbO to PSII stays similar (Murakami *et al.* 2005; Lundin *et al.* 2007a). Lundin *et al.* (2007a) found the amount of photosystem I (PSI) to be unaffected, whereas Suorsa *et al.* (2016) and Liu *et al*. (2009) reported reduced amounts of PSI. The PSI/PSII ratio measured by EPR spectroscopy was 1.54 in *psbo1* compared to 0.91 in WT (Allahverdiyeva *et al.* 2009), meaning that the amount of PSII was affected more than the amount of PSI. The level of ATP synthase seems to be unaffected (Lundin *et al.* 2007a; Suorsa *et al.* 2016), while the level of cytochrome b_6f complex was reported to be unaffected (Suorsa *et al.* 2016) or even increased (Liu *et al.* 2009). The somewhat discrepant results between the publications (Murakami *et al.* 2005; Lundin *et al.* 2007a; Suorsa *et al.* 2016) might be caused by different western blot protocols (Janes 2015), different growth conditions and age of the plants, analyzing either thylakoid membranes or whole leaves or normalisation to either chlorophyll amount or total proteins.

The abundance of various PSII supercomplexes is also altered in *psbo1* mutant. The mutant has less PSII-LHCII supercomplexes (Lundin *et al.* 2008; Allahverdiyeva *et al.* 2009) and PSII dimers, while it has relatively more PSII monomers and CP43-less PSII monomers (Lundin *et al.* 2008). This is in line with higher ratio of PSIIβ centres to PSIIα centres, where PSIIβ centres are mostly PSII complexes with less antenna complexes located in stroma-exposed thylakoids, while PSIIα centres are mostly PSII-LHCII supercomplexes in stacked grana membranes (Liu *et al.* 2007, 2009).

The *psbo1* mutant has significantly altered the function of PSII. The maximum quantum yield of PSII (F_V/F_M) is 0.8, whereas values for *psbo1* are about 0.5-0.6 (Murakami *et al.* 2002; Lundin *et al.* 2007a; Allahverdiyeva *et al.* 2009), rising up to 0.7 for the mature plants (Murakami *et al.* 2005). The lower values are mainly due to high F_O (Murakami *et al.* 2002; Allahverdiyeva *et al.* 2009).

Various measurements indicated that the function of PSII in *psbo1* mutant is altered both at the donor and acceptor sides (Liu *et al.* 2007; Allahverdiyeva *et al.* 2009). The oxygen evolution of isolated thylakoid membranes is lower for *psbo1* compared to WT (Murakami *et al.* 2002; Lundin *et al.* 2007a; Bricker & Frankel 2008; Allahverdiyeva *et al.* 2009). Interestingly, some of the defects measured on isolated thylakoid membranes of *psbo1* (S_2 and S_3 state dark decay and oxygen yield) were reversed after addition of $CaCl_2$ (Bricker & Frankel 2008). However, Allahverdiyeva *et al.* (2009) did not observe any similar effect of the $CaCl_2$.

The effects of *psbo1* mutation were reverted also by sufficient expression of N-terminally His-tagged PsbO1 protein (Liu *et al.* 2009).

The *psbo1* mutant has also some differences in non-photochemical quenching (NPQ) and cyclic electron transfer around PSI. The induction of NPQ is faster in *psbo1* compared to WT. The level of steady-state NPQ is higher in *psbo1* under low light, while it is lower under higher intensity of illumination (Allahverdiyeva *et al.* 2009; Suorsa *et al.* 2016). Cyclic electron transfer around PSI seems to be elevated in *psbo1* (Allahverdiyeva *et al.* 2009). The level of plastid terminal oxidase (PTOX), involved in chlororespiration, is increased in *psbo1* (Allahverdiyeva *et al.* 2009; Suorsa *et al.* 2016).

Reversible phosphorylation of PSII proteins and LHCII has an influence on PSII-LHCII supercomplex stability, PSII repair process and balancing excitation between PSII and PSI (state transitions, Järvi *et al.* 2015; Rantala *et al.* 2020). Suorsa *et al.* (2016) reported that state transitions, the redistribution of LHCII complexes and thus energy between PSII and PSI, are impaired in *psbo1*. They also showed that there are different phosphorylation patterns of PSII core subunits and LHCII under various light conditions in *psbo1* compared to WT. Lundin *et al.* (2007a) also showed different phosphorylation levels of PSII core subunits in *psbo1*, however, it is difficult to compare the levels of phosphorylated subunits when the data shown in the publication are not corrected for the amount of PSII subunits (both with and without phosphorylation). The difference in phosphorylation patterns can be connected to changes in levels of phosphatases required for LHCII and PSII dephosphorylation. While the level of TAP38/PPH1, dephosphorylating LHCII, is decreased in *psbo1* compared to WT, the level of PBCP, dephosphorylating PSII core subunits, is increased in *psbo1*. The levels of kinases STN7 and STN8 are similar in *psbo1* and WT (Suorsa *et al.* 2016).

Interestingly, the PSII defects are not exacerbated under high light (HL) conditions, but the difference from WT is rather diminished. After long-term HL, leaf weight, proportion of open PSII centres (*qP*) and maximum quantum yield of PSII (F_V/F_M) of *psbo1* become closer to values for WT (Lundin *et al.* 2007a; Allahverdiyeva *et al.* 2009). The high F_O value of chlorophyll fluorescence of *psbo1* becomes lower in HL-grown plants, which is in contrast to WT, where HL treatment causes increase in F_O. Similar is reaction of F_O to short-term (3 h) HL (Allahverdiyeva *et al.* 2009). As Allahverdiyeva *et al.* (2009) point out, this suggests that *psbo1* mutant has reduced PQ-pool at growth light (GL) conditions, whereas exposure to HL results in more oxidised PQ-pool.

The decrease of F_V/F_M after short-term HL and subsequent recovery is similar in WT and *psbo1*. Only after HL treatment in presence of lincomycin, the decrease of F_V/F_M was much stronger in *psbo1* compared to WT. Lincomycin is an inhibitor of chloroplast protein synthesis, thus inhibiting also PSII repair. This result suggests that PSII in *psbo1* is more prone to photodamage compared to WT (Allahverdiyeva *et al.* 2009).

Lundin *et al.* (2008) analysed levels of various types of PSII complexes (supercomplexes, PSII dimers, PSI monomers etc.) under GL and long-term HL. However, the results presented in table and several figures seems to be discrepant and thus it is only possible to conclude that the relative proportion of PSII monomer and CP43-less monomer increases upon HL in *psbo1* and probably also in WT, while the relative proportion of PSII-LHCII supercomplexes and PSII dimers decreases.

1.2.4.2.2 Mutant *psbo2*

The *psbo2* mutant, lacking PsbO2 protein and producing only PsbO1 protein, is described in two different ways in available literature. While Lundin *et al.* (2007a, 2008) describes the phenotype of the *psbo2* mutant and also many measured characteristics to be markedly different from WT, subsequent publications (Allahverdiyeva *et al.* 2009; Suorsa *et al.* 2016) describe the mutant to be practically indistinguishable from WT, both in terms of phenotype and measured characteristics.

According to Lundin *et al.* (2007a), the *psbo2* mutant grew faster than *psbo1* but slower than WT. The leaves of *psbo2* were dark green, more elongated and with bent edges. The level of PsbO1 protein in *psbo2* was about 125% of the total PsbO level in WT. Correspondingly, the amount of PSII subunits increased to about 138%, while the levels of PSI and ATP synthase were similar to WT. The leaves of *psbo2* were described to contain more thylakoids and PSII-LHCII supercomplexes. The oxygen evolution of thylakoids isolated from *psbo2* was higher (145%) compared to WT, due to the higher content of PSII. The maximum quantum yield of PSII (F_V/F_M) was similar in *psbo2* and WT (Lundin *et al.* 2007a).

Lundin *et al.* (2007a) also reported that the *psbo2* mutant had problems during long-term HL. They state that after 15 days under HL (1000 μmol photons m^{-2} s^{-1}), the leaf weight of *psbo2* was markedly reduced, while after 28 days, the leaves were completely withered.[3] The authors show that during short-term HL, the F_V/F_M values and the amount of D1 protein decline faster in presence of lincomycin in *psbo1* and WT. In *psbo2*, there was almost no difference between samples with and without lincomycin, suggesting that the repair of PSII is impaired in the *psbo2* mutant. They also showed that *in vitro* D1 dephosphorylation was impaired in *psbo2* (Lundin *et al.* 2007a).

In the subsequent publication, Lundin *et al.* (2008) showed that there is higher proportion of PSII-LHCII supercomplexes among other types of PSII complexes in *psbo2* compared to WT. However, upon HL, the relative proportion of PSII-LHCII supercomplexes and PSII dimers decreased more than in WT and the proportion of CP43-less PSII monomers increased (Lundin *et al.* 2008).

In contrast to the results described above, Allahverdiyeva *et al.* (2009) did not find any difference in the function of PSII in *psbo2* mutant and WT or in the phenotype of the plants. The flash-induced fluorescence yield and its subsequent relaxation in darkness, thermoluminescence characteristics, EPR spectra, oxygen evolution of thylakoid membranes, NPQ induction and $P700^+$ re-reduction in darkness all showed differences between *psbo1* and WT, but no significant differences between *psbo2* and WT. Also the F_V/F_M values and their reaction to long-term HL, short-term HL or short-term HL in the presence of lincomycin were similar in *psbo2* and WT. These results do not support the hypothesis that the PSII repair is impaired in the *psbo2* mutant.

Similar results were obtained by Suorsa *et al.* (2016), who did not observe any differences between *psbo2* and WT in phenotype or growth rate. Also levels of leaf pigments, levels of various types of PSII complex, state transitions, quantum yield and various other characteristics measured by chlorophyll a fluorescence were not significantly different between *psbo2* and WT. The only small difference was in the level of several proteins and in phosphorylation of PSII subunits and LHCII. The level of PsbO1 protein was reported to be only 47% of the total PsbO level in WT[4] and the level of PsbP was decreased

[3] Unfortunately, the documentation of this experiment by Lundin *et al.* (2007a) is very poor. It is not clear if fresh or dry weight of leaves was measured, if all the leaves of plants were measured and if the given number of measurements is for leaves or plants. There is no documentation for the state of the plants after 28 days of HL, it is only described in the text.

[4] Such a low level of PsbO in *psbo2* mutant seems to be unlikely without any effect on PSII and phenotype of the mutant, as shown by Dwyer *et al.* (2012) and by us in the Chapter 4.3. Because also the other mutants were reported by Suorsa *et al.* (2016) to have very low amount of PsbO (only 17% of WT levels for *psbo1*), there was probably some problem with the quantification of PsbO in this publication.

similarly. However, the amount of other PSII subunits, including PsbQ, was unaffected, as well as levels of PSI subunits, cytochrome b_6f subunits, ATP synthase subunit and other investigated proteins. Interestingly, there were some differences between *psbo2* and WT in phosphorylation patterns of PSII core subunits and LHCII under various light conditions. The levels of phosphorylated D1 and D2 subunits were higher in *psbo2* after dark treatment and levels of phosphorylated CP43 and LHCII were higher under PSI-favouring light (Suorsa *et al.* 2016).

It is not clear why the results on *psbo2* mutant are so discrepant. Lundin *et al.* (2007a, 2008) and Allahverdiyeva *et al.* (2009) used the same T-DNA insertion mutant line (SALK_024720). Suorsa *et al.* (2016) used transposon insertion mutant line (CSHL_ET9214), but they state that there were no differences from the previously described mutant line (SALK_024720). The main difference in cultivation conditions is that Lundin *et al.* (2007a, 2008) used hydroponic cultivation, while cultivation in soil was used in the subsequent publications (Allahverdiyeva *et al.* 2009; Suorsa *et al.* 2016). The possibility that hydroponic cultivation caused so strong manifestation of otherwise veiled phenotype of *psbo2* mutation prompts for further investigation.

1.2.4.2.3 Similarity between plants with reduced level of PsbO and *psbo1* mutant

Interestingly, the *psbo1* mutants of *A. thaliana* show many features similar to plants with suppressed expression of both *psbO* genes by RNA interference (RNAi). Yi *et al.* (2005) used RNAi construct silencing mainly *psbO2*, while Dwyer *et al.* (2012) used construct silencing mainly *psbO1*. Both of the constructs affected levels of both isoforms, however, the PsbO1/PsbO2 ratio was changed to different directions. Nevertheless, the results were similar. Plants with low PsbO levels grew more slowly than WT and their leaves were pale green (Yi *et al.* 2005; Dwyer *et al.* 2012). Their leaves were also thinner and chloroplasts contained less thylakoid layers per granum (Dwyer *et al.* 2012).

The decrease of the amount of PsbO led to a reduction of other PSII subunits (Yi *et al.* 2005; Dwyer *et al.* 2012), resulting in lower amount of functional PSII centres (Dwyer *et al.* 2012). PSI content also decreased, but not as much as PSII. The levels of LHCII, cytochrome b_6f, ATP synthase and ribulose-1,5-bisphosphate carboxylase-oxygenase (rubisco) were not affected (Yi *et al.* 2005; Dwyer *et al.* 2012).

The chlorophyll fluorescence characteristics of plants with decreased amount of PsbO also resembled *psbo1* mutant. The reduction of PsbO led to an increase of F_O value and concomitant decrease of F_V/F_M, the maximum quantum yield of PSII (Yi *et al.* 2005; Dwyer *et al.* 2012). Also the quantum yield for oxygen evolution was lower in such plants, while maximum rates of oxygen evolution measured under saturating irradiances were independent of PsbO content. Similarly, the PSII photochemical efficiency measured from

chlorophyll fluorescence (Φ_{PSII}) was lower in low PsbO plants at low irradiance, but at saturating irradiances there were no differences (Dwyer *et al.* 2012). The NPQ was higher in low PsbO plants than in WT at lower irradiances, while it got lower under higher irradiances (Dwyer *et al.* 2012), again resembling the *psbo1* mutant (Suorsa *et al.* 2016).

The high similarity between the *psbo1* mutant and the plants with decreased amount of both PsbO isoforms suggests that the phenotype of the *psbo1* is caused mainly by the decrease of the total level of PsbO and not by the absence of PsbO1. In line with this hypothesis is an observation that plants devoid of PsbO2 and heterozygous at the *psbO1* locus (*psbo2 psbO1/psbo1*) showed phenotype intermediate between *psbo1* and WT (Suorsa *et al.* 2016).

2 Aims of the thesis

My research of PsbO started with the finding that potato (*Solanum tuberosum*) mutant with enhanced formation of tubers lacks one isoform of PsbO (Fischer *et al.* 2008). It was also known that *Arabidopsis thaliana* has two isoforms that differ in their functions, as published by Lundin *et al.* (2007a, 2008). Since basic sequence comparison of PsbO isoforms from these two species surprisingly suggested that they evolved independently, the first aim of my thesis was to investigate in detail the evolution of PsbO in plants with focus on the origin of isoforms and differences in their sequences. The obtained results together with many gaps that we found in the knowledge about the function of PsbO isoforms in *A. thaliana* (partly connected with serious doubts about the reliability of results presented by Lundin and his co-workers), resulted in the main aim of this thesis to unravel auxiliary functions of PsbO and functional differences between PsbO isoforms.

The particular aims covered in this thesis were:

- To investigate evolution of PsbO in plants with focus on the origin of the isoforms.
- To compare properties of isolated PsbO isoforms from higher plants and PsbO from algae.
- To test a hypothesis that PsbO changes its conformation depending on pH in physiologically relevant range.
- To find the extent to which the phenotype of *psbo1* mutant of *A. thaliana* is caused by decreased level of PsbO and the extent to which it is caused by the absence of PsbO1 isoform.
- To investigate changes in the proteome of *A. thaliana* induced by decreased level of PsbO and by presence of only one PsbO isoform.

3 Materials and methods

3.1 Plant material, genotyping and sequencing of T-DNA insertion site

Seeds of *A. thaliana* WT plants (Col-0, N60000), *psbo1* (SALK_093396C, N682662) and *psbo2* (SALK_024720C, N658148) were obtained from Nottingham Arabidopsis Stock Centre. The mutants were checked for homozygous insertion of T-DNA by PCR. The primers used for WT allele were 5‘-GGCCCATTAGCTCAGTTGGT-3‘ and 5‘-ACTCTGGAGGAGCGTTCTTG-3‘ (*psbo1*) or 5‘-TCACACCCTACTTGAATTCACCT-3‘ and 5‘-TTCGAGCCCACTTCCTTCAC-3‘ (*psbo2*). For mutant alleles, we used primer for the left border of T-DNA (5‘-CTTGCTGCAACTCTCTCAGG-3‘) and either 5‘-GGCCCATTAGCTCAGTTGGT-3‘ (*psbo1*) or 5‘-TTCGAGCCCACTTCCTTCAC-3‘ (*psbo2*). The same primers were used for genotyping of the F2 generation of crosses. For mapping of T-DNA insertion sites, we used the same primers as for the mutant alleles of *psbo1* and *psbo2* and also primer 5‘-ATTGGTTTAGGTGTTCTCAAGTGC-3‘ with the primer for the left border of T-DNA (5‘-CTTGCTGCAACTCTCTCAGG-3‘) to amplify the other end of the T-DNA insertion in *psbo1* mutant. Similar PCR with the primer for the right border of the T-DNA (5‘-GAGCTCGAAACGATCCAGATCCGGTG-3‘) gave no product. We failed to amplify the other end of the T-DNA insertion in *psbo2* mutant. The obtained PCR products were sequenced using the primer for the left border of T-DNA (5‘-CTTGCTGCAACTCTCTCAGG-3‘).

3.2 Growth conditions

Seeds were stratified in water at 4 °C for several days. After sowing, the pellets were placed directly to the particular light conditions. Plants were grown in Jiffy peat pellets, periodically watered with solution of Kristalon Start fertilizer (Agro CS), under 8-hour photoperiod and day/night temperature 23/18 °C. The intensity of growth light (GL) was around 125 µmol photons m^{-2} s^{-1} (PAR, 109–135 µmol photons m^{-2} s^{-1} throughout the cultivation area) and was provided by white LEDs supplemented with far red LEDs. The high light (HL) intensity was around 850 µmol photons m^{-2} s^{-1} (PAR, 688–933 µmol photons m^{-2} s^{-1} throughout the cultivation area) and was provided by LumiGrow Pro 325 lights with red and blue LEDs supplemented with white LEDs of lower intensity.

3.3 Fluorescence imaging

Before measurement, plants were dark adapted for at least 30 minutes. Fluorescence of chlorophyll a imaging was performed with FluorCam (Photon Systems Instruments, Czech Republic) with blue measuring light and white saturation flashes of 1 s duration and intensity 3700 µmol photons m^{-2} s^{-1}. NPQ induction was measured under blue actinic light of intensity 79 µmol photons m^{-2} s^{-1}. NPQ was calculated as $(F_M - F_M‘)/F_M‘$. Directly after NPQ

induction measurement, giving 4 minutes of acclimation to blue light of intensity 79 μmol photons m^{-2} s^{-1}, rapid light curves (RLC) were measured by stepwise increases in white light intensity from 74 μmol photons m^{-2} s^{-1} to 1893 μmol photons m^{-2} s^{-1} in 30s steps. Relative electron transport rate (rETR) was calculated as PAR × $(F_M - F_t)/F_M$. Initial slope of the RLC (α) and maximum relative electron transport rate ($rETR_{max}$) were calculated according to Ralph & Gademann (2005). The curves were fitted using *nls* function implemented in R according to Ralph & Gademann (2005), using only growing part of the curve and simplified version of equation without photoinhibition (β = 0). The rosette area was measured as the top view of photosynthetic area as measured by FluorCam. The statistical analyses were performed in R v. 3.5.3 using ANOVA with Tukey's HSD post-hoc test ($p < 0.05$).

3.4 Western blotting

Proteins were isolated from leaves according to Martínez-García *et al.* (1999). Samples in the loading buffer were denatured by incubation in 95 °C for 5 min and 30 μg of proteins was loaded on 10% SDS-PAGE gel and subjected to electrophoresis. Proteins were transferred to polyvinylidene difluoride (PVDF) membrane (Serva Fluorobind) and immunodecorated with Anti-PsbO1 (AS14 2824) and Anti-PsbO2 (AS14 2825) antibodies obtained from Agrisera (Vännäs, Sweden). Secondary antibody conjugated with horseradish peroxidase (ADI-SAB-300) was obtained from Enzo Life Sciences and visualised using Pierce ECL Western Blotting Substrate (Thermo Sientific).

3.5 Proteome analysis

3.5.1 Plant material

Three biological replicates for each genotype were analysed, samples consisted of one plant (WT) or two plants (*psbo1* and *psbo1*psbo2*, because of their smaller size). 49 days old plants grown under GL conditions were used. Whole rosettes (without roots) were carefully homogenised in liquid nitrogen to avoid any bias caused by differences between young and old leaves. An aliquot of the resulting powder was used for protein isolation.

3.5.2 Protein isolation and digestion[5]

Plant material was lysed by boiling at 95°C for 10 min in 100mM TEAB (triethylammonium bicarbonate) containing 2% SDC (sodium deoxycholate), 40mM chloroacetamide, 10mM TCEP (Tris(2-carboxyethyl)phosphine) and further sonicated (Bandelin Sonoplus Mini 20, MS 1.5). Protein concentration was determined using BCA

[5] This text was provided by Laboratory of Mass Spectrometry at Biocev research centre, which performed the described method.

protein assay kit (Thermo) and 30 µg of protein per sample was used for MS sample preparation.

Samples were further processed using SP3 beads according to Hughes *et al.* (2019). Briefly, 5 µl of SP3 beads was added to 30 µg of protein in lysis buffer and filled to 50 µl with 100mM TEAB. Protein binding was induced by addition of ethanol to 60% (vol./vol.) final concentration. Samples were mixed and incubated for 5 min at RT. After binding, the tubes were placed into magnetic rack and the unbound supernatant was discarded. Beads were subsequently washed two times with 180 µl of 80% ethanol. After washing, samples were digested with trypsine (trypsin/protein ratio 1/30) reconstituted in 100mM TEAB at 37 °C overnight. After digestion, samples were acidified with TFA to 1% final concentration and peptides were desalted using in-house made stage tips packed with C18 disks (Empore) according to Rappsilber *et al.* (2007).

3.5.3 nLC-MS/MS Analysis[6]

Nano reversed phase columns (EASY-Spray column, 50 cm x 75 µm ID, PepMap C18, 2 µm particles, 100 Å pore size) were used for LC-MS analysis. Mobile phase buffer A was composed of water and 0.1% formic acid . Mobile phase B was composed of acetonitrile and 0.1% formic acid. Samples were loaded onto the trap column (C18 PepMap100, 5 µm particle size, 300 µm x 5 mm, Thermo Scientific) for 4 min at 18 µl/min. Loading buffer was composed of water, 2% acetonitrile and 0.1% trifluoroacetic acid . Peptides were eluted with Mobile phase B gradient from 4% to 35% B in 120 min. Eluting peptide cations were converted to gas-phase ions by electrospray ionization and analyzed on a Thermo Orbitrap Fusion (Q-OT-qIT, Thermo Scientific). Survey scans of peptide precursors from 350 to 1400 m/z were performed in orbitrap at 120K resolution (at 200 m/z) with a 5×10^5 ion count target. Tandem MS was performed by isolation at 1,5 Th with the quadrupole, HCD fragmentation with normalized collision energy of 30, and rapid scan MS analysis in the ion trap. The MS2 ion count target was set to 10^4 and the max injection time was 35 ms. Only those precursors with charge state 2–6 were sampled for MS2. The dynamic exclusion duration was set to 30 s with a 10 ppm tolerance around the selected precursor and its isotopes. Monoisotopic precursor selection was turned on. The instrument was run in top speed mode with 2 s cycles (Hebert *et al.* 2014).

3.5.4 Label-free quantification[6]

All data were analyzed and quantified with the MaxQuant software version 2.0.2.0 (Cox & Mann 2008). The false discovery rate (FDR) was set to 1% for both proteins and peptides

[6] This text was provided by Laboratory of Mass Spectrometry at Biocev research centre, which performed the described method.

and we specified a minimum peptide length of seven amino acids. The Andromeda search engine was used for the MS/MS spectra search against the *A. thaliana* protein database (Araport11 genome release, version from 2021-03-08, downloaded from https://www.arabidopsis.org, containing 48 359 entries). Enzyme specificity was set as C-terminal to Arg and Lys, also allowing cleavage at proline bonds and a maximum of two missed cleavages. Dithiomethylation of cysteine was selected as fixed modification and N-terminal protein acetylation and methionine oxidation as variable modifications. The "match between runs" feature of MaxQuant was used to transfer identifications to other LC-MS/MS runs based on their masses and retention time (maximum deviation 0.7 min) and this was also used in quantification experiments. Quantifications were performed with the label-free algorithm in MaxQuant (Cox *et al.* 2014).

3.5.5 Data analysis

Data were further processed using R v. 3.5.3. Quantification results in the form of LFQ intensities, as generated by MaxQuant, were first filtered from the proteins assigned by MaxQuant as contaminants, reverse hits or "only identified by site". Second, only proteins quantified in at least two replicates in at least one genotype were retained, giving the final set of 3030 proteins (or "protein groups", as called in MaxQuant). Binary logarithm of the LFQ intensities was calculated and used in all further calculations. Normalisation of replicates was performed by normalising the third quartile of the log-LFQ intensities of proteins that were quantified in all samples. We checked that the normalisation is proper by observation that the levels of nuclear proteins were not changed in average between genotypes (Fig. 4.11).

Annotations were obtained from UniProt, downloaded on 2021-10-15 for the reference proteome of *A. thaliana* (https://www.uniprot.org/uniprot/?query=proteome%3Aup000006548). AtSubP prediction of subcellular localisation of proteins (Kaundal *et al.* 2010) was downloaded from https://www.arabidopsis.org/download_files/Genes/Araport11_genome_release/Araport11-Subcellular_Predictions (version 2020-02-20).

Categorisation of thylakoid proteins in complexes and functional groups was based on Flannery *et al*. (2021), supplemented with information from other publications (Ifuku *et al.* 2011; Järvi *et al.* 2013, 2015; Shikanai 2016; Rantala *et al.* 2020) and photosynthetic proteins from KEGG database (https://www.genome.jp/brite/ath00194).

For the analysis of changes in the levels of protein categories, the mean of $\log_2$(fold change) for each comparison of genotypes was first normalised to zero. The statistical significance of the difference of the mean of each category from zero was calculated through randomisations and corrected by Benjamini-Hochberg FDR ($q < 0.05$).

The results were further processed using Perseus v. 1.6.15.0 (Tyanova *et al.* 2016). Proteins with significantly different levels between genotypes were identified by one-way ANOVA ($q < 0.05$, permutation-based FDR) with Tukey's HSD post-hoc test ($q < 0.05$). For principal component analysis (PCA), the missing values were replaced from normal distribution (width 0.3, down shift 1.8). Gene ontology (GO) enrichment analysis was done using Fischer exact test (with Benjamini-Hochberg FDR, $q < 0.05$) with frequencies in the whole set of 3030 proteins used as baseline.

4 Results

4.1 Parallel subfunctionalisation of PsbO protein isoforms in angiosperms revealed by phylogenetic analysis and mapping of sequence variability onto protein structure (PUBLICATION 1)

Duchoslav M., Fischer L. (**2015**) Parallel subfunctionalisation of PsbO protein isoforms in angiosperms revealed by phylogenetic analysis and mapping of sequence variability onto protein structure. *BMC Plant Biology* **15**: 133. DOI: https://doi.org/10.1186/s12870-015-0523-4

These published results, referred as PUBLICATION 1 in the thesis, can be found in Attachment.

Summary: In this publication, we present analysis of expressed *psbO* sequences from 49 land plant species. We found that many species express two *psbO* paralogs. Interestingly, phylogenetic analysis revealed that *psbO* duplication occurred many times independently, generally at the roots of modern angiosperm families. Moreover, mapping of the differences on the protein tertiary structure showed that the isoforms in individual species differ from each other on similar positions, mostly on the luminally exposed end of the β-barrel and on β1-β2 loop. We suggest that similar subfunctionalisation of PsbO isoforms occurred parallelly in various lineages.

My contribution: I performed all of the *in silico* analyses and I significantly contributed to the study design and results interpretation. I wrote most parts of the manuscript.

4.2 Dynamic pH-induced conformational changes of the PsbO protein in the fluctuating acidity of the thylakoid lumen (PUBLICATION 2)

Carius A.B., Rogne P., Duchoslav M., Wolf-Watz M., Samuelsson G., Shutova T. (**2019**) Dynamic pH-induced conformational changes of the PsbO protein in the fluctuating acidity of the thylakoid lumen. *Physiologia Plantarum* **166**: 288–299. DOI: https://doi.org/10.1111/ppl.12948

These published results, referred as PUBLICATION 2 in the thesis, can be found in Attachment.

Summary: In this publication, we investigated PsbO proteins from green alga *Chlamydomonas reinhardtii* (WT version and truncated version ΔS145K187 without large flexible domain, β5-β6 loop) and higher plant *Solanum tuberosum* (StPsbO1 and StPsbO2 isoforms). The proteins were expressed in bacteria, purified and studied *in vitro*. CD (circular dichroism) spectra of the proteins showed that all of them had very similar secondary structure. However, the small differences between CD spectrum of StPsbO1 and StPsbO2 show that their conformation is not completely identical. The intrinsic fluorescence spectra, originating mainly from single tryptophan residue in PsbO, show again overall similarity of PsbO from higher plants and from algae, but small differences between StPsbO1 and StPsbO2. Titration experiments using the hydrophobic fluorescence probe ANS revealed that PsbO proteins exhibit acid–base hysteresis. He hypothesised that the pH-dependent dynamic behaviour at physiological pH ranges is a common feature of PsbO proteins and causes reversible conformational changes of their β-barrel domain in response to the fluctuating acidity of the thylakoid lumen.

My contribution: I performed all of the experiments with StPsbO1 and StPsbO2 proteins from *Solanum tuberosum* (preparation of constructs, expression in bacteria, purification, measurement of CD spectra). I measured the intrinsic fluorescence spectra of StPsbO1 and StPsbO2 with assistance of Radovan Fišer. I participated in the writing of the manuscript.

4.3 Functional differences between PsbO1 and PsbO2 proteins of *Arabidopsis thaliana* are smaller than anticipated (unpublished results)

This part of the thesis, consisting of unpublished results, will be submitted as a manuscript in near future.

My contribution: I performed all of the experiments and measurements of chlorophyll a fluorescence. Ondřej Nykles, student under my supervision, provided partial technical assistance with sowing and harvesting of the plants. Proteome analysis (protein isolation, nLC-MS/MS analysis and initial processing in MaxQuant software) was performed by Laboratory of Mass Spectrometry at Biocev research centre (Faculty of Science, Charles University). I performed all of the analyses of the results. I designed the study and interpreted the results together with my supervisor.

4.3.1 Isolation of *psbo1*psbo2* double mutant with partially restored expression of *psbO1*

The *psbo2* mutant of *A. thaliana* is very similar to WT plants (Allahverdiyeva *et al.* 2009; Suorsa *et al.* 2016). In order to be able to observe subtle changes in the phenotype of the *psbo2* and also *psbo1* mutant, we crossed these mutants to obtain WT plants (in the F2 generation) that would be genetically and epigenetically very similar to *psbo* mutants. As the *psbo1psbo2* double mutant was reported to be seedling lethal (Suorsa *et al.* 2016) and the plants with a strongly silenced expression of *psbO* genes were unable to grow photoautotrophically (Yi *et al.* 2005), we did not expect to find any double mutants in the F2 generation, which we grew photoautotrophically in the soil. Unexpectedly, genotyping of the F2 population revealed 2 plants out of 31 to be homozygous mutants in both *psbO1* and *psbO2* genes. The obtained proportion of *psbo1psbo2* double mutants (2/31) is very close to the theoretical proportion of 1/16 that would be expected if the *psbo1psbo2* double mutant was not seedling lethal and was able to grow photoautotrophically in the soil. This unexpected result led us to a more detailed investigation of these plants.

The phenotype of the *psbo1psbo2* plants was similar to the phenotype of the *psbo1* mutant, showing retarded growth and pale green leaves (Fig. 4.1). As the previous reports show that plants are not able to grow photoautotrophically without PsbO (Yi *et al.* 2005; Suorsa *et al.* 2016), we expected that the expression of at least one of the *psbO* genes had to be restored. Immunoblots with specific anti-PsbO1 and anti-PsbO2 antibodies showed that the *psbo1psbo2* plants contained the PsbO1 protein, but not the PsbO2 protein (Fig. 4.2). Thus, it was evident that the expression of the *psbO1* gene with T-DNA insertion was somehow restored during the crossing of *psbo1* and *psbo2*, so we designated the resulting double mutant as *psbo1*psbo2*.

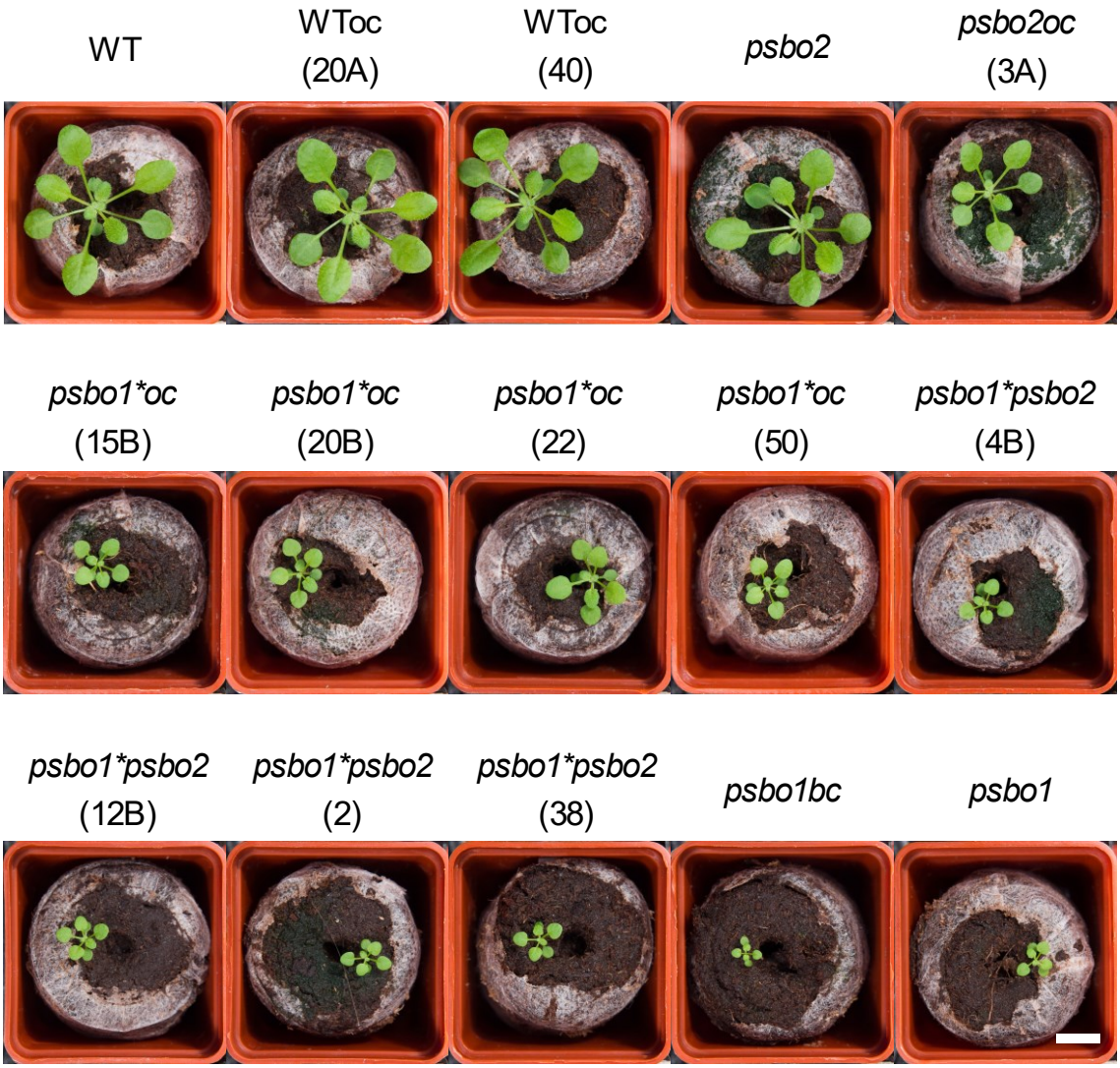

Fig. 4.1: Phenotypes of WT, *psbo2*, *psbo1* and progeny of their crosses. WToc were plants with WT genotype, *psbo2oc* were plants with *psbo2* genotype, *psbo1*oc* were plants with *psbo1* genotype and partially restored expression of *psbO1* gene and *psbo1*psbo2* were plants with *psbo1psbo2* genotype and partially restored expression of *psbO1* gene. The particular line, resulting from single genotyped plant in the F2 generation, is given in parenthesis. The lines 20A, 3A, 15B, 20B, 4B and 20B are from the cross *psbo2*×*psbo1*, while the lines 40, 22, 50, 2 and 38 are from the reciprocal cross *psbo1*×*psbo2*. The *psbo1bc* was a plant with a *psbo1* genotype from the back-cross WT×*psbo1*. The plants were 26 days old and of the F3 generation, with exception of *psbo1bc*, which was of the F2 generation. The scale bar is 10 mm long.

On the immunoblots, faint bands were visible also for PsbO1 in the *psbo1* mutant and for PsbO2 in the *psbo2* mutant. It is not clear at this time whether there is very low expression of mutant alleles also in the original *psbo1* and *psbo2* mutants, or whether the anti-PsbO1 and anti-PsbO2 antibodies have a low level of cross-reactivity with the other PsbO isoform (the mature PsbO1 and PsbO2 proteins differ in only 11 amino acid residues).

We investigated also single homozygous mutants from the F2 generation of the *psbo2*×*psbo1* cross (referred to as **o**ut-**c**rossed mutants *psbo1oc* and *psbo2oc*). The *psbo2oc* plants were similar to *psbo2* and WT. However, the *psbo1oc* plants showed intermediate

phenotype between *psbo1* and WT (Fig. 4.1 and Fig. 4.3), suggesting that the expression of *psbO1* was partially restored also in these plants. Thus, we named these plants *psbo1*oc*.

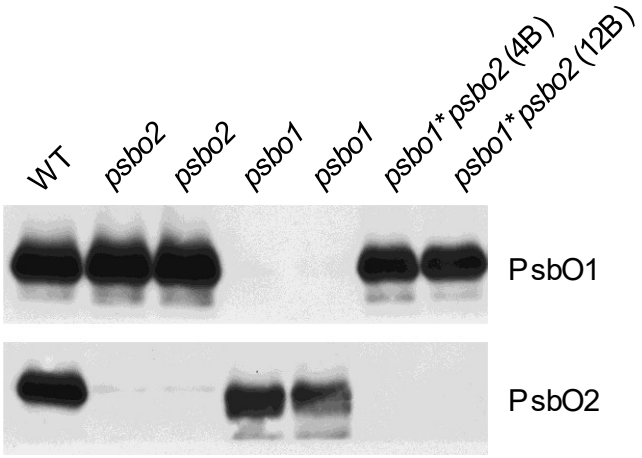

Fig. 4.2: Immunoblot analysis of proteins isolated from leaves of WT and mutant plants. Identical samples isolated from *psbo1* and *psbo2* were run in two adjacent lanes. The samples from *psbo1*psbo2* double mutants were from two plants (4B and 12B) from F2 generation. The plants were 115 days old. Proteins in amount of 30 µg were loaded in each lane.

In order to verify that the crossing of *psbo1* with *psbo2* caused the restoration of *psbO1* expression, we made also a reciprocal cross (*psbo1*×*psbo2*) and a back-cross to WT (WT×*psbo1*). The result of the reciprocal cross (*psbo1*×*psbo2*) was the same as of the *psbo2*×*psbo1* cross. In the F2 generation we found several *psbo1*psbo2* double mutants with a fenotype similar to that of the *psbo1* mutant. All *psbo1*oc* mutants found by genotyping had a phenotype intermediate between that of *psbo1* and WT, suggesting that the partial restoration of *psbO1* expression had already happened in the F1 generation regardless of the crossing direction and was retained in F2.

The back-cross (WT×*psbo1*) yielded F2 progeny where 11 plants out of 40 had *psbo1*-like phenotype (designated as *psbo1bc*) and the rest had WT-like phenotype. No plants with intermediate phenotype were observed, suggesting that the crossing of *psbo1* with WT did not cause restoration of *psbO1* expression.

The phenotypes of the plants with a partially restored *psbO1* expression (*psbo1*psbo2* double mutants and *psbo1*oc* mutants) were stable also in the next generation (F3) after self-pollination. We measured rosette size and maximum quantum yield of PSII (F_V/F_M) in F3 lines derived from several individual plants of the F2 generation originating from both *psbo2*×*psbo1* and *psbo1*×*psbo2* crosses (Fig. 4.3). The F_V/F_M showed the differences between the genotypes better than the rossette area due to lower variance. The values fall clearly into four distinct groups with different levels of F_V/F_M: First group with the lowest F_V/F_M values consiting of *psbo1* and *psbo1bc*, second group of *psbo1*psbo2* double mutant

lines with only slightly higher values, third group of *psbo1*oc* lines with intermediate values and a fourth group with WT-like values consisting of WT, WToc (WT outcrossed from the crosses of *psbo1* and *psbo2*), *psbo2* and *psbo2oc*. The measurement of the rosette area revealed that WToc plants were slightly bigger than the original WT line (Col-0, used for the creation of the SALK T-DNA mutants), while the F_V/F_M values were the same. The higher rosette size may have resulted from some compensatory epigenetic changes that had occurred in the *psbo1* background. For this reason and because of higher variability of WToc than WT, we decided to use the original WT in subsequent analyses.

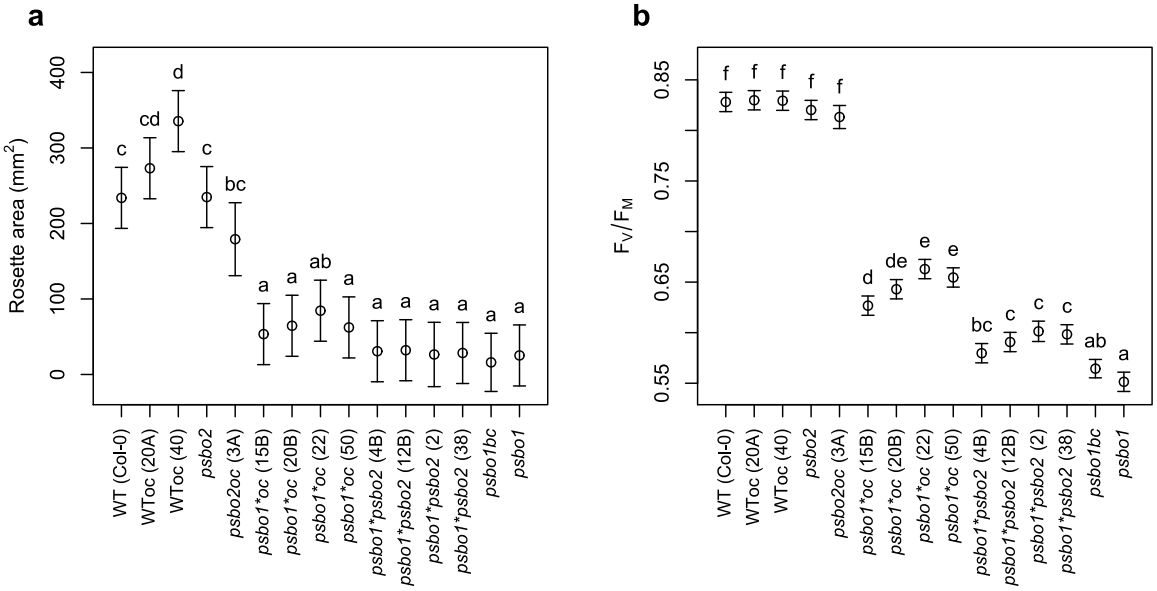

Fig. 4.3: Characteristics of WT, *psbo1*, *psbo2* and progeny of their crosses measured by chlorophyll fluorescence imaging. **a** Rosette area was measured as top view of the photosynthetic area. **b** Maximum quantum yield of PSII (F_V/F_M) of individual plants was measured as the mean value of the projected photosynthetic area of the plant. Individual lines were F3 progeny of single plants from F2 generation with the exception of *psbo1bc*, where F2 plants identified as homozygous mutants in *psbO1* were measured. Plants were 26 days old. Means of 7–11 individual plants and 95% confidence intervals are shown. Significant differences, as identified by Tukey's HSD post-hoc test, are designated by different letters.

4.3.2 Location of T-DNA insertion and possible mechanism of *psbO1* expression restoration

In order to better understand the mechanism of *psbO1* reactivation in the T-DNA mutant line, we mapped the precise position of the T-DNA insertions in both *psbo1* and *psbo2* mutants (Fig. 4.4), confirming previously published positions (Lundin *et al.* 2007a). We found that the T-DNA in *psbo2* mutant is inserted in the last exon (54 bases upstream of the stop codon), excluding a possibility that the full-length PsbO2 protein can be synthesized. In the case that the transcription and translation would happen, the mutant gene might produce PsbO2 protein with the last 19 amino acid residues at C-terminus (GAKVPKDVKIQGVWYGQIE) exchanged for 13 different residues (AVQDILWCKQIDA). However, such protein was not found during proteomic analysis

(Chapter 4.3.3.3). Also, no significant amount of PsbO2 protein was found by immunoblotting (Fig. 4.2), although the specific epitop used for immunization should be present in such protein (Fig. 4.4).

The *psbo1* mutant has the T-DNA insertion in 5‘ untranslated region (UTR) of *psbO* gene, 72 bases upstream of the start codon. Thus, if the transcription and proper translation of the coding region would happen, the mutated *psbO1* gene can produce full-length PsbO1 protein without any changes. PCR amplification and sequencing of the insertion site also revealed that at least part of the T-DNA is present as an inverted repeat, because genomic regions from both sides of the insertion were amplified using the same primer for left border of T-DNA and a primer for right border gave no product.

Although the mechanism of reactivation remains unclear, similar losses of mutant phenotypes by interaction with another T-DNA locus were already described in intronic T-DNA lines (Xue *et al.* 2012; Gao & Zhao 2013; Osabe *et al.* 2017). This phenomenon, called T-DNA suppression, was observed after crossing of SALK T-DNA mutants with other mutants with epigenetically silenced T-DNAs inserted in different loci. High DNA methylation of silenced T-DNA triggers DNA methylation in the second T-DNA locus by canonical RNA-directed DNA methylation pathway in F1 generation after crossing of the mutants. This DNA methylation probably causes heterochromatinisation and allows for unterminated read-through transcription of the whole T-DNA by RNA polymerase II. Subsequently, transcripts containing such copy of T-DNA in the intron can be efficiently spliced and produce native proteins (Osabe *et al.* 2017).

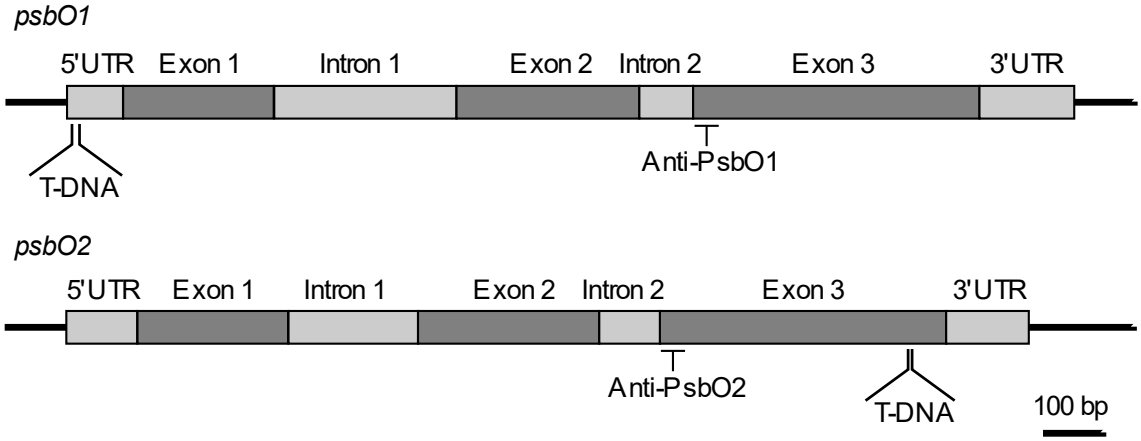

Fig. 4.4: Scheme of *psbO1* and *psbO2* genes. T-DNA insertions in mutant lines *psbo1* (SALK_093396) and *psbo2* (SALK_024720) are marked as T-DNA. Parts of the genes encoding for peptides used for creating of specific antibodies (anti-PsbO1: ASDGSVNFKEEDG, anti-PsbO2: GSDGSVKFKEEDG, Peter Gollan, personal communication) are marked as Anti-PsbO1 and Anti-PsbO2. The size of all elements in the scheme is proportional to their length.

As in the case of *psbo1*psbo2* and *psbo1*oc*, such loss of mutant phenotype (T-DNA suppression) is reproducible and stable in subsequent generations (Osabe *et al.* 2017). Also,

the epigenetic silencing of the T-DNA in *psbo2* mutant can be deduced from inactive kanamycin resistance in the *psbo2* mutant, while the resistance gene was still active in the *psbo1* mutant (Magdalena Metličková, unpublished data). This suggests that the T-DNA from *psbo2* can cause an increase of methylation of the T-DNA in *psbo1*, causing a specific change of its overall epigenetic status and in turn the possibility of weak *psbO1* gene expression.

4.3.3 Characterisation of mutants with various levels of PsbO1 and PsbO2

4.3.3.1 Growth characteristics and maximum quantum yield of PSII (F_V/F_M)

The gaining of *psbo1*psbo2* and *psbo1*oc* mutants provided an opportunity to investigate pallette of plants with various amounts of PsbO1 and PsbO2 proteins. The *psbo2* and *psbo2oc* plants have probably the total levels of PsbO similar to WT, while they only have the PsbO1 protein. The *psbo1*oc* plants have probably the PsbO1 level lower than WT while the PsbO2 level similar as WT or slightly higher. Finally, the *psbo1* and *psbo1*psbo2* plants have the lowest level of total PsbO. The *psbo1* mutants have only the PsbO2 isoforms at level similar to WT or slightly higher. The *psbo1*psbo2* plants have only the PsbO1 isoform in lower amount than WT. For determining the functional differences between PsbO1 and PsbO2, it would be especially valuable to compare phenotypically similar pairs (1) WT with *psbo2* (or *psbo2oc*) that both have the WT phenotype and (2) *psbo1*psbo2* with *psbo1* that both have strongly retarded growth and pale green leaves.

In order to utilise this opportunity, we characterised several plant lines more deeply. First, we compared growth characteristics and basic chlorophyll a fluorescence parameters of the plants. The plants were repeatedly measured during their growth by chlorophyll fluorescence imager, providing non-destructive measurement of rosette area and F_V/F_M value (maximum quantum yield of PSII). The results (Fig. 4.5) show that the growth rate and F_V/F_M values are positively correlated with each other. WT, *psbo2* and *psbo2oc* were the fastest growing genotypes, *psbo1*oc* plants had intermediate growth rates and *psbo1*psbo2* plants grew only slightly faster than the slowest *psbo1* plants.

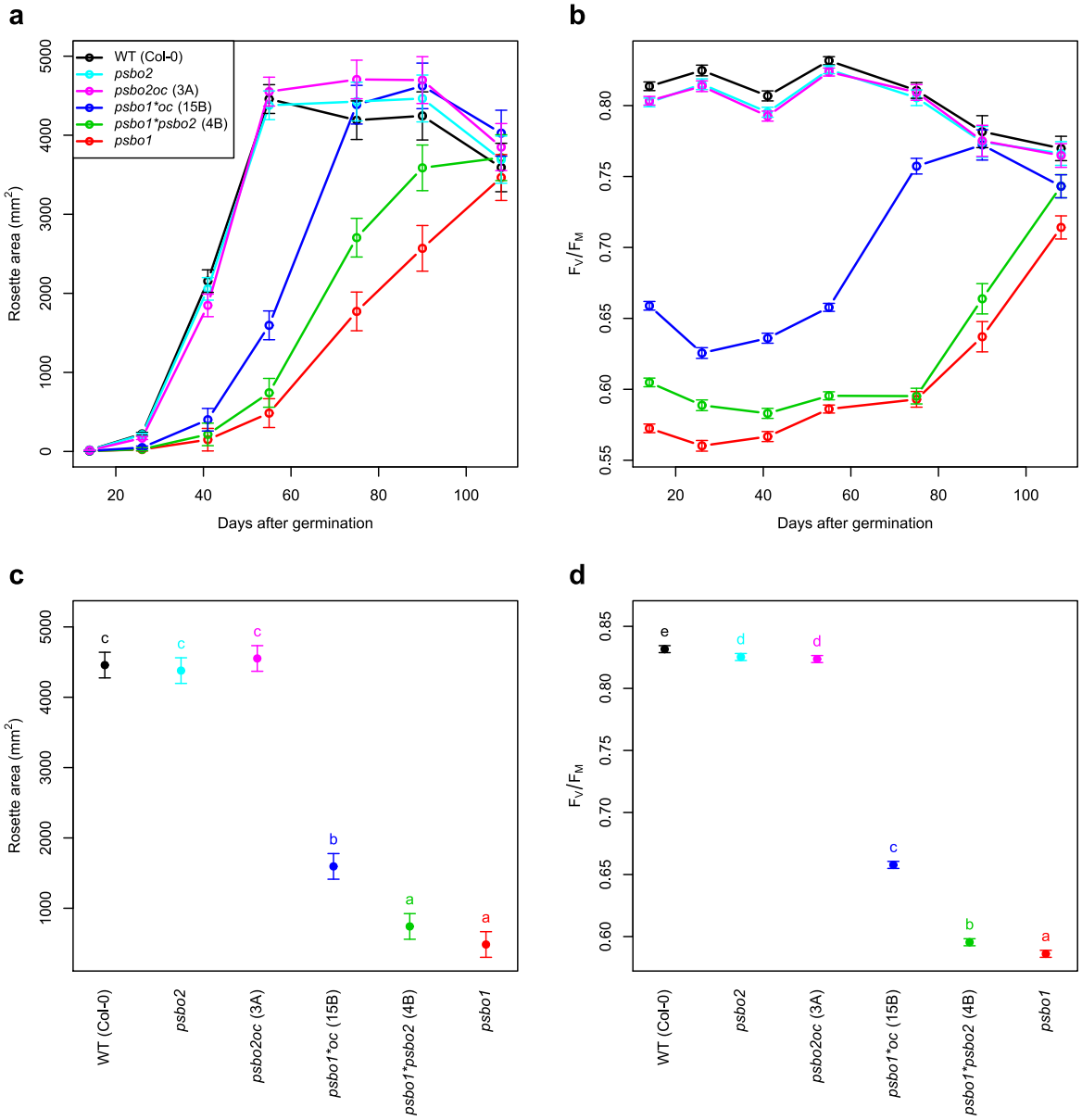

Fig. 4.5: Characteristics of WT, *psbo2*, *psbo2oc* (line 3A), *psbo1*oc* (line 15B), *psbo1*psbo2* (line 4B) and *psbo1* plants measured by chlorophyll fluorescence imaging throughout their growth. **a** Rosette area was measured as top view of photosynthetic area. **b** Maximum quantum yield of PSII (F_V/F_M) of individual plants was measured as mean value of the projected photosynthetic area of the plant. **c, d** Values of rosette area (**c**) and F_V/F_M (**d**) in the fourth time point (55 days) of the plots **a** and **b** depicted to show statistical significance of the differences (Tuckey's HSD post-hoc test, designated by letters). Individual lines (in parenthesis) were F3 progeny of single plants from F2 generation as in Fig. 4.3. Means of 20 individual plants for each genotype (18–20 in the last two time points) and 95% confidence intervals are shown. Note that the difference in F_V/F_M values between WT and *psbo2* with *psbo2oc* was significant in the first four measurements of this experiment, while it was not significant in the experiment presented in Fig. 4.3. This is caused by higher *n* and lower number of lines in this experiment, resulting in higher power of the post-hoc test.

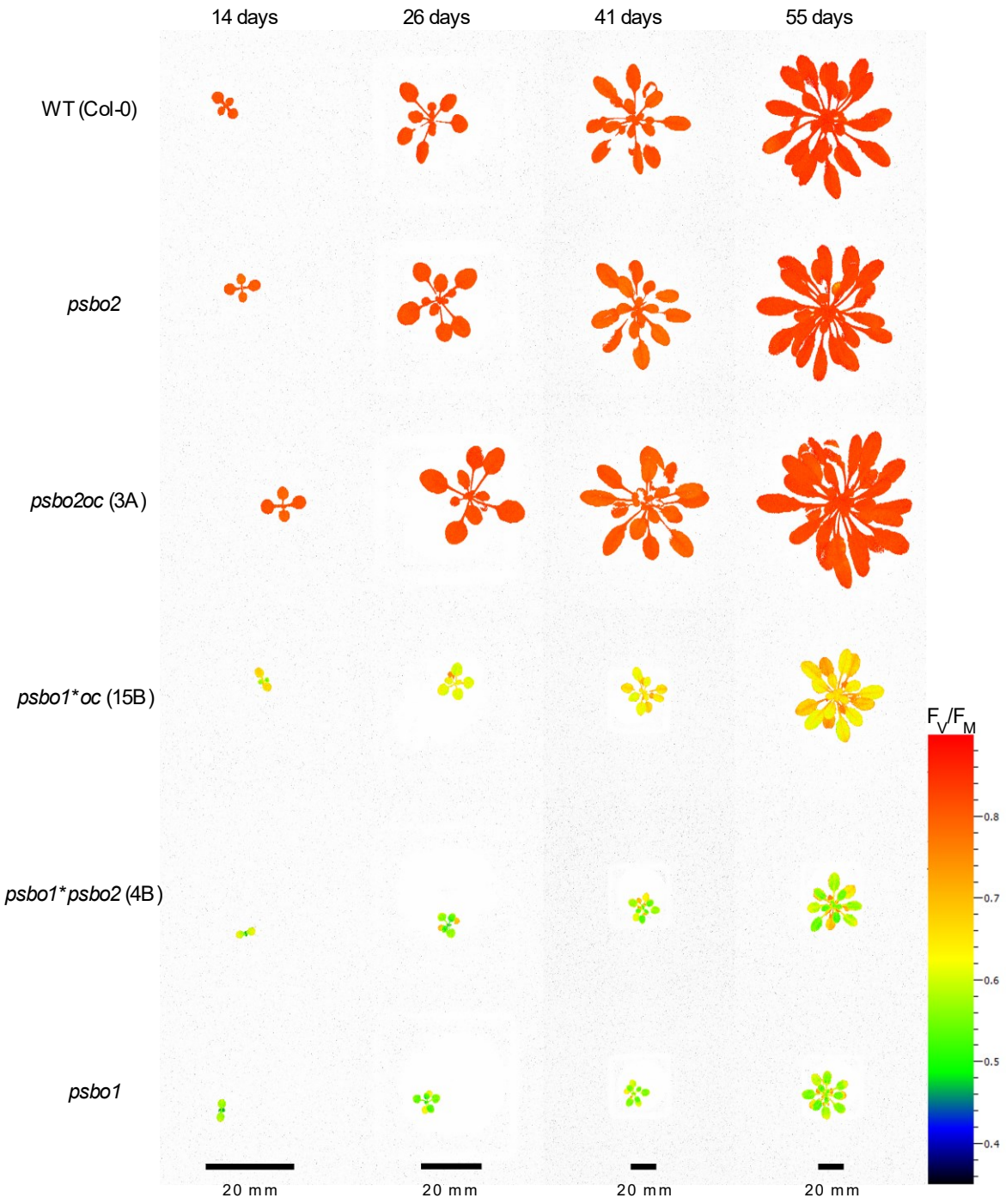

Fig. 4.6: Chlorophyll fluorescence images of WT, *psbo2*, *psbo2oc* (line 3A), *psbo1*oc* (line 15B), *psbo1*psbo2* (line 4B) and *psbo1* plants in several time points. The maximum quantum yield of PSII (F_V/F_M) is shown in false colours. The same individual plants are shown in the different time points. Scale bars, different for each time point, are shown below. The plants are from the same experiment as shown in Fig. 4.5.

The measured F_V/F_M values were somewhat fluctuating during the growth of the plants (Fig. 4.5), possibly because of different temperature on the days of measurement (the plants were cultivated in a growth room with controlled conditions, however, the measurements were done in a room without temperature control). Nevertheless, the F_V/F_M values of *psbo2* and *psbo2oc* were always slightly lower compared to WT. The difference was significant

during the first two months of growth, even it was only 1–2%. The F_V/F_M values of *psbo1*oc* plants were again intermediate, while *psbo1*psbo2* plants had low values, but slightly higher than that of the *psbo1* plants. After three months of growth, senescence caused slight decline of the F_V/F_M values for WT, *psbo2* and *psbo2oc*. In contrary, the F_V/F_M values of *psbo1*oc*, *psbo1*psbo2* and *psbo1* increased during the growth of the plants, as was already observed for *psbo1* mutant (Murakami *et al.* 2005). The senescence of these slowly growing genotypes was delayed, as was bolting under the short-day conditions of the experiment.

The chlorophyll fluorescence imaging allowed us to observe also differences in chlorophyll fluorescence within a plant. We noticed that the mutants with low F_V/F_M values (*psbo1*oc*, *psbo1*psbo2* and *psbo1*) show very low levels of F_V/F_M especially in young leaves, while in older leaves the values were higher (Fig. 4.6). The pattern stayed similar during the growth of the plants. The increase of the F_V/F_M values of whole plants during the growth (Fig. 4.5b) was probably caused by increasing proportion of older leaves visible in the rosette (Fig. 4.6). WT, *psbo2* and *psbo2oc* plants had the F_V/F_M values uniform throughout the whole rosette (Fig. 4.6).

4.3.3.2 Reaction to high light (HL) treatment

Lundin *et al.* (2007a) reported problems of *psbo2* mutant during prolonged high light (HL) conditions and suggested that PsbO2 protein is involved in PSII repair after D1 protein damage. To test whether PsbO1 and PsbO2 proteins differ in their ability to cope with HL and associated increase in PSII turnover, we exposed our set of mutants with various levels of PsbO isoforms to long-term HL conditions.

All of the genotypes tested performed better under HL conditions (850 µmol photons m^{-2} s^{-1}) compared to growth light (GL) conditions (125 µmol photons m^{-2} s^{-1}). The plants were bigger after 26 days of growth under HL compared to control (GL) conditions (Fig. 4.7 and Fig. 4.8a). The maximum quantum yield of PSII (F_V/F_M) was higher in all of the mutant plants, while it did not change in the WT (Fig. 4.8b). In the *psbo2* mutant, where the F_V/F_M was only slightly lower than in WT under GL, it increased to the WT level under HL conditions. In the mutants with decreased level of PsbO (*psbo1*oc*, *psbo1*psbo2* and *psbo1*), the increase of F_V/F_M values under HL was much more pronounced, with the highest increase in *psbo1*oc* (Fig. 4.8d). The increase in the rosette area was similar in WT, *psbo2*, *psbo1*psbo2* and *psbo1*, while it was somewhat higher in *psbo1*oc* (Fig. 4.8c). We measured the same characteristics also after 32 days of growth and the results were very similar (data not shown).

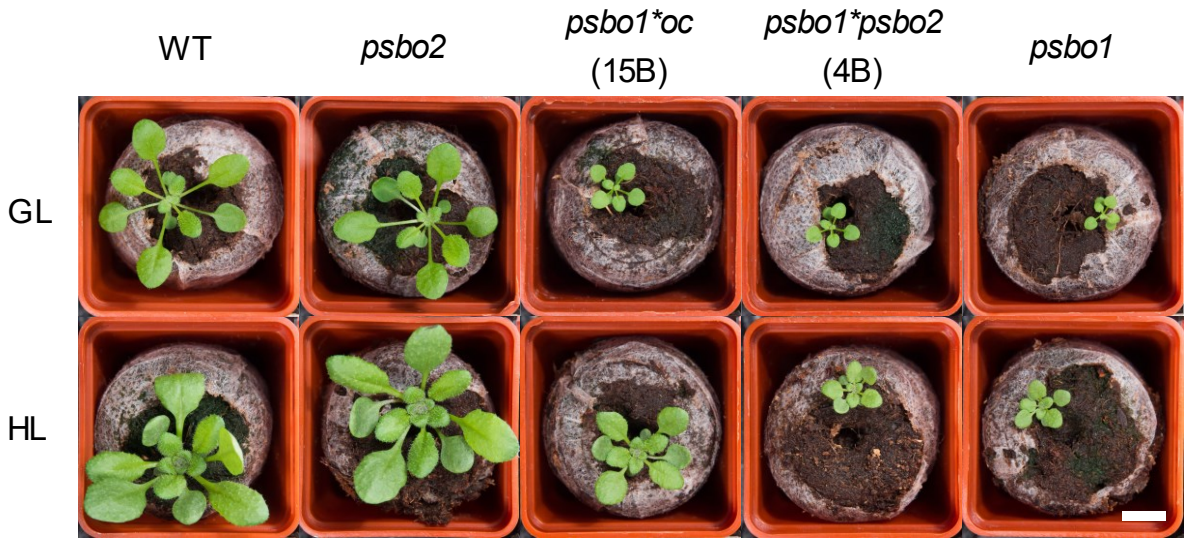

Fig. 4.7: Phenotypes of WT, *psbo2*, *psbo1*oc* (line 15B), *psbo1*psbo2* (line 4B) and *psbo1* plants cultivated under growth light (GL) conditions (125 µmol photons m^{-2} s^{-1}) and high light (HL) conditions (850 µmol photons m^{-2} s^{-1}). The plants were 26 days old and cultivated under the particular light conditions already from germination. The plants from GL are the same as in Fig. 4.1. The scale bar is 10 mm long.

Non-photochemical quenching (NPQ) allows plants to dissipate excess light energy absorbed by antenna proteins safely as heat. It is one of the mechanisms used to cope with HL (Ruban 2016). Therefore, we compared induction of non-photochemical quenching (NPQ) of plants grown under HL and GL conditions. Fig. 4.9a shows that upon exposure of dark adapted plants to actinic light, the plants with decreased level of PsbO (*psbo1*oc*, *psbo1*psbo2* and *psbo1*) developed the NPQ faster than WT and *psbo2*. However, the steady state NPQ was lowest in *psbo1*psbo2* and *psbo1* and intermediate in *psbo1*oc*. When comparing HL-grown and GL-grown plants, the plants of all genotypes grown at HL had faster induction of NPQ and higher initial peak. After about 2 minutes of light, NPQ of HL-grown plants dropped to the same level as in GL-grown plants.

Rapid light curves (RLC, response of electron transport rate to rapidly increasing irradiance) allow estimation of saturation characteristics of electron transport (Ralph & Gademann 2005). We measured RLC of plants previously grown at either HL or GL (Fig. 4.9b–d). The calculated initial slope of the RLC (α; Fig. 4.9c) corresponds well to the F_V/F_M values (Fig. 4.8b) – the already high values of WT and *psbo2* almost did not change under HL, while the lower values of *psbo1*oc*, *psbo1*psbo2* and *psbo1* increased under HL. The calculated maximum of relative electron transport rate ($rETR_{max}$), describing a capacity of the electron transport chain, was lowest in *psbo1* and *psbo1*psbo2*, intermediate in *psbo1*oc* and highest in WT and *psbo2*. It was 1.8–2.7 times higher in all genotypes when grown at HL, with the lowest relative increase in *psbo2* and highest in *psbo1*oc* (Fig. 4.9d).

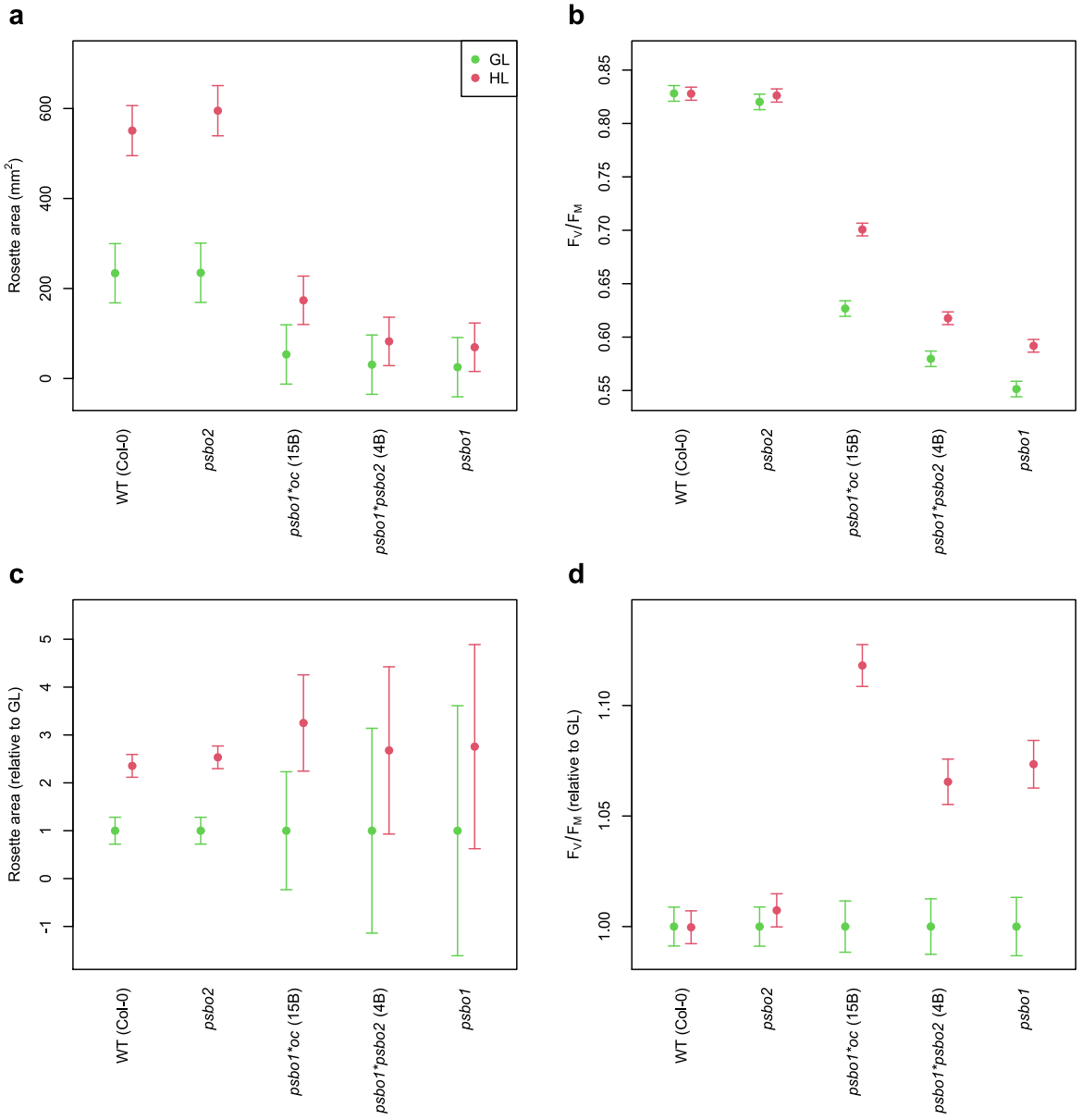

Fig. 4.8: Impact of long-term high light (HL, 850 µmol photons m^{-2} s^{-1}) conditions compared to growth light (GL, 125 µmol photons m^{-2} s^{-1}) conditions on rosette area and F_V/F_M of plants with various levels of PsbO1 and PsbO2 proteins. **a** Rosette area was measured as top view of photosynthetic area. **b** Maximum quantum yield of PSII (F_V/F_M) of individual plants was measured as mean value of the projected photosynthetic area of the plant. **c, d** Relative change of the values shown in plots a and b, respectively (values were divided by the GL value for the particular genotype). Plants were cultivated in GL or HL conditions already from germination and measured 26 days after germination. Means of 10 (GL) or 14-15 (HL) individual plants and 95% confidence intervals are shown. The data from GL are the same as data shown in Fig. 4.3.

Our results show that plants with similar phenotype at GL conditions, but different representation of PsbO1 and PsbO2, practically does not differ in reaction to long-term high light. Similarly, there was almost no difference in the reaction to rapid increase of light intensity (see RLC of GL-grown plants, Fig. 4.9b, d). The *psbo1*psbo2* mutant, with PsbO1 isoform only, was in our measurements always very similar to *psbo1* mutant, which has only PsbO2 isoform. The *psbo1*psbo2* plants were always only slightly closer to WT values. Likewise, there was almost no difference between WT and *psbo2* mutant, which has only

PsbO1 isoform. Our data suggest that PsbO1 and PsbO2 does not markedly differ in the support of PSII repair or related processes, in contrast to the hypothesis presented by Lundin *et al.* (2007a).

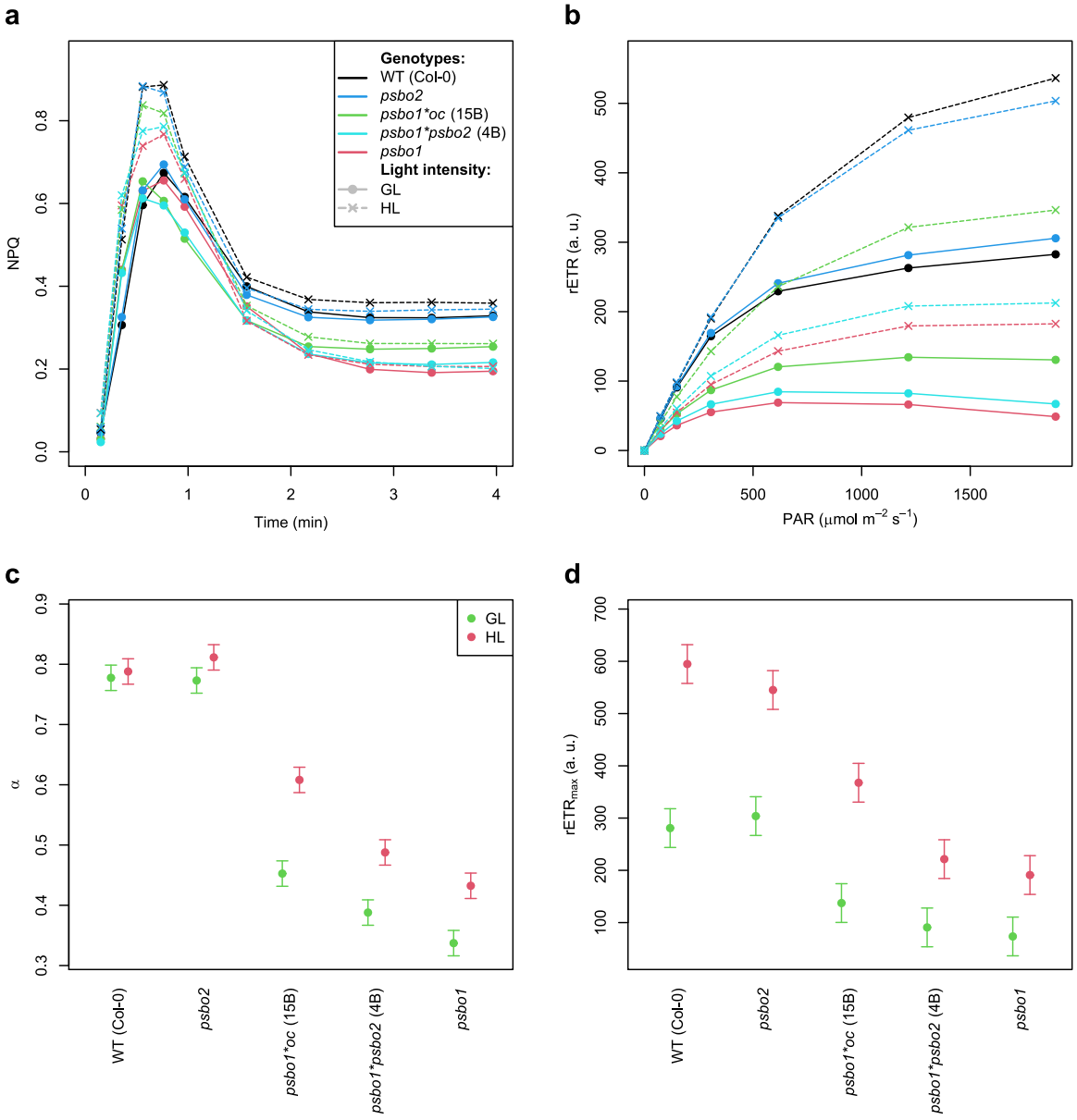

Fig. 4.9: Impact of long-term high light conditions (HL, 850 µmol photons m^{-2} s^{-1}) compared to growth light conditions (GL, 125 µmol photons m^{-2} s^{-1}) on induction of non-photochemical quenching (NPQ) and rapid light curves (RLC) of plants with various levels of PsbO1 and PsbO2 proteins. **a** NPQ of dark-adapted plants exposed to actinic light (blue light, 79 µmol photons m^{-2} s^{-1}, switched on at time 0). **b** Rapid light curves (relative electron transport rate plotted against irradiance by photosynthetically active radiation, PAR). **c** Initial slope of the RLC (α) calculated from RLC shown in **b**. **d** Maximum relative electron transport rate ($rETR_{max}$) calculated from RLC shown in **b**. Plants were cultivated in GL or HL conditions already from germination and measured 32 days after germination. Means of 6 individual plants per genotype are shown, with 95% confidence intervals in **c** and **d**.

4.3.3.3 Proteome of *psbo1*psbo2* and *psbo1* mutants and WT

In order to learn what could be the difference in function of PsbO1 and PsbO2, we analysed proteomes of *psbo1*psbo2*, *psbo1* and WT plants. As shown above, the

*psbo1*psbo2* and *psbo1* mutants differ in the retained PsbO isoform, but have very similar phenotype characterized by strongly retarded growth due to reduced photosynthetic performance. If PsbO1 and PsbO2 functionally differ, proteomic comparison of these two mutants should help to understand the difference between PsbO1 and PsbO2. Moreover, the comparison of both mutants (*psbo1*psbo2* and *psbo1*) with WT should reveal consequences of reduction of the total PsbO level. Using nano liquid chromatography connected to mass spectrometer (nLC-MS), we analysed abundances of proteins isolated from whole leaves (Table 9.1 in Attachments). Analysis of whole leaves without any fractionation allowed us to assess not only direct changes in the photosynthetic apparatus, but also consequent changes in other parts of the cell.

First, we compared levels of PsbO isoforms in WT and mutant plants. As PsbO1 and PsbO2 proteins have some tryptic peptides indistinguishable and some different, it was possible to calculate approximate amount of PsbO in mutants compared to WT and also ratio of PsbO1 and PsbO2 in WT. Our calculations revealed that PsbO2 accounted for 32–36% of total PsbO in WT. The total amount of PsbO was reduced to 39–44% in *psbo1* mutant, which means that the amount of PsbO2 rose to approximately 120% compared to WT. In *psbo1*psbo2* mutant, the total PsbO level was reduced to 31–32%, which means that the level of PsbO1 was reduced to 47–50% compared to WT. We found also trace amounts of some PsbO1 peptides in *psbo1* mutant and trace amounts of some PsbO2 peptides in *psbo1*psbo2*, however, this could be caused by sample carry-over in liquid chromatography column. Anyway, even if present, the amount of PsbO isoforms that were expected to be missing in particular mutants was surely lower than 3% of the amount of that isoform in WT.

While the exact numbers calculated from intensities of several peptides need to be taken with caution, the results nicely confirmed our expectation that *psbo1*psbo2* mutant have virtually only PsbO1 protein, in level comparable to the level of PsbO2 in *psbo1* mutant.

The proteomic analysis identified and quantified 3030 proteins (or protein groups, where the mass spectrometry did not distinguish similar proteins; Table 9.1 in Attachments), out of which 787 were significantly enriched or depleted in one or both of the mutants ($q < 0.05$, ANOVA with permutation-based false discovery rate correction). Only 145 proteins differed between any two genotypes with a ratio higher than 2.

As expected from the previous characterisation of the *psbo1*, *psbo1*psbo2* and WT plants, the proteomes of mutants were closer to each other than to WT proteome. Tukey's HSD test revealed only 162 proteins with levels different between *psbo1* and *psbo1*psbo2*, while there were 693 and 470 proteins with different levels between the pairs *psbo1* – WT and *psbo1*psbo2* – WT, respectively. Very similar pattern can be seen from the position of the samples on the first two components of a principal component analysis (PCA, Fig. 4.10). The mutants were closer to each other than to WT, with the distance between WT and

*psbo1*psbo2* being slightly shorter than the distance between WT and *psbo1*. The first component of PCA correlated well with the total amount of PsbO and even better with F_V/F_M (Fig. 4.5d), whereas the second component correlated well with the ratio of PsbO isoforms (*psbo1* has only PsbO2 isoform, *psbo1*psbo2* has only PsbO1 isoform, WT is in between).

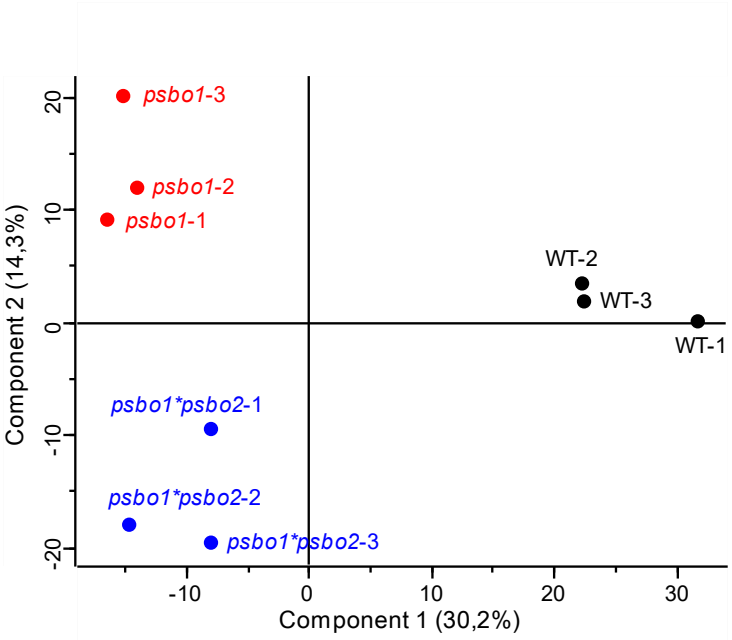

Fig. 4.10: Principal component analysis (PCA) of WT, *psbo1* and *psbo1*psbo2* leaf proteomes. Biological replicates of each genotype are depicted separately. The first and the second components describe 30.2% and 14.3% of the overall variability of the samples, respectively. Based on log-transformed intensities of 3030 proteins. The values missing in some samples were imputed (details are described in Materials and Methods).

To assess overall changes in the cells of mutant plants, we compared levels of proteins predicted to be localised in various cell compartments or extracellular (Fig. 4.11). The average amount of nuclear, plasma membrane and Golgi apparatus proteins was not significantly enriched or depleted in mutants compared to WT. Interestingly, chloroplast proteins were in average significantly enriched in both *psbo1* and *psbo1*psbo2*, while mitochondrial, cytoplasmic and extracellular proteins were depleted in the mutants (Fig. 4.11). Comparison of *psbo1*psbo2* and *psbo1* revealed that the levels of chloroplast proteins was lower in *psbo1*psbo2*, while the levels of mitochondrial and extracellular proteins were higher. This suggests again that the proteome of *psbo1*psbo2* was in average slightly closer to WT than *psbo1* proteome. Levels of plasma membrane proteins and proteins with unknown localisation were also increased in *psbo1*psbo2* compared to *psbo1* (Fig. 4.11).

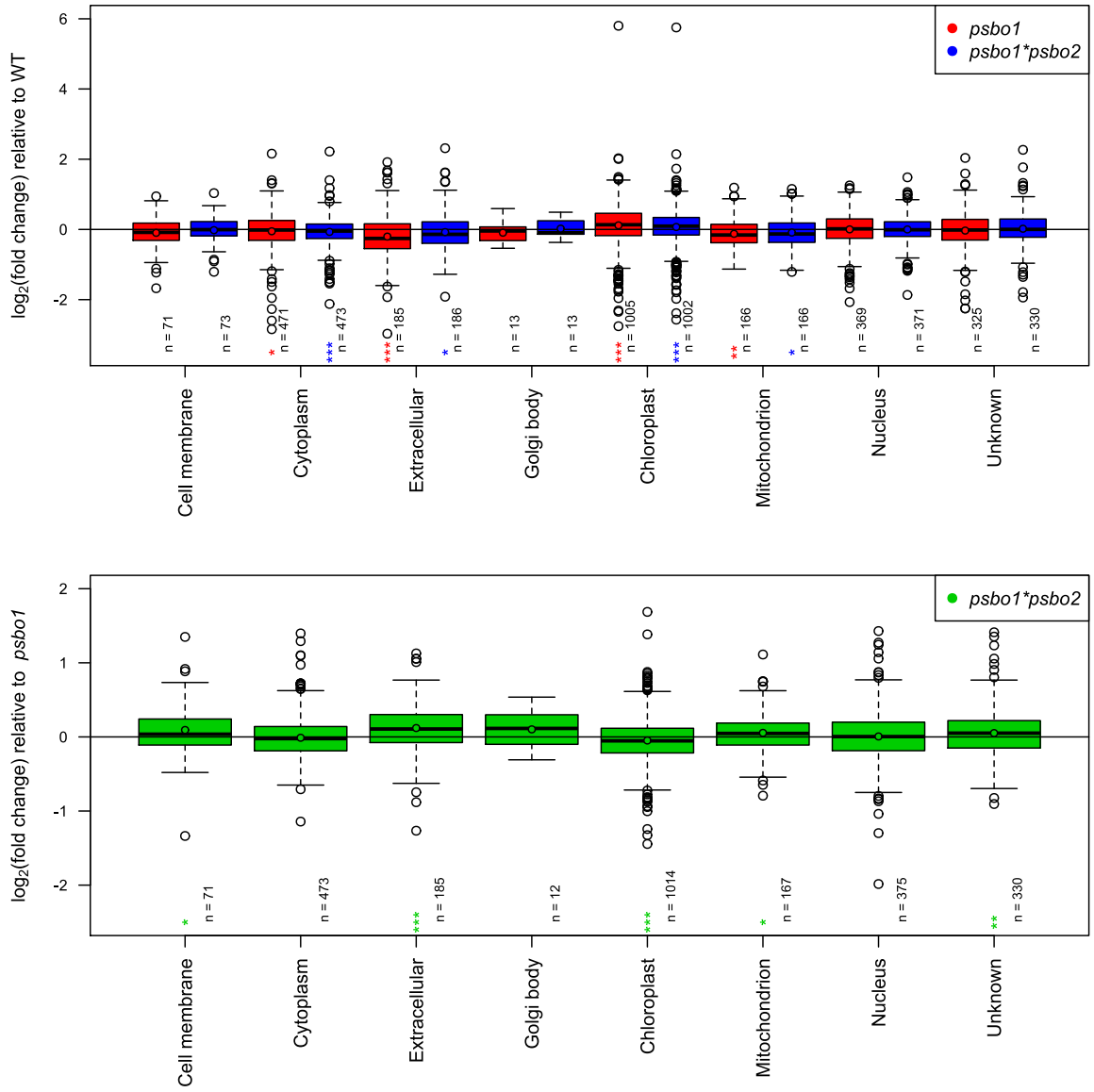

Fig. 4.11: Differences in the levels of proteins predicted to distinct cell compartments. The boxes range from lower to upper quartile, median is shown by bold line and mean by a coloured dot. Number of proteins (protein groups) in category and particular comparison is given by number. The overall mean of $\log_2$(fold change) for each comparison of genotypes was normalised to zero. The statistical significance of the difference of the mean of each category from zero, as calculated through randomisations, is shown as stars (* $q < 0.05$, ** $q < 0.01$, *** $q < 0.001$). Proteins (protein groups) with more than one predicted subcellular localisation were omitted from the analysis.

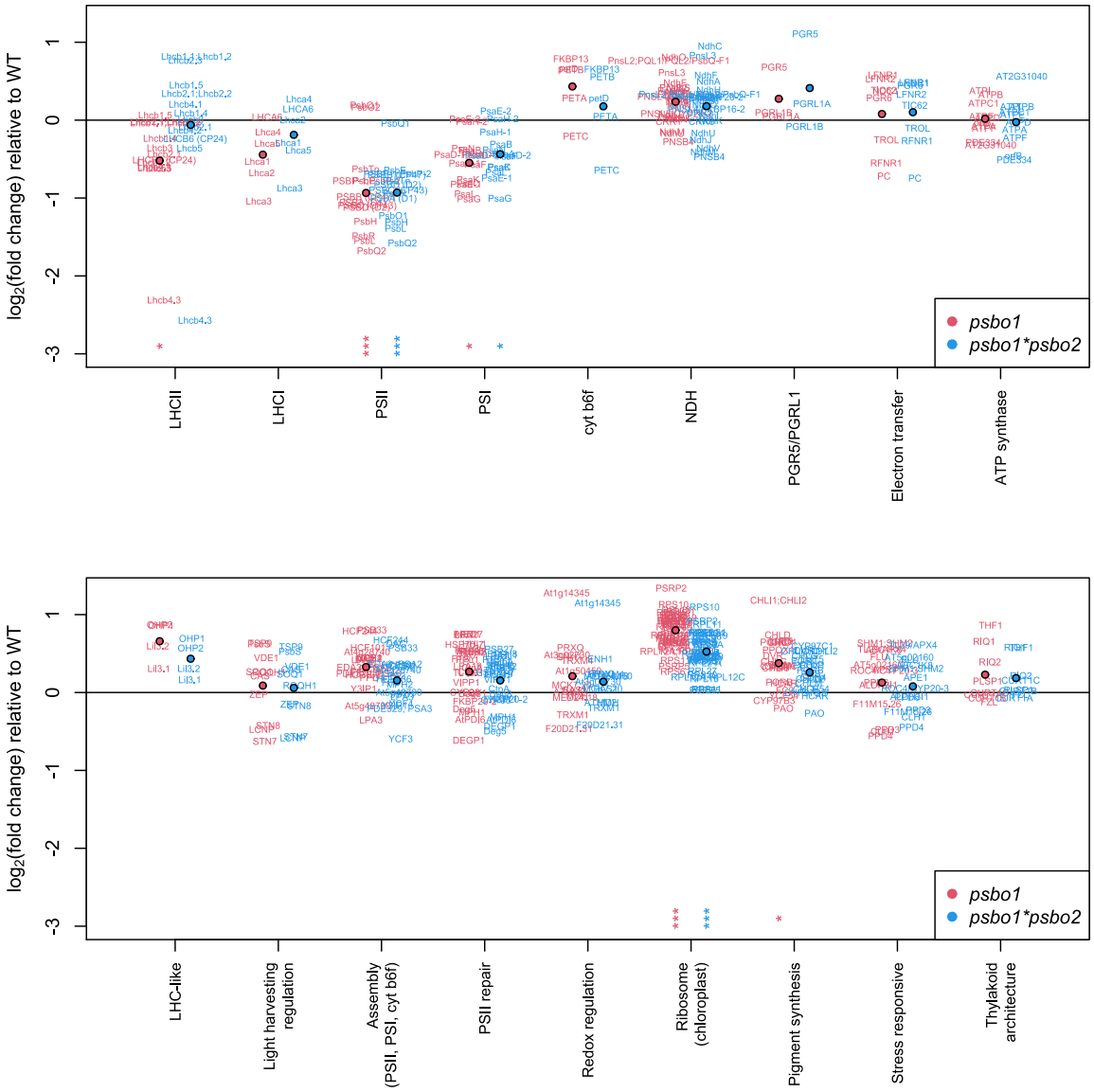

Fig. 4.12: Changes in the levels of electron transport chain complexes and some other groups of chloroplast proteins (*psbo1* and *psbo1*psbo2* mutants compared to WT). The proteins were categorised according to Flannery *et al*. (2021) and several other publications (see Materials and methods for details). The mean for each group is shown as a dot. The overall mean of $\log_2$(fold change) for each comparison of genotypes was normalised to zero. The statistical significance of the difference of the mean of each category from zero, as calculated through randomisations, is shown as stars (* $q < 0.05$, ** $q < 0.01$, *** $q < 0.001$).

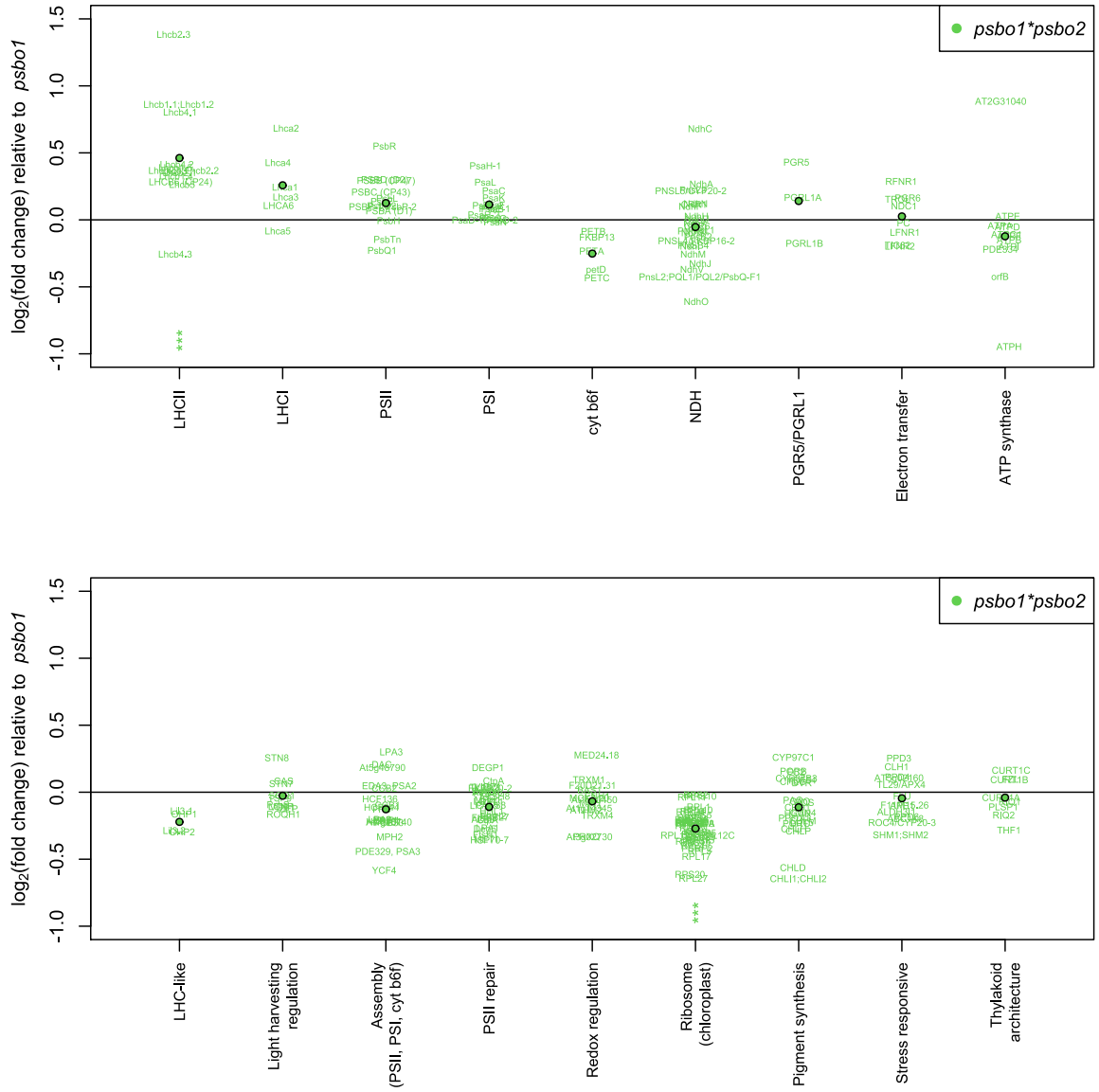

Fig. 4.13: Changes in the levels of electron transport chain complexes and some other groups of chloroplast proteins (*psbo1*psbo2* mutant compared to *psbo1* mutant). The proteins were categorised according to Flannery *et al*. (2021) and several other publications (see Materials and methods for details). The mean for each group is shown as a dot. The overall mean of $\log_2$(fold change) for each comparison of genotypes was normalised to zero. The statistical significance of the difference of the mean of each category from zero, as calculated through randomisations, is shown as stars (* $q < 0.05$, ** $q < 0.01$, *** $q < 0.001$).

While the chloroplast proteins were in average enriched in both mutants, not all of the chloroplast proteins followed the same pattern. Out of the 1056 quantified proteins predicted to chloroplast, 199 and 152 were significantly enriched in *psbo1* and *psbo1*psbo2*, respectively, whereas 103 and 67 were significantly depleted. In order to characterise the photosynthetic apparatus of *psbo1* and *psbo1*psbo2* mutants in detail, we have analysed changes in the levels of electron transport chain complexes and some other groups of chloroplast proteins, as categorised by Flannery *et al*. (2021) (Fig. 4.12, 4.13 and Table 9.1 in Attachments). Levels of cytochrome b_6f complex and ATP synthase were not significantly

changed in the mutants, as well as the levels of complexes involved in cyclic electron flow (NDH complex and PGR5/PGRL1 complex). As expected, the level of PSII proteins was decreased in both of the mutants. The average amount of PSII proteins in mutants was about 50% of WT, indicating that the decrease of PSII was similar to the decrease of the total PsbO level in the mutants. Interestingly, the PsbQ2 protein was one of the most reduced in the mutants, while the level of PsbQ1 protein did not change. Thus, the decrease of total PsbQ is similar to other PSII proteins, but the ratio of PsbQ1 to PsbQ2 was higher in the mutants.

The level of PSI was also decreased in the mutants, but not so strongly as PSII, only to about 70% of the level in WT. Antenna proteins of PSII (LHCII) were significantly reduced (to about 70%) only in *psbo1*. The average level of LHCII was not changed in *psbo1*psbo2* compared to WT. This means that the LHCII to PSII ratio is increased in *psbo1* and even more increased in *psbo1*psbo2*. It is also important to note that not all of the LHCII proteins were influenced similarly. The most outstanding was a Lhcb4.3 (CP29.3) protein, which is strongly depleted in both mutants (Fig. 4.12). The reduction of the average level of LHCI proteins, the antenna proteins of PSI, was not significant. However, regarding the fold change, it was similar to the reduction of PSI.

Stress responsive chloroplast proteins and light harvesting regulation proteins were not affected in the mutants as whole categories (Fig. 4.12). However, some of the proteins had significantly different levels in mutants. For example, PsbS protein, involved in NPQ, was increased to about 140–150% in both mutants, which might explain the faster induction of NPQ (Fig. 4.9a). STN7 kinase, involved in state transitions through phosphorylation of LHCII trimers, was significantly decreased in both of the mutants to about 60–70% (Table 9.1 in Attachments).

Proteins involved in assembly of electron transport chain complexes in thylakoid membrane and proteins involved in PSII repair were in average slightly increased in both of the mutants, but the changes were just below the level of significance (Fig. 4.12). Nevertheless, some of the individual proteins were significantly enriched in the mutants, like Psb33, Psb27, TL18.3, MET1, HHL1, PPL1 and several FtsH proteases. Out of the proteins in the categories “Assembly” and “PSII repair”, only DegP1 protease, involved in degradation of D1 protein (Järvi *et al.* 2015), was significantly decreased in the mutants (Table 9.1 in Attachments).

The levels of chloroplast proteins involved in pigment synthesis were slightly increased in both mutants, but the increase was statistically significant only in *psbo1*. Interestingly, the highest increase from the investigated groups of proteins was in chloroplast ribosomal proteins, with the average increase to 174% and 144% (*psbo1* and *psbo1*psbo2*, respectively) compared to WT (Fig. 4.12). This might mean that the proteosynthesis in chloroplasts was increased in the mutants compared to WT.

Fig. 4.12 shows that the changes in all of the investigated groups of chloroplast proteins had the same direction in both mutants, suggesting that the decrease in the total amount of PsbO was the main driving force behind the changes. Most of the changes were more pronounced in *psbo1* compared to *psbo1*psbo2*. Fig. 4.13 shows comparison of the levels of the same groups of proteins between *psbo1* and *psbo1*psbo2*. The only significantly different categories were LHCII proteins and chloroplast ribosomal proteins.

Table 4.1: Gene ontology (GO) term enrichment in groups of proteins with significantly increased or decreased levels between pairs of genotypes. The groups of proteins are based on significant difference determined by Tukey's HSD post-hoc test and the genotype where the level is higher (i.e. the group "WT > *psbo1*" contains proteins, which have significantly higher level in WT compared to *psbo1*). First seven GO terms of categories "biological process" and "cellular component" with the lowest *q*-value are shown for each group. Note that only six GO terms were below the treshold ($q < 0.05$) in the group "*psbo1* > *psbo1*psbo2*".

GO description	Enrichment factor	*q*-value	GO description	Enrichment factor	*q*-value
WT > *psbo1*			***psbo1* > WT**		
secretory vesicle	2.6	<0.0001	chloroplast	1.8	<0.0001
mitochondrial membrane	5.6	0.0002	chloroplast stroma	2.3	<0.0001
plasmodesma	1.6	0.0002	translation	3.7	<0.0001
cell wall	1.8	0.0014	chloroplast envelope	2.1	<0.0001
plasma membrane	1.4	0.0016	ribosome	3.6	<0.0001
protein-chromophore linkage	4.2	0.0017	chloroplast thylakoid membrane	1.8	<0.0001
apoplast	1.8	0.0036	chloroplast thylakoid	1.9	0.0003
WT > *psbo1*psbo2*			***psbo1*psbo2* > WT**		
mitochondrion	1.6	0.0013	chloroplast	1.8	<0.0001
response to cadmium ion	2.2	0.0018	chloroplast stroma	2.2	<0.0001
tricarboxylic acid cycle	4.8	0.0082	chloroplast envelope	2.2	<0.0001
plasmodesma	1.6	0.0147	chloroplast thylakoid membrane	2.2	<0.0001
cell wall	1.8	0.0165	chloroplast thylakoid	2.4	<0.0001
mitochondrial membrane	5.4	0.0207	translation	2.6	0.0002
endoplasmic reticulum lumen	4.5	0.0208	ribosome	2.8	0.0029
psbo1*psbo2* > *psbo1			***psbo1* > *psbo1*psbo2***		
protein-chromophore linkage	11.9	<0.0001	chloroplast stroma	2.3	0.0025
photosystem I	11.6	<0.0001	cytosolic ribosome	3.9	0.0047
photosynthesis, light harvesting in photosystem I	14.9	<0.0001	translation	4.2	0.0144
plastoglobule	6.0	<0.0001	cytosolic large ribosomal subunit	5.0	0.0179
photosystem II	9.9	<0.0001	polysomal ribosome	4.8	0.0209
secretory vesicle	3.7	0.0025	ribosome	4.7	0.0232
apoplast	2.7	0.0070			

To find further differences in the proteomes of the investigated genotypes, we performed gene ontology (GO) enrichment analysis to find terms enriched in groups of proteins significantly increased or decreased between pairs of genotypes. The results (Table 4.1) show similar information as the previous analyses (Fig. 4.11, 4.12, 4.13). It shows that a group of extracelular proteins (described by terms "secretory vesicle", "cell wall", "apoplast", "plasmodesma" and "endoplasmic reticulum lumen") and a group of mitochondrial proteins (described by terms "mitochondrion", "mitochondrial membrane" and "tricarboxylic acid cycle") were decreased in mutants compared to WT. The LHCII proteins (term "protein-chromophore linkage") had decreased levels specifically in *psbo1*. Proteins increased in mutants included many chloroplast and ribosomal proteins. Close investigation revealed that not only chloroplast ribosomes, as showed in Fig. 4.12, but also cytoplasmic ribosomes had increased levels in the mutants (Table 9.1 in Attachments).

GO enrichment analysis of proteins with levels differing between *psbo1* and *psbo1*psbo2* did not show any specific feature of *psbo1*psbo2* and confirmed again that, regarding protein levels, this mutant lied between WT and *psbo1*. Compared to *psbo1* mutant, *psbo1*psbo2* had higher levels of LHC proteins (which drives also the enrichment of terms "photosystem I", "photosystem II" and "plastoglobule") and of the same group of extracellular proteins that had even higher levels in WT. Complementarily, proteins increased in *psbo1* compared to *psbo1*psbo2* encompassed chloroplast and ribosomal proteins.

To find specific differences, we investigated proteins with the most different levels between *psbo1*psbo2* and *psbo1*. Table 4.2 shows the only six significant proteins that have more than two times different levels between *psbo1*psbo2* and *psbo1*. These proteins are very various and localised in different parts of cell, like chloroplast, extracellular space and cytoplasm. Therefore, we were not able to identify any clear specific feature of *psbo1*psbo2*.

Table 4.2: Proteins with more than two times different levels between *psbo1*psbo2* and *psbo1*. Only proteins with significant differences according to ANOVA with Tukey's HSD post-hoc test are listed.

Gene ID		Description	Subcellular localisation	Fold change		
				*psbo1*psbo2*/ *psbo1*	*psbo1*/WT	*psbo1*psbo2*/ WT
AT2G10940		Bifunctional inhibitor/lipid-transfer protein/seed storage 2S albumin superfamily protein	Extracellular/ Chloroplast	**0.41**	1.70	0.69
AT1G31070; AT2G35020	GlcNAc1pUT1; GlcNAc1pUT2	N-acetylglucosamine-1-phosphate uridylyltransferase 1; N-acetylglucosamine-1-phosphate uridylyltransferase 2	Cytoplasm	**0.47**	1.58	0.74
AT1G20190	EXP11	Expansin 11	Extracellular	**2.14**	0.42	0.90
AT2G32810	BGAL9	Beta-galactosidase 9	Extracellular	**2.25**	0.66	1.49
AT2G23070	CK2-alpha4	Casein kinase II subunit alpha-4	Chloroplast	**2.44**	NaN[a]	NaN[a]
AT1G12900	GAPA-2	Glyceraldehyde 3-phosphate dehydrogenase A subunit 2	Chloroplast	**3.32**	1.00	3.31

[a] The protein CK2-alpha4 was not quantified in WT, thus the fold changes between mutants and WT could not be calculated.

4.3.4 Discussion of unpublished results

4.3.4.1 Restoration of *psbO* expression in *psbo1*oc* and *psbo1*psbo2* is probably caused by epigenetic changes

Unexpectedly, by crossing *psbo1* and *psbo2* knock-out mutants, we have obtained double mutants *psbo1*psbo2* and single mutants *psbo1*oc* that have partially restored expression of the *psbO1* gene despite the retained insertion of T-DNA in 5'UTR. A similar phenomenon of epigenetic suppression of T-DNA mutant phenotype was observed after a crossing of mutants where T-DNA was inserted in an intron (Xue *et al.* 2012; Gao & Zhao 2013; Osabe *et al.* 2017). Multiple evidence suggests that the epigenetic interaction between the two SALK T-DNA insertions, likely an induction of T-DNA methylation in *psbo1* triggered by the silenced T-DNA in *psbo2*, occurred also in our case. Suorsa *et al.* (2016) reported that the *psbo1psbo2* double mutant in their case was unable to grow autotrophically, but they crossed a different *psbo2* mutant (CSHL_ET9214), which did not contain T-DNA and thus could not cause the same T-DNA suppression.

Although we did not find any report showing the phenomenon of T-DNA suppression for insertion in 5‘UTR, we expect that the mechanism is similar to that for the intronic T-DNA insertions. The *psbO1* mRNA was shown to be present already in the original *psbo1* mutant (Lundin *et al.* 2007a). We believe that epigenetic modifications such as DNA methylation allowed a splicing-out of the T-DNA copy from the transcript and thus also enabled its translation. Although there is no intron in the 5‘UTR of the *psbO1* gene, the splicing with low efficiency might be possible, because Yadav *et al.* (2018) showed that a transposon inserted in an exon can also be spliced out in some cases. However, the precise mechanism for the partial restoration of *psbO1* expression in *psbo1*psbo2* and *psbo1*oc* needs further elucidation.

4.3.4.2 Most of the changes in psbo1 mutant are caused by reduction of the total amount of PsbO

It is obvious from the published studies describing the *psbo1* mutant (Murakami *et al.* 2002, 2005; Liu *et al.* 2007, 2009; Lundin *et al.* 2007a, 2008; Bricker & Frankel 2008; Allahverdiyeva *et al.* 2009; Suorsa *et al.* 2016) and plants with a decreased amount of both PsbO isoforms (Yi *et al.* 2005; Dwyer *et al.* 2012) that the differences from WT are very similar in both cases (as described in detail in Introduction). This resulted in a question which features of *psbo1* mutant are specifically caused by the absence of PsbO1 isoform and which are caused only by the reduction of the total amount of PsbO. The newly obtained *psbo1*psbo2* and *psbo1*oc* lines supplemented the original *psbo1* and *psbo2* mutants and allowed us to characterise a set of mutants with various amounts of PsbO1 and PsbO2 proteins, making it possible to answer this question. Especially the comparison of *psbo1* and *psbo1*psbo2* mutants is interesting, as these plants have a similar phenotype and comparable levels of PsbO, but different isoforms (*psbo1* has only PsbO2 isoform, while *psbo1*psbo2* has only PsbO1 isoform). They are thus much better suited to elucidate the specific functions of PsbO1 and PsbO2 than the comparison of *psbo1* and *psbo2*, used in previous publications (Lundin *et al.* 2007a, 2008; Allahverdiyeva *et al.* 2009), with completely different phenotypes likely due to very different levels of PsbO.

Our results showed that most of the changes in the *psbo1* mutant were caused by the decrease of the total PsbO level and not by the absence of the PsbO1 isoform. We did not find any qualitative difference between *psbo1* and *psbo1*psbo2* in the growth rate (Fig. 4.5a, c), maximum quantum yield of PSII (F_V/F_M, Fig. 4.5b, d), NPQ induction (Fig. 4.9a), reaction to rapid increase of light intensity (Fig. 4.9b–d) or reaction to long-term high light (Fig. 4.8, Fig. 4.9). Complementarily, most changes in protein levels were similar in *psbo1* and *psbo1*psbo2*.

4.3.4.3 Decreased PsbO level has pleiotropic effects

The decrease of the total PsbO level caused many changes. The level of PSII was decreased to about 50% in both mutants (Fig. 4.12), which was somewhat higher than the levels of PsbO (31–44% of WT level). Dwyer *et al.* (2012) showed that the reduction of PsbO causes equivalent reduction of functional PSII centres. However, since PsbO was in our mutants slightly more decreased than PSII, there is still a possibility that some fraction of PsbO in WT is free in the lumen, unassembled to PSII, as proposed by Hashimoto *et al.* (1996), while the free PsbO might be missing or decreased in the mutants.

Our results show that the decrease of the PsbO level causes not only a reduction in the amount of PSII, but also in the amount of PSI, while the levels of cytochrome b_6f complex, ATP synthase, NDH complex and PGR5/PGRL1 complex are unaffected or even slightly increased (Fig. 4.12), which is in line with most of the previously published results (Murakami *et al.* 2005; Yi *et al.* 2005; Lundin *et al.* 2007a; Liu *et al.* 2009; Dwyer *et al.* 2012; Suorsa *et al.* 2016). Of interest is our finding that Lhcb4.3 (CP29.3) antenna protein of PSII is strongly decreased and that the ratio of PsbQ1 and PsbQ2, isoforms of PSII extrinsic protein PsbQ, is increased, while the total amount of PsbQ is similarly decreased as other PSII subunits. Levels of both Lhcb4.3 and PsbQ2 strongly differ also between low light-grown and HL-grown plants (Lhcb4.3 increases and PsbQ2 decreases in HL; Flannery *et al.* 2021), but they are regulated differently in *psbo1* and *psbo1*psbo2* mutants, where both Lhcb4.3 and PsbQ2 decrease. The differences in levels of these two proteins might be related to changes in PSII-LHCII supercomplex organisation, as the Lhcb4 (CP29) proteins are bound between PSII core, M-LHCII trimer, S-LHCII trimer and CP24. PsbQ is bound near S-LHCII trimer and CP26 (Fig. 1.2). It was already shown that *psbo1* mutants have different ratios of various PSII supercomplexes (Liu *et al.* 2007, 2009; Lundin *et al.* 2008; Allahverdiyeva *et al.* 2009; Suorsa *et al.* 2016).

We found that the decrease of the PsbO level causes an increase in the amount of ribosomal proteins, localised both in the cytoplasm and chloroplast (Fig. 4.12, Table 4.1). Moreover, the amount of chloroplast proteins involved in pigment synthesis and some of the proteins involved in PSII assembly and repair was also increased (Fig. 4.12). This might be a result of a malfunction of PSII, which is more susceptible to photodamage and needs more frequent repair, as suggested for *psbo1* mutant (Lundin *et al.* 2007a, 2008; Allahverdiyeva *et al.* 2009). However, we did not observe any qualitative difference between *psbo1* and *psbo1*psbo2* in this regard, suggesting that the susceptibility to photodamage is not caused by the presence of PsbO2 and a lack of PsbO1, as previously proposed (Lundin *et al.* 2007a, 2008; Allahverdiyeva *et al.* 2009), but by the low total amount of PsbO. The second possible explanation of the increase in the amount of ribosomal proteins, not mutually exclusive, is that the lack of energy from photosynthesis (while the amount of light is sufficient) triggers

higher production of chloroplast proteins in an attempt to support photosynthetic assimilation. However, this comes to the limit imposed by low amount of PsbO. This might explain the overall increase in the amount of chloroplast proteins in the *psbo1* and *psbo1*psbo2* mutants (Fig. 4.11, Table 4.1).

In contrast, both *psbo1* and *psbo1*psbo2* mutants have a slightly lower amount of mitochondrial proteins. This could be a compensatory reaction to a slowly running electron transport chain in the chloroplast, as chloroplasts and mitochondria are tightly connected through redox signalling. Mitochondria serve to alleviate overreduction under photorespiratory conditions (Dietz *et al.* 2016), which are unlikely to occur in mutants with a severely reduced chloroplast linear electron transport.

A lower amount of some extracellular proteins in *psbo1* and *psbo1*psbo2* mutants is intriguing (Fig. 4.11, Table 4.1). There is no obvious direct connection between impaired PSII and proteins secreted to the extracellular space. However, chloroplasts and extracellular proteins seem to be connected by some signalling pathways (Bobik & Burch-Smith 2015). Chloroplasts participate in the defence against pathogens (Serrano *et al.* 2016), which also includes changes in secreted proteins and restructuring of the cell wall. Moreover, it was shown that for example mutation in a chloroplast-localised DEVH-type RNA helicase, which causes overall impairment of chloroplast function, also affects the expression of cell wall- and plasmodesmata-related genes as well as the function of plasmodesmata (Burch-Smith *et al.* 2011). Note that "plasmodesma" was one of the GO terms enriched among proteins depleted in mutants (Table 4.1). The existence of signalling pathways between the chloroplast and extracellular proteins is supported also by the finding of proteins that interact both with chloroplast proteins and with extracellular proteins. For example, AtNHR2A and AtNHR2B proteins, involved in plant immunity, were shown to be localised among other sites to chloroplast and to interact both with chloroplast and extracellular proteins (Singh *et al.* 2018, 2020). Moreover, RACK1a protein was shown to interact with many chloroplast proteins, including PsbO, but also with some extracellular proteins (Kundu *et al.* 2013; Guo *et al.* 2019).

4.3.4.4 Phenotypic changes in the mutants with decreased PsbO level are stronger in younger leaves

The effect of the mutations was not uniform throughout the plants. As we showed by chlorophyll fluorescence imaging, younger leaves were affected more severely than older ones (Fig. 4.6). The increase of F_V/F_M values in older leaves might be caused by increasing amount of PsbO, as suggested by Murakami *et al.* (2005). It is not clear if PsbO is so long-lived that it can slowly accumulate to higher amounts in the old leaves despite the slow expression, or if the mature leaves are able to increase *psbO* expression. However, the use

of various leaves and plants of various age might explain some variation in the published data about the *psbo1* mutant, for example in the levels of proteins (summarised in Introduction). Interestingly, Dwyer *et al.* (2012) did not observe the difference in F_V/F_M between young and old leaves of plants with the level of PsbO decreased by RNA interference. The discrepancy might be caused by a different dynamics of *psbO* expression during leaf maturation in mutant and RNAi plants.

4.3.4.5 PsbO1 and PsbO2 differ in function only subtly

Most of the differences in protein levels were slightly more pronounced in *psbo1* and less in *psbo1*psbo2*, similarly as the growth rate retardation and F_V/F_M decrease. The fact that the changes are stronger in *psbo1*, together with the observation that there was probably slightly less of PsbO1 in *psbo1*psbo2* (31–32% of total WT level) compared to PsbO2 in *psbo1* (39–44% of total WT level), suggests that PsbO1 and PsbO2 are not completely equal in supporting of PSII activity. At least under the conditions of our experiments, PsbO1 probably supports the activity of PSII better than PsbO2. This *in vivo* observation is in accordance with previously published *in vitro* measurements, where maximum oxygen-evolving activity of PSII with PsbO2 was about 80% of that with PsbO1 (Murakami *et al.* 2005; Lundin *et al.* 2007a).

While most of the PSII proteins were at a very similar level in both mutants (Fig. 4.12), PSII core proteins D2 and CP47 were significantly enriched (to about 125%) in *psbo1*psbo2* compared to *psbo1* (Table 9.1 in Attachments). This gives a possibility that *psbo1*psbo2* has a slightly more functional PSII than *psbo1*. Better function of PSII in *psbo1*psbo2* compared to *psbo1* might be related also to higher amount of LHCII proteins, which is one of the major differences between *psbo1*psbo2* and *psbo1*.

Taken together, our results showed interesting consequences of a decrease in the PsbO level. However, we did not identify clear functional difference between PsbO1 and PsbO2 proteins other than that PsbO1 probably supports the function of PSII slightly better than PsbO2. Our experiments with HL did not show any difference in the acclimation of the mutants and neither the analysis of the proteomes did provide any good clue for any functional difference. While it is tempting to conclude that PsbO2 is just a dispensable, partially broken version of PsbO1, it is not likely. First, a useless protein would not be expressed and retained in evolution. Second, the F_V/F_M values of *psbo2* and *psbo2oc* mutants were only slightly, but reproducibly lower compared to WT (Fig. 4.5b, d), suggesting that the PsbO2 protein is not fully dispensable. And third, although not many, there were some differences between the proteomes of *psbo1* and *psbo1*psbo2* (Fig. 4.10, Table 4.2). Therefore, we suggest that the functional difference between PsbO1 and PsbO2 is not large but might lie in fine-tuning of some process in the thylakoids. However, the identification

of such process would need further research. Especially valuable would be to identify the conditions under which the mutants lacking PsbO2 would perform worse than other genotypes.

5 General discussion

5.1 Difference between the function of PsbO1 and PsbO2 is probably smaller than anticipated

The presence of two slightly different PsbO proteins in *A. thaliana* and many other plant species (Murakami *et al.* 2002; PUBLICATION 1) raises a question: What is the functional difference between PsbO1 and PsbO2, if there is any at all?

Lundin *et al.* (2007a) suggested that in *A. thaliana*, PsbO1 mainly supports normal oxygen evolution by PSII and PsbO2 regulates the phosphorylation state and turnover of the D1 protein. In a further publication (Lundin *et al.* 2008), the authors suggested that the role of PsbO2 in the turnover of D1 protein is connected with its higher GTPase activity. However, there are several problems with these publications (thorough critics was presented in Bricker & Frankel 2011). Mainly, if the PsbO2 protein would be needed for D1 turnover and PSII repair, the *psbo2* mutant lacking PsbO2 protein should exhibit impairment of PSII and thus growth retardation, at least under photoinhibitory conditions. While Lundin *et al.* (2007a) observed a phenotype of *psbo2* different from WT and described the devastating effect of prolonged high light (HL) on its fitness, in none of later studies such effect of *psbo2* mutation was observed, even when using the same T-DNA insertional lines (Allahverdiyeva *et al.* 2009; Suorsa *et al.* 2016). We also investigated the same mutant lines as Lundin *et al.* (2007a). As we have shown in Chapter 4.3, the *psbo2* plants were practically indistinguishable from WT, both under growth light (GL) conditions and under HL conditions (Fig. 4.7 in Chapter 4.3). The only small, but significant difference was a 1–2% decrease in the maximum quantum yield of PSII (F_V/F_M) under GL (Fig. 4.5 in Chapter 4.3). Similarly, also the plants with decreased total amount of PsbO, but different isoform present (*psbo1* and *psbo1*psbo2*) did not differ in their ability to acclimate to HL (Fig. 4.8 in Chapter 4.3). Allahverdiyeva *et al.* (2009) explained that the difference in *psbo2* observed by Lundin *et al.* (2007a) was caused by prolonged hydroponic cultivation. However, we did not observe any difference in *psbo2* phenotype from WT, although we used the same hydroponic cultivation (Nykles and Duchoslav, unpublished results). Thus, the results obtained by Lundin *et al.* (2007a, 2008) using *psbo2* mutant need to be taken with caution.

The *psbo1* mutant, lacking the PsbO1 protein, has pale green leaves, retarded growth and defective PSII (see Introduction for more details). This led to a conclusion that the role of PsbO1 is to support PSII function, while PsbO2 is insufficient in this role (Lundin *et al.* 2007a; Allahverdiyeva *et al.* 2009). Nevertheless, our results presented in Chapter 4.3 show that most of the characteristics of the *psbo1* mutant are caused by a decrease in the total PsbO amount and not by the missing PsbO1 isoform itself. The *psbo1*psbo2* plants with the PsbO1 protein only (at a level comparable to PsbO2 in the *psbo1* mutant) had very similar

characteristics to *psbo1*. Complementarily, our preliminary results show that increased expression of *psbO2* gene in *psbo1* plants is able to increase F_V/F_M and growth rate to WT levels (Nykles, Hlavsová and Duchoslav, unpublished results). Our results agree with the previous work on plants with decreased amount of both PsbO isoforms by RNA interference, which had also characteristics very similar to *psbo1* (Yi *et al.* 2005; Dwyer *et al.* 2012).

The above-presented arguments suggest that the difference in the function of PsbO1 and PsbO2 is small, if any. Thus, we can return to the question at the beginning and reformulate it: Do we have any evidence that PsbO1 and PsbO2 have different functions?

5.2 Ample evidence suggests that there is some divergence in the function of PsbO1 and PsbO2

The first line of evidence is based on evolution of *psbO* genes in plants. We have shown in PUBLICATION 1 that orthologues of *psbO1* and *psbO2* genes are expressed also in other species from Brassicaceae family, not only in *A. thaliana* (Fig. 1 in PUBLICATION 1). It is improbable that a dispensable gene would be retained without bigger changes and expressed in all investigated members of the family in the long term. Moreover, Brassicaceae is not the only family with two PsbO isoforms. Majority of the investigated angiosperm species express two *psbO* genes (Additional file 3 in PUBLICATION 1). Although the duplication of the *psbO* gene occurred many times independently (mostly in a common ancestor of each plant family; Fig. 1 in PUBLICATION 1), the extent of differences between PsbO isoforms stays similar (2–9% of mature PsbO protein sequence). We also found that although independently evolved, the differences between PsbO isoforms are in the same parts of the PsbO structure, which are partially different from the generally variable parts of the PsbO structure (Fig. 4 in PUBLICATION 1). This strongly suggests that there is some functional difference between PsbO isoforms that is beneficial for plants and thus evolved repeatedly throughout the phylogenetic tree of land plants. However, the existence of species and whole families that flourish with only one PsbO isoform suggests that the difference would not be big or the advantage of having two PsbO isoforms can be compensated by some other adaptation.

The second evidence for the partially different and complementary function of PsbO isoforms is the slightly lower F_V/F_M of the *psbo2* mutant compared to WT (Fig. 4.5 in Chapter 4.3). A similar result was obtained also by Allahverdiyeva *et al.* (2009), but they measured only several plants and did not perform statistical analysis of significance of the difference. We obtained the same result also using *psbo2* mutants created independently by CRISPR-Cas9 mutagenesis (Hlavsová 2020). Although the conditions under which the phenotype of *psbo2* mutant would be more strongly manifested were still not identified, this suggests that the PsbO2 protein cannot be fully substituted by PsbO1. However, it is still

possible that the decrease of F_V/F_M value in *psbo2* is caused only by a different total level of PsbO compared to WT. Since literature data showing the change of PsbO1 level in *psbo2* mutant are contradictory (Lundin *et al.* 2007a; Suorsa *et al.* 2016), further analyses are required.

The third evidence for the functional divergence of PsbO1 and PsbO2 is that the proteomes of *psbo1* and *psbo1*psbo2* are slightly different (Chapter 4.3). Although most of the differences are in line with the low-PsbO mutant phenotype, which is a little more pronounced in *psbo1*, there are several proteins that do not follow the pattern that the level of a particular protein in *psbo1*psbo2* is in between the levels in WT and *psbo1*. This qualitative difference between proteomes of the two mutants was clearly indicated by the principal component analysis (Fig. 4.10 in Chapter 4.3). Importantly, a slightly different function or organisation of PSII in plants having different PsbO isoforms is evident from a different ratio of LHCII proteins to PSII proteins (Fig. 4.12 in Chapter 4.3) and PsbO to PSII proteins in *psbo1* and *psbo1*psbo2* mutants (Chapter 4.3). This could be somehow related to different phosphorylation patterns of PSII core subunits and LHCII under various light conditions in *psbo2* compared to WT (Suorsa *et al.* 2016). However, no visible reorganisation of various forms of PSII supercomplexes in *psbo2* was observed using blue native PAGE (Suorsa *et al.* 2016).

The fourth evidence is that PsbO2 probably supports the oxygen evolution activity of PSII slightly worse than PsbO1. This was demonstrated by Murakami *et al.* (2005) *in vitro* using recombinant PsbOs and PSII particles isolated from spinach, by Lundin *et al.* (2007a) using PSII-LHCII supercomplexes isolated from *psbo1* and *psbo2* mutants and finally by our *in vivo* analysis (Chapter 4.3). We observed that the performance of the *psbo1*psbo2* mutant in various aspects was slightly better compared to *psbo1*, while the level of PsbO1 in *psbo1*psbo2* mutant was probably slightly lower than the level of PsbO2 in *psbo1* mutant (Chapter 4.3).

Although all the four lines of evidence suggesting that the functions of PsbO1 and PsbO2 differ have some uncertainty, they are in accordance with each other.

5.3 Divergence of PsbO1 and PsbO2 probably helps in tuning some process on PSII

As we have laid above several indices that PsbO1 and PsbO2 have slightly different functions, we can return to the main question at the beginning: What is the functional difference between PsbO1 and PsbO2?

In *A. thaliana, b*oth *psbO* genes are expressed stably in all green parts of the plant. The ratio between *psbO1* and *psbO2* mRNAs or between PsbO1 and PsbO2 proteins almost does not change during development of the plants or during various short-term stresses (Lundin

et al. 2008). We obtained similar results also by searching microarray and RNAseq data from Genevestigator (Hruz *et al.* 2008). There seem to be no tissues, developmental stages or perturbations showing a larger change in the ratio of *psbO1* and *psbO2* mRNAs, although the two isoforms slightly differ in the co-expressed gene clusters. This suggests three possibilities regarding the functional difference between PsbO1 and PsbO2, either (1) both isoforms are needed all the time or very often, or (2) the conditions when one of the isoforms is needed can come suddenly and are unpredictable, or (3) the isoforms are needed in different types of cells or chloroplasts that are constantly present in the plant.

We have shown that the differences between PsbO isoforms in various species are located mostly at the end of the β-barrel protruding into the thylakoid lumen (Fig. 4 in PUBLICATION 1). Some of the differences are often located also on the β1-β2 loop, which interacts with the CP47 subunit of the other monomer of PSII. PsbO isoforms from *A. thaliana* also follow this pattern, only one difference (V/S on position 186) is located outside these regions. We have also found that the part of PsbO facing PSII is very conserved, suggesting that the influence of the PsbO isoform on the function of PSII is rather indirect (Fig. 5 in PUBLICATION 1). Nevertheless, the differences between isoforms on the β1-β2 loop might influence the dimerisation of PSII.

The differences at the end of the β-barrel protruding into the lumen might modulate interaction with some interactor of PsbO. While no published work searching for interactors of PsbO is available to our knowledge, PsbO appeared in several searches for interactors of other proteins. PsbO interacts with stromatal chaperone HSP90C, which probably helps its translocation through the stroma to the thylakoid lumen (Jiang *et al.* 2017, 2020). Another interactor, luminal disulfide-bond forming enzyme LTO1 (lumen thiol oxidoreductase1), probably catalyses the formation of a disulfide bond in PsbO (Karamoko *et al.* 2011). PsbO might interact also with thioredoxins, as shown for thioredoxin h3 (Marchand *et al.* 2004). PsbO was shown to interact also with CV (chloroplast vesiculation) protein, which is highly expressed during senescence and abiotic stresses and triggers degradation of chloroplasts (Wang & Blumwald 2014). There was proposed also some interaction of PsbO with immunophilin CYP38 (cyclophilin38); nevertheless, the direct interaction was not documented (Wang *et al.* 2015). There are also reports about PsbO interactors from other species than *A. thaliana*. PsbO was reported to be phosphorylated by WKS1 (wheat kinase START1) in wheat, however, this kinase is present only in some cultivars of wheat, resistant to fungal patogen *Puccinia striiformis* (Wang *et al.* 2019). Abbink *et al.* (2002) reported interaction of PsbO with RNA helicase domain of the Tobacco mosaic virus replicase protein in tobacco. Unfortunately, none of the publications tested the difference in the binding of a particular interactor with PsbO1 and PsbO2. Thus, the hypothesis that the differences

between PsbO isoforms modulate the binding of some interactor cannot be endorsed without further experiments.

Lundin *et al.* (2007b, 2008) proposed that PsbO is a non-canonical GTPase and that the isoforms have different GTPase activity. PSII membranes isolated from the *psbo1* mutant had higher GTPase activity compared to membranes isolated from *psbo2* mutants or WT (Lundin *et al.* 2008). A similar result was obtained by Wang *et al.* (2015). It might be possible that the different GTPase activity was caused for example by different arrangement of PSII-LHCII supercomplexes in the mutants rather than by a different GTPase activity of PsbO1 and PsbO2 itself. However, our preliminary results show that isolated, heterologously produced PsbO isoforms from potato (*Solanum tuberosum*), StPsbO1 and StPsbO2 used in PUBLICATION 2, also differ in GTPase activity (Duchoslav, unpublished results). Some parts of the proposed GTP-binding site on PsbO (Lundin *et al.* 2007b) differ frequently between isoforms (Additional file 2 in PUBLICATION 1). One of the proposed switches, the regions that should change conformation between GDP- and GTP-bound states, is the β1-β2 loop that interacts with the other monomer of PSII (Lundin *et al.* 2007b). It is therefore possible that the GTPase activity of PsbO influences the dimerisation of PSII. Unfortunately, the regulation of the PsbO GTPase cycle is unknown, as no GTPase activating proteins or guanine nucleotide exchange factors are known for PsbO.

PsbO was proposed to be a part of a hydrogen-bond network around the Mn_4CaO_5 cluster, which provides rapid transport of protons and acts as a "proton antenna" (Shutova *et al.* 2007; Bondar & Dau 2012; Lorch *et al.* 2015; Barry *et al.* 2017; Guerra *et al.* 2018; Gerland *et al.* 2020). It seems that pK_a of the carboxylic groups on PsbO, involved in such a network, is important for such a function (Gerland *et al.* 2020). Moreover, the conformation of PsbO changes depending on pH (Fig. 4 in PUBLICATION 2; Shutova *et al.* 2005; Gerland *et al.* 2020). As we show in PUBLICATION 2, there is probably some cooperativity in the conformational changes, as the titration curve of PsbO forms a hysteresis loop (Fig. 4 in PUBLICATION 2). This suggests that there might be some feedback regulation of PSII activity by PsbO, slowing down the oxygen evolution by PSII when the pH in lumen is low (PUBLICATION 2; Shutova *et al.* 2005). However, another possibility, although very speculative, is that PsbO might "sense" through the hydrogen-bond network if the Mn_4CaO_5 cluster works properly or if the D1 protein is damaged. We hypothesise that the conditions when protons are not flowing regularly from the Mn_4CaO_5 cluster (which means that D1 might be damaged), while the bulk of the lumen is acidic (which means that the other PSIIs are running), might induce some change in PsbO conformation. This might trigger GTP digestion, which in turn causes a bigger change (switch) in the conformation of the β1-β2 loop and a monomerisation of the PSII dimer. Monomeric PSII can be then labelled for repair

by phosphorylation by STN8 kinase, causing its transport to grana margins and exchange of the D1 subunit (Järvi *et al.* 2015).

Independent of which hypothesis about the function of the pH-dependent conformational changes of PsbO is valid, differences between PsbO isoforms might modulate such process. We have shown that most frequent differences between PsbO isoforms are mutual exchanges between glutamic (E) and aspartic (D) acid residues (Fig. 3 in PUBLICATION 1). Three out of eleven different residues between *A. thaliana* PsbO1 and PsbO2 are such E/D exchanges. Although these residues are seemingly synonymous, such substitutions might modulate the pK_a of the particular residues and in turn the response of PsbO to pH changes. We found that these substitutions are strongly conserved in orthologous isoforms within plant families and in some cases even shared across more families (Additional file 2 in PUBLICATION 1).

Obviously, further experiments are needed to test whether the PsbO isoforms differ in pH-dependent conformational changes. However, much more research is necessary to elucidate the role of such conformational changes and the function of GTPase activity of PsbO.

6 Conclusions (English version)

Our phylogenetic analysis showed that not only *A. thaliana*, but also many other species express two *psbO* genes. Interestingly, the duplication of the gene occurred many times (in each plant family) independently. Nevertheless, the differences between isoforms are in the same parts of the structure, suggesting that the functional differences between the isoforms might also be similar in various species despite their independent origin.

Biochemical characterisation of PsbO from the green alga *Chlamydomonas reinhardtii* and the higher plant *Solanum tuberosum* showed that the PsbO proteins from various photosynthetic organisms are very similar and that the conformation of the β-barrel part of PsbO is influenced by pH.

We have found that the expression of the *psbO1* gene might be partially restored in the commonly used *psbo1* T-DNA mutant of *A. thaliana*, probably due to epigenetic interaction with another T-DNA. Thanks to this, we have obtained a *psbo1*psbo2* mutant, which has low amount of PsbO1 protein and no PsbO2 protein. Growth of *psbo1*psbo2* mutant was strongly retarded, similarly to the *psbo1* mutant, which contains PsbO2 at a level similar to that of PsbO1 in the *psbo1*psbo2* mutant.

Comparison of plants with various amounts of PsbO1 and PsbO2 revealed that the total level of PsbO has a fundamental effect on PSII function and phenotype of the plants regardless of which isoform is present. Plants with different PsbO isoforms, but at a similar total level, also did not significantly differ in their reaction to long-term high light conditions.

An analysis of the proteome confirmed that the mutant plants with only PsbO1 or PsbO2 differ marginally. However, changes caused by the decrease of the total level of PsbO were more pronounced in the plants with PsbO2 than in the plants with PsbO1, even though the level of PsbO2 was probably slightly higher in the compared plants. The same was true for the comparison of phenotypes, suggesting that PsbO2 is slightly less effective in supporting PSII activity. The plants with PsbO1 also had a higher ratio of antenna proteins to PSII compared to the plants with PsbO2. The analysis of the proteome unravelled also interesting consequences of a low amount of PsbO in the plants, for example a decrease in the amount of mitochondrial proteins and of a group of extracellular proteins and an increase in the amount of ribosomal proteins.

Interpreting our results, we propose that PsbO isoforms do not have fundamentally different functions, but rather differ in a fine modulation of some process. We hypothesise that the frequent D-E (aspartate – glutamate) substitutions between isoforms might tune the pH-dependent conformational changes of PsbO. However, functional significance of these conformational changes and potential connection with GTPase activity of PsbO needs to be revealed by further experiments.

7 Závěry (česká verze)

Naše fylogenetická analýza ukázala, že nejenom huseníček (*Arabidopsis thaliana*), ale i mnoho dalších druhů exprimuje dva geny psbO. Duplikace genu psbO proběhla kupodivu mnohokrát (v různých čeledích) nezávisle. Přesto mají izoformy z různých čeledí rozdíly ve stejných částech struktury, což naznačuje, že funkční rozdíly mezi izoformami mohou být v různých druzích podobné i přes nezávislý vznik.

Biochemická charakterizace PsbO ze zelené řasy *Chlamydomonas reinhardtii* a z bramboru (*Solanum tuberosum*) ukázala, že proteiny PsbO z různých fotosyntetizujících organismů jsou velmi podobné a že konformace β-soudkové části PsbO je ovlivňována změnami pH.

Zjistili jsme, že exprese genu *psbO1* v běžně používaném T-DNA inzerčním mutantovi *psbo1* může být částečně obnovena, pravděpodobně díky epigenetické interakci s další T-DNA. Díky tomu jsme získali mutanta *psbo1*psbo2*, který má malé množství proteinu PsbO1 a žádný protein PsbO2. Mutant *psbo1*psbo2* rostl velmi pomalu, podobně jako mutant *psbo1*, který obsahuje pouze izoformu PsbO2 (množství PsbO1 v mutantovi *psbo1*psbo2* je srovnatelné s množstvím PsbO2 v mutantovi *psbo1*).

Porovnáním mutantů huseníčku s různými množstvími PsbO1 a PsbO2 jsme zjistili, že celkové množství PsbO v rostlině má zásadní vliv na funkci fotosystému II (PSII) a fenotyp rostlin, nezávisle na tom, která izoforma je v rostlině přítomná. Rostliny se stejnou celkovou hladinou PsbO, ale různými izoformami, se nelišily také svojí reakcí na dlouhodobou vysokou ozářenost.

Analýza proteomu potvrdila, že mutantní rostliny, které mají buď jen PsbO1, nebo PsbO2, se liší minimálně. Nicméně změny způsobené snížením celkové hladiny PsbO se v rostlinách s PsbO2 projevily více než v rostlinách s PsbO1, přestože hladina PsbO2 byla v porovnávaných rostlinách pravděpodobně trochu vyšší. To samé platilo pro porovnání fenotypů, z čehož vyplývá, že izoforma PsbO2 je pravděpodobně o něco méně efektivní při podporování aktivity PSII. Rostliny s PsbO1 měly také vyšší poměr anténních proteinů k PSII v porovnání s rostlinami s PsbO2. Analýza proteomu odhalila rovněž zajímavé změny související s nízkou hladinou PsbO v rostlinách, například snížení množství mitochondriálních proteinů a skupiny extracelulárních proteinů a zvýšení množství ribozomálních proteinů.

Na základě našich výsledků navrhujeme, že izoformy PsbO nemají zásadně odlišnou funkci, ale spíše jemně modulují nějaký proces. Spekulujeme, že časté záměny aspartát – glutamát mezi izoformami PsbO by mohly ladit konformační změny, které probíhají v závislosti na pH. Nicméně funkci těchto konformačních změn a potenciální souvislost s GTPázovou aktivitou PsbO je potřeba odhalit pomocí dalšího výzkumu.

8 References

Abbink T.E.M., Peart J.R., Mos T.N.M., Baulcombe D.C., Bol J.F., Linthorst H.J.M. (**2002**) Silencing of a Gene Encoding a Protein Component of the Oxygen-Evolving Complex of Photosystem II Enhances Virus Replication in Plants. *Virology* **295**: 307–319. doi: 10.1006/viro.2002.1332

Ago H., Adachi H., Umena Y., Tashiro T., Kawakami K., Kamiya N., Tian L., Han G., Kuang T., Liu Z., Wang F., Zou H., Enami I., Miyano M., Shen J.-R. (**2016**) Novel Features of Eukaryotic Photosystem II Revealed by Its Crystal Structure Analysis from a Red Alga. *The Journal of biological chemistry* **291**: 5676–5687. doi: 10.1074/jbc.m115.711689

Allahverdiyeva Y., Mamedov F., Holmström M., Nurmi M., Lundin B., Styring S., Spetea C., Aro E.-M. (**2009**) Comparison of the electron transport properties of the psbo1 and psbo2 mutants of Arabidopsis thaliana. *Biochimica et Biophysica Acta (BBA) - Bioenergetics* **1787**: 1230–1237. doi: 10.1016/j.bbabio.2009.05.013

Barber J. (**2016**) 'Photosystem II: the water splitting enzyme of photosynthesis and the origin of oxygen in our atmosphere.' *Quarterly Reviews of Biophysics* **49**. doi: 10.1017/S0033583516000093

Barry B.A., Brahmachari U., Guo Z. (**2017**) Tracking Reactive Water and Hydrogen-Bonding Networks in Photosynthetic Oxygen Evolution. *Accounts of Chemical Research* **50**: 1937–1945. doi: 10.1021/acs.accounts.7b00189

Bentley F.K., Eaton-Rye J.J. (**2008**) The Effect of Removing Photosystem II Extrinsic Proteins on Dimer Formation and Recovery from Photodamage in Synechocystis sp. PCC 6803. In: Allen JF, Gantt E, Golbeck JH, Osmond B (eds) Photosynthesis. Energy from the Sun. Springer Netherlands, Dordrecht, pp 715–717. doi: 10.1007/978-1-4020-6709-9_159

Betts S.D., Ross J.R., Hall K.U., Pichersky E., Yocum C.F. (**1996**) Functional reconstitution of photosystem II with recombinant manganese-stabilizing proteins containing mutations that remove the disulfide bridge. *Biochimica et Biophysica Acta (BBA) - Bioenergetics* **1274**: 135–142. doi: 10.1016/0005-2728(96)00023-0

Bezouwen L.S. van, Caffarri S., Kale R.S., Kouřil R., Thunnissen A.-M.W.H., Oostergetel G.T., Boekema E.J. (**2017**) Subunit and chlorophyll organization of the plant photosystem II supercomplex. *Nature Plants* **3**: nplants201780. doi: 10.1038/nplants.2017.80

Biesiadka J., Loll B., Kern J., Irrgang K.-D., Zouni A. (**2004**) Crystal structure of cyanobacterial photosystem II at 3.2 Å resolution: a closer look at the Mn-cluster. *Physical Chemistry Chemical Physics* **6**: 4733–4736. doi: 10.1039/B406989G

Blankenship R.E. (**2014**) *Molecular Mechanisms of Photosynthesis*. Wiley.

Bobik K., Burch-Smith T.M. (**2015**) Chloroplast signaling within, between and beyond cells. *Frontiers in Plant Science* **6**

Boekema E.J., van Breemen J.F.L., van Roon H., Dekker J.P. (**2000**) Conformational Changes in Photosystem II Supercomplexes upon Removal of Extrinsic Subunits. *Biochemistry* **39**: 12907–12915. doi: 10.1021/bi0009183

Bommer M., Bondar A.-N., Zouni A., Dobbek H., Dau H. (**2016**) Crystallographic and Computational Analysis of the Barrel Part of the PsbO Protein of Photosystem II: Carboxylate–Water Clusters as Putative Proton Transfer Relays and Structural Switches. *Biochemistry* **55**: 4626–4635. doi: 10.1021/acs.biochem.6b00441

Bondar A.-N., Dau H. (**2012**) Extended protein/water H-bond networks in photosynthetic water oxidation. *Biochimica et Biophysica Acta (BBA) - Bioenergetics* **1817**: 1177–1190. doi: 10.1016/j.bbabio.2012.03.031

Bricker T.M. (**1992**) Oxygen evolution in the absence of the 33-kilodalton manganese-stabilizing protein. *Biochemistry* **31**: 4623–4628. doi: 10.1021/bi00134a012

Bricker T.M., Frankel L.K. (**2008**) The psbo1 Mutant of Arabidopsis Cannot Efficiently Use Calcium in Support of Oxygen Evolution by Photosystem II. *Journal of Biological Chemistry* **283**: 29022–29027. doi: 10.1074/jbc.M805122200

Bricker T.M., Frankel L.K. (**2011**) Auxiliary functions of the PsbO, PsbP and PsbQ proteins of higher plant Photosystem II: A critical analysis. *Journal of Photochemistry and Photobiology B: Biology* **104**: 165–178. doi: 10.1016/j.jphotobiol.2011.01.025

Bricker T.M., Roose J.L., Fagerlund R.D., Frankel L.K., Eaton-Rye J.J. (**2012**) The extrinsic proteins of Photosystem II. *Biochimica et Biophysica Acta (BBA) - Bioenergetics* **1817**: 121–142. doi: 10.1016/j.bbabio.2011.07.006

Burch-Smith T.M., Brunkard J.O., Choi Y.G., Zambryski P.C. (**2011**) Organelle–nucleus cross-talk regulates plant intercellular communication via plasmodesmata. *Proceedings of the National Academy of Sciences* **108**: E1451–E1460. doi: 10.1073/pnas.1117226108

Burnap R.L., Sherman L.A. (**1991**) Deletion mutagenesis in Synechocystis sp. PCC6803 indicates that the manganese-stabilizing protein of photosystem II is not essential for oxygen evolution. *Biochemistry* **30**: 440–446. doi: 10.1021/bi00216a020

Cox J., Hein M.Y., Luber C.A., Paron I., Nagaraj N., Mann M. (**2014**) Accurate Proteome-wide Label-free Quantification by Delayed Normalization and Maximal Peptide Ratio Extraction, Termed MaxLFQ. *Molecular & Cellular Proteomics* **13**: 2513–2526. doi: 10.1074/mcp.M113.031591

Cox J., Mann M. (**2008**) MaxQuant enables high peptide identification rates, individualized p.p.b.-range mass accuracies and proteome-wide protein quantification. *Nature Biotechnology* **26**: 1367–1372. doi: 10.1038/nbt.1511

Cox N., Pantazis D.A., Lubitz W. (**2020**) Current Understanding of the Mechanism of Water Oxidation in Photosystem II and Its Relation to XFEL Data. *Annual Review of Biochemistry* **89**: 795–820. doi: 10.1146/annurev-biochem-011520-104801

De Las Rivas J., Balsera M., Barber J. (**2004**) Evolution of oxygenic photosynthesis: genome-wide analysis of the OEC extrinsic proteins. *Trends in Plant Science* **9**: 18–25. doi: 10.1016/j.tplants.2003.11.007

De Las Rivas J., Barber J. (**2004**) Analysis of the Structure of the PsbO Protein and its Implications. *Photosynthesis Research* **81**: 329–343. doi: 10.1023/B:PRES.0000036889.44048.e4

Dietz K.-J., Turkan I., Krieger-Liszkay A. (**2016**) Redox- and Reactive Oxygen Species-Dependent Signaling into and out of the Photosynthesizing Chloroplast. *Plant Physiology* **171**: 1541–1550. doi: 10.1104/pp.16.00375

Dwyer S.A., Chow W.S., Yamori W., Evans J.R., Kaines S., Badger M.R., Caemmerer S. von (**2012**) Antisense reductions in the PsbO protein of photosystem II leads to decreased quantum yield but similar maximal photosynthetic rates. *Journal of Experimental Botany* **63**: 4781–4795. doi: 10.1093/jxb/ers156

Ferreira K.N., Iverson T.M., Maghlaoui K., Barber J., Iwata S. (**2004**) Architecture of the Photosynthetic Oxygen-Evolving Center. *Science* **303**: 1831–1838. doi: 10.1126/science.1093087

Fischer W.W., Hemp J., Johnson J.E. (**2016**) Evolution of Oxygenic Photosynthesis. *Annual Review of Earth and Planetary Sciences* **44**: 647–683. doi: 10.1146/annurev-earth-060313-054810

Fischer L., Lipavska H., Hausman J.-F., Opatrny Z. (**2008**) Morphological and molecular characterization of a spontaneously tuberizing potato mutant: an insight into the regulatory mechanisms of tuber induction. *BMC Plant Biology* **8**: 117. doi: 10.1186/1471-2229-8-117

Flannery S.E., Hepworth C., Wood W.H.J., Pastorelli F., Hunter C.N., Dickman M.J., Jackson P.J., Johnson M.P. (**2021**) Developmental acclimation of the thylakoid proteome to light intensity in Arabidopsis. *The Plant Journal* **105**: 223–244. doi: 10.1111/tpj.15053

Gabdulkhakov A., Guskov A., Broser M., Kern J., Müh F., Saenger W., Zouni A. (**2009**) Probing the Accessibility of the Mn4Ca Cluster in Photosystem II: Channels Calculation, Noble Gas Derivatization, and Cocrystallization with DMSO. *Structure* **17**: 1223–1234. doi: 10.1016/j.str.2009.07.010

Gao Y., Zhao Y. (**2013**) Epigenetic Suppression of T-DNA Insertion Mutants in Arabidopsis. *Molecular Plant* **6**: 539–545. doi: 10.1093/mp/sss093

Gerland L., Friedrich D., Hopf L., Donovan E.J., Wallmann A., Erdmann N., Diehl A., Bommer M., Buzar K., Ibrahim M., Schmieder P., Dobbek H., Zouni A., Bondar A.-N., Dau H., Oschkinat H. (**2020**) pH-Dependent Protonation of Surface Carboxylate Groups in PsbO Enables Local Buffering and Triggers Structural Changes. *ChemBioChem* **21**: 1597–1604. doi: 10.1002/cbic.201900739

Graça A.T., Hall M., Persson K., Schröder W.P. (**2021**) High-resolution model of Arabidopsis Photosystem II reveals the structural consequences of digitonin-extraction. *Scientific reports* **11**: 15534. doi: 10.1038/s41598-021-94914-x

Grinzato A., Albanese P., Marotta R., Swuec P., Saracco G., Bolognesi M., Zanotti G., Pagliano C. (**2020**) High-Light versus Low-Light: Effects on Paired Photosystem II Supercomplex Structural Rearrangement in Pea Plants. *International Journal of Molecular Sciences* **21**: 8643. doi: 10.3390/ijms21228643

Guerra F., Siemers M., Mielack C., Bondar A.-N. (**2018**) Dynamics of Long-Distance Hydrogen-Bond Networks in Photosystem II. *The Journal of Physical Chemistry B* **122**: 4625–4641. doi: 10.1021/acs.jpcb.8b00649

Guo J., Hu Y., Zhou Y., Zhu Z., Sun Y., Li J., Wu R., Miao Y., Sun X. (**2019**) Profiling of the Receptor for Activated C Kinase 1a (RACK1a) interaction network in Arabidopsis thaliana. *Biochemical and Biophysical Research Communications* **520**: 366–372. doi: 10.1016/j.bbrc.2019.09.142

Guskov A., Kern J., Gabdulkhakov A., Broser M., Zouni A., Saenger W. (**2009**) Cyanobacterial photosystem II at 2.9-Å resolution and the role of quinones, lipids, channels and chloride. *Nature Structural & Molecular Biology* **16**: 334–342. doi: 10.1038/nsmb.1559

Hashimoto A., Yamamoto Y., Theg S.M. (**1996**) Unassembled subunits of the photosynthetic oxygen-evolving complex present in the thylakoid lumen are long-lived and assembly-competent. *FEBS Letters* **391**: 29–34. doi: 10.1016/0014-5793(96)00686-2

Hebert A.S., Richards A.L., Bailey D.J., Ulbrich A., Coughlin E.E., Westphall M.S., Coon J.J. (**2014**) The One Hour Yeast Proteome. *Molecular & Cellular Proteomics* **13**: 339–347. doi: 10.1074/mcp.M113.034769

Hellmich J., Bommer M., Burkhardt A., Ibrahim M., Kern J., Meents A., Müh F., Dobbek H., Zouni A. (**2014**) Native-like Photosystem II Superstructure at 2.44 Å Resolution through Detergent Extraction from the Protein Crystal. *Structure* **22**: 1607–1615. doi: 10.1016/j.str.2014.09.007

Hlavsová K. (**2020**) *Mutageneze genů psbO1 a psbO2 v Arabidopsis thaliana pomocí metody CRISPR-Cas9*. Diploma thesis, Univerzita Karlova, Přírodovědecká fakulta (http://hdl.handle.net/20.500.11956/122188)

Ho F.M., Styring S. (**2008**) Access channels and methanol binding site to the CaMn4 cluster in Photosystem II based on solvent accessibility simulations, with implications for substrate water access. *Biochimica et Biophysica Acta (BBA) - Bioenergetics* **1777**: 140–153. doi: 10.1016/j.bbabio.2007.08.009

Hruz T., Laule O., Szabo G., Wessendorp F., Bleuler S., Oertle L., Widmayer P., Gruissem W., Zimmermann P. (**2008**) Genevestigator V3: A Reference Expression Database for the Meta-Analysis of Transcriptomes. *Advances in Bioinformatics* **2008**

Hughes C.S., Moggridge S., Müller T., Sorensen P.H., Morin G.B., Krijgsveld J. (**2019**) Single-pot, solid-phase-enhanced sample preparation for proteomics experiments. *Nature Protocols* **14**: 68–85. doi: 10.1038/s41596-018-0082-x

Ifuku K., Endo T., Shikanai T., Aro E.-M. (**2011**) Structure of the Chloroplast NADH Dehydrogenase-Like Complex: Nomenclature for Nuclear-Encoded Subunits. *Plant and Cell Physiology* **52**: 1560–1568. doi: 10.1093/pcp/pcr098

Janes K.A. (**2015**) An analysis of critical factors for quantitative immunoblotting. *Science Signaling* **8**: rs2–rs2. doi: 10.1126/scisignal.2005966

Järvi S., Gollan P.J., Aro E.-M. (**2013**) Understanding the roles of the thylakoid lumen in photosynthesis regulation. *Frontiers in Plant Science* **4**. doi: 10.3389/fpls.2013.00434

Järvi S., Suorsa M., Aro E.-M. (**2015**) Photosystem II repair in plant chloroplasts — Regulation, assisting proteins and shared components with photosystem II biogenesis. *Biochimica et Biophysica Acta (BBA) - Bioenergetics* **1847**: 900–909. doi: 10.1016/j.bbabio.2015.01.006

Jiang T., Mu B., Zhao R. (**2020**) Plastid chaperone HSP90C guides precursor proteins to the SEC translocase for thylakoid transport. *Journal of Experimental Botany* **71**: 7073–7087. doi: 10.1093/jxb/eraa399

Jiang T., Oh E.S., Bonea D., Zhao R. (**2017**) HSP90C interacts with PsbO1 and facilitates its thylakoid distribution from chloroplast stroma in Arabidopsis. *PLOS ONE* **12**: e0190168. doi: 10.1371/journal.pone.0190168

Kamiya N., Shen J.-R. (**2003**) Crystal structure of oxygen-evolving photosystem II from Thermosynechococcus vulcanus at 3.7-Å resolution. *Proceedings of the National Academy of Sciences* **100**: 98–103. doi: 10.1073/pnas.0135651100

Karamoko M., Cline S., Redding K., Ruiz N., Hamel P.P. (**2011**) Lumen Thiol Oxidoreductase1, a Disulfide Bond-Forming Catalyst, Is Required for the Assembly of Photosystem II in Arabidopsis[C][W]. *The Plant Cell* **23**: 4462–4475. doi: 10.1105/tpc.111.089680

Kaundal R., Saini R., Zhao P.X. (**2010**) Combining Machine Learning and Homology-Based Approaches to Accurately Predict Subcellular Localization in Arabidopsis. *Plant Physiology* **154**: 36–54. doi: 10.1104/pp.110.156851

Kern J., Chatterjee R., Young I.D., Fuller F.D., Lassalle L., Ibrahim M., Gul S., Fransson T., Brewster A.S., Alonso-Mori R., Hussein R., Zhang M., Douthit L., Lichtenberg C. de, Cheah M.H., Shevela D., Wersig J., Seuffert I., Sokaras D., Pastor E., Weninger C., Kroll T., Sierra R.G., Aller P., Butryn A., Orville A.M., Liang M., Batyuk A., Koglin J.E., Carbajo S., Boutet S., Moriarty N.W., Holton J.M., Dobbek H., Adams P.D., Bergmann U., Sauter N.K., Zouni A., Messinger J., Yano J., Yachandra V.K. (**2018**) Structures of the intermediates of Kok's photosynthetic water oxidation clock. *Nature* **563**: 421–425. doi: 10.1038/s41586-018-0681-2

Kouřil R., Dekker J.P., Boekema E.J. (**2012**) Supramolecular organization of photosystem II in green plants. *Biochimica et Biophysica Acta (BBA) - Bioenergetics* **1817**: 2–12. doi: 10.1016/j.bbabio.2011.05.024

Kundu N., Dozier U., Deslandes L., Somssich I.E., Ullah H. (**2013**) Arabidopsis scaffold protein RACK1A interacts with diverse environmental stress and photosynthesis related proteins. *Plant Signaling & Behavior* **8**: e24012. doi: 10.4161/psb.24012

Liu H., Frankel L.K., Bricker T.M. (**2007**) Functional Analysis of Photosystem II in a PsbO-1-Deficient Mutant in Arabidopsis thaliana. *Biochemistry* **46**: 7607–7613. doi: 10.1021/bi700107w

Liu H., Frankel L.K., Bricker T.M. (**2009**) Functional complementation of the Arabidopsis thaliana psbo1 mutant phenotype with an N-terminally His6-tagged PsbO-1 protein in photosystem II. *Biochimica et Biophysica Acta (BBA) - Bioenergetics* **1787**: 1029–1038. doi: 10.1016/j.bbabio.2009.03.006

Loll B., Kern J., Saenger W., Zouni A., Biesiadka J. (**2005**) Towards complete cofactor arrangement in the 3.0 Å resolution structure of photosystem II. *Nature* **438**: 1040–1044. doi: 10.1038/nature04224

Long S.P., Marshall-Colon A., Zhu X.-G. (**2015**) Meeting the Global Food Demand of the Future by Engineering Crop Photosynthesis and Yield Potential. *Cell* **161**: 56–66. doi: 10.1016/j.cell.2015.03.019

Lorch S., Capponi S., Pieront F., Bondar A.-N. (**2015**) Dynamic Carboxylate/Water Networks on the Surface of the PsbO Subunit of Photosystem II. *The Journal of Physical Chemistry B* **119**: 12172–12181. doi: 10.1021/acs.jpcb.5b06594

Lundin B., Hansson M., Schoefs B., Vener A.V., Spetea C. (**2007a**) The Arabidopsis PsbO2 protein regulates dephosphorylation and turnover of the photosystem II reaction centre D1 protein. *The Plant Journal* **49**: 528–539. doi: 10.1111/j.1365-313X.2006.02976.x

Lundin B., Nurmi M., Rojas-Stuetz M., Aro E.-M., Adamska I., Spetea C. (**2008**) Towards understanding the functional difference between the two PsbO isoforms in Arabidopsis thaliana—insights from phenotypic analyses of psbo knockout mutants. *Photosynthesis Research* **98**: 405–414. doi: 10.1007/s11120-008-9325-y

Lundin B., Thuswaldner S., Shutova T., Eshaghi S., Samuelsson G., Barber J., Andersson B., Spetea C. (**2007b**) Subsequent events to GTP binding by the plant PsbO protein: Structural changes, GTP hydrolysis and dissociation from the photosystem II complex. *Biochimica et Biophysica Acta (BBA) - Bioenergetics* **1767**: 500–508. doi: 10.1016/j.bbabio.2006.10.009

Marchand C., Maréchal P.L., Meyer Y., Miginiac-Maslow M., Issakidis-Bourguet E., Decottignies P. (**2004**) New targets of Arabidopsis thioredoxins revealed by proteomic analysis. *PROTEOMICS* **4**: 2696–2706. doi: 10.1002/pmic.200400805

Martínez-García J.F., Monte E., Quail P.H. (**1999**) A simple, rapid and quantitative method for preparing Arabidopsis protein extracts for immunoblot analysis. *The Plant Journal* **20**: 251–257. doi: 10.1046/j.1365-313x.1999.00579.x

Mayfield S.P., Bennoun P., Rochaix J.D. (**1987**) Expression of the nuclear encoded OEE1 protein is required for oxygen evolution and stability of photosystem II particles in Chlamydomonas reinhardtii. *The EMBO Journal* **6**: 313–318.

Murakami R., Ifuku K., Takabayashi A., Shikanai T., Endo T., Sato F. (**2002**) Characterization of an Arabidopsis thaliana mutant with impaired psbO, one of two genes encoding extrinsic 33-kDa proteins in photosystem II. *FEBS Letters* **523**: 138–142. doi: 10.1016/S0014-5793(02)02963-0

Murakami R., Ifuku K., Takabayashi A., Shikanai T., Endo T., Sato F. (**2005**) Functional dissection of two Arabidopsis PsbO proteins. *FEBS Journal* **272**: 2165–2175. doi: 10.1111/j.1742-4658.2005.04636.x

Murray J.W., Barber J. (**2006**) Identification of a Calcium-Binding Site in the PsbO Protein of Photosystem II†. *Biochemistry* **45**: 4128–4130. doi: 10.1021/bi052503t

Murray J.W., Barber J. (**2007**) Structural characteristics of channels and pathways in photosystem II including the identification of an oxygen channel. *Journal of Structural Biology* **159**: 228–237. doi: 10.1016/j.jsb.2007.01.016

Nikitina J., Shutova T., Melnik B., Chernyshov S., Marchenkov V., Semisotnov G., Klimov V., Samuelsson G. (**2008**) Importance of a single disulfide bond for the PsbO protein of photosystem II: protein structure stability and soluble overexpression in <i>Escherichia coli</i> *Photosynthesis Research* **98**: 391–403. doi: 10.1007/s11120-008-9327-9

Nowaczyk M., Berghaus C., Stoll R., Rögner M. (**2004**) Preliminary structural characterisation of the 33 kDa protein (PsbO) in solution studied by site-directed mutagenesis and NMR spectroscopy. *Physical Chemistry Chemical Physics* **6**: 4878–4881. doi: 10.1039/B407316A

Osabe K., Harukawa Y., Miura S., Saze H. (**2017**) Epigenetic Regulation of Intronic Transgenes in Arabidopsis. *Scientific Reports* **7**: 45166. doi: 10.1038/srep45166

Pagliano C., Saracco G., Barber J. (**2013**) Structural, functional and auxiliary proteins of photosystem II. *Photosynthesis Research* **116**: 167–188. doi: 10.1007/s11120-013-9803-8

Pettersen E.F., Goddard T.D., Huang C.C., Meng E.C., Couch G.S., Croll T.I., Morris J.H., Ferrin T.E. (**2021**) UCSF ChimeraX: Structure visualization for researchers, educators, and developers. *Protein Science* **30**: 70–82. doi: 10.1002/pro.3943

Ralph P.J., Gademann R. (**2005**) Rapid light curves: A powerful tool to assess photosynthetic activity. *Aquatic Botany* **82**: 222–237. doi: 10.1016/j.aquabot.2005.02.006

Rantala M., Rantala S., Aro E.-M. (**2020**) Composition, phosphorylation and dynamic organization of photosynthetic protein complexes in plant thylakoid membrane. *Photochemical & Photobiological Sciences* **19**: 604–619. doi: 10.1039/D0PP00025F

Rappsilber J., Mann M., Ishihama Y. (**2007**) Protocol for micro-purification, enrichment, pre-fractionation and storage of peptides for proteomics using StageTips. *Nature Protocols* **2**: 1896–1906. doi: 10.1038/nprot.2007.261

Renger G., Renger T. (**2008**) Photosystem II: The machinery of photosynthetic water splitting. *Photosynthesis Research* **98**: 53–80. doi: 10.1007/s11120-008-9345-7

Roose J.L., Frankel L.K., Mummadisetti M.P., Bricker T.M. (**2016**) The extrinsic proteins of photosystem II: update. *Planta*: 1–20. doi: 10.1007/s00425-015-2462-6

Roose J.L., Kashino Y., Pakrasi H.B. (**2007**) The PsbQ protein defines cyanobacterial Photosystem II complexes with highest activity and stability. *Proceedings of the National Academy of Sciences* **104**: 2548–2553. doi: 10.1073/pnas.0609337104

Ruban A.V. (**2016**) Nonphotochemical Chlorophyll Fluorescence Quenching: Mechanism and Effectiveness in Protecting Plants from Photodamage. *Plant Physiology* **170**: 1903–1916. doi: 10.1104/pp.15.01935

Sato N. (**2010**) Phylogenomic and structural modeling analyses of the PsbP superfamily reveal multiple small segment additions in the evolution of photosystem II-associated PsbP protein in green plants. *Molecular Phylogenetics and Evolution* **56**: 176–186. doi: 10.1016/j.ympev.2009.11.021

Seidler A. (**1996**) The extrinsic polypeptides of Photosystem II. *Biochimica et Biophysica Acta (BBA) - Bioenergetics* **1277**: 35–60. doi: 10.1016/S0005-2728(96)00102-8

Serrano I., Audran C., Rivas S. (**2016**) Chloroplasts at work during plant innate immunity. *Journal of Experimental Botany* **67**: 3845–3854. doi: 10.1093/jxb/erw088

Shen L., Huang Z., Chang S., Wang W., Wang J., Kuang T., Han G., Shen J.-R., Zhang X. (**2019**) Structure of a C2S2M2N2-type PSII-LHCII supercomplex from the green alga Chlamydomonas reinhardtii. *Proceedings of the National Academy of Sciences of the United States of America* **116**: 21246–21255. doi: 10.1073/pnas.1912462116

Sheng X., Watanabe A., Li A., Kim E., Song C., Murata K., Song D., Minagawa J., Liu Z. (**2019**) Structural insight into light harvesting for photosystem II in green algae. *Nature Plants* **5**: 1320–1330. doi: 10.1038/s41477-019-0543-4

Shi L.-X., Hall M., Funk C., Schröder W.P. (**2012**) Photosystem II, a growing complex: Updates on newly discovered components and low molecular mass proteins. *Biochimica et Biophysica Acta (BBA) - Bioenergetics* **1817**: 13–25. doi: 10.1016/j.bbabio.2011.08.008

Shikanai T. (**2016**) Chloroplast NDH: A different enzyme with a structure similar to that of respiratory NADH dehydrogenase. *Biochimica et Biophysica Acta (BBA) - Bioenergetics* **1857**: 1015–1022. doi: 10.1016/j.bbabio.2015.10.013

Shutova T., Klimov V.V., Andersson B., Samuelsson G. (**2007**) A cluster of carboxylic groups in PsbO protein is involved in proton transfer from the water oxidizing complex of Photosystem II. *Biochimica et Biophysica Acta (BBA) - Bioenergetics* **1767**: 434–440. doi: 10.1016/j.bbabio.2007.01.020

Shutova T., Nikitina J., Deikus G., Andersson B., Klimov V., Samuelsson G. (**2005**) Structural Dynamics of the Manganese-Stabilizing ProteinEffect of pH, Calcium, and Manganese†. *Biochemistry* **44**: 15182–15192. doi: 10.1021/bi0512750

Singh R., Lee S., Ortega L., Ramu V.S., Senthil-Kumar M., Blancaflor E.B., Rojas C.M., Mysore K.S. (**2018**) Two Chloroplast-Localized Proteins: AtNHR2A and AtNHR2B, Contribute to Callose Deposition During Nonhost Disease Resistance in Arabidopsis. *Molecular Plant-Microbe Interactions®* **31**: 1280–1290. doi: 10.1094/MPMI-04-18-0094-R

Singh R., Liyanage R., Gupta C., Lay J.O., Pereira A., Rojas C.M. (**2020**) The Arabidopsis Proteins AtNHR2A and AtNHR2B Are Multi-Functional Proteins Integrating Plant Immunity With Other Biological Processes. *Frontiers in Plant Science* **11**: 232. doi: 10.3389/fpls.2020.00232

Spetea C., Hundal T., Lohmann F., Andersson B. (**1999**) GTP bound to chloroplast thylakoid membranes is required for light-induced, multienzyme degradation of the photosystem II D1 protein. *Proceedings of the National Academy of Sciences* **96**: 6547–6552. doi: 10.1073/pnas.96.11.6547

Spetea C., Hundal T., Lundin B., Heddad M., Adamska I., Andersson B. (**2004**) Multiple evidence for nucleotide metabolism in the chloroplast thylakoid lumen. *Proceedings of the National Academy of Sciences of the United States of America* **101**: 1409–1414. doi: 10.1073/pnas.0308164100

Spetea C., Lundin B. (**2012**) Evidence for nucleotide-dependent processes in the thylakoid lumen of plant chloroplasts – an update. *FEBS Letters* **586**: 2946–2954. doi: 10.1016/j.febslet.2012.07.005

Su X., Ma J., Wei X., Cao P., Zhu D., Chang W., Liu Z., Zhang X., Li M. (**2017**) Structure and assembly mechanism of plant C2S2M2-type PSII-LHCII supercomplex. *Science* **357**: 815–820. doi: 10.1126/science.aan0327

Suga M., Akita F., Hirata K., Ueno G., Murakami H., Nakajima Y., Shimizu T., Yamashita K., Yamamoto M., Ago H., Shen J.-R. (**2015**) Native structure of photosystem II at 1.95 Å resolution viewed by femtosecond X-ray pulses. *Nature* **517**: 99–103. doi: 10.1038/nature13991

Suga M., Akita F., Yamashita K., Nakajima Y., Ueno G., Li H., Yamane T., Hirata K., Umena Y., Yonekura S., Yu L.-J., Murakami H., Nomura T., Kimura T., Kubo M., Baba S., Kumasaka T., Tono K., Yabashi M., Isobe H., Yamaguchi K., Yamamoto M., Ago H., Shen J.-R. (**2019**) An oxyl/oxo mechanism for oxygen-oxygen coupling in PSII revealed by an x-ray free-electron laser. *Science* **366**: 334–338. doi: 10.1126/science.aax6998

Suorsa M., Rossi F., Tadini L., Labs M., Colombo M., Jahns P., Kater M.M., Leister D., Finazzi G., Aro E.-M., Barbato R., Pesaresi P. (**2016**) PGR5-PGRL1-Dependent Cyclic Electron Transport Modulates Linear Electron Transport Rate in Arabidopsis thaliana. *Molecular Plant* **9**: 271–288. doi: 10.1016/j.molp.2015.12.001

Suorsa M., Sirpiö S., Allahverdiyeva Y., Paakkarinen V., Mamedov F., Styring S., Aro E.-M. (**2006**) PsbR, a Missing Link in the Assembly of the Oxygen-evolving Complex of Plant Photosystem II *. *Journal of Biological Chemistry* **281**: 145–150. doi: 10.1074/jbc.M510600200

Svensson B., Tiede D.M., Barry B.A. (**2002**) Small-Angle X-ray Scattering Studies of the Manganese Stabilizing Subunit in Photosystem II. *J Phys Chem B* **106**: 8485–8488. doi: 10.1021/jp0258199

Tanaka A., Fukushima Y., Kamiya N. (**2017**) Two Different Structures of the Oxygen-Evolving Complex in the Same Polypeptide Frameworks of Photosystem II. *Journal of the American Chemical Society* **139**: 1718–1721. doi: 10.1021/jacs.6b09666

Tanaka S., Kawata Y., Wada K., Hamaguchi K. (**1989**) Extrinsic 33-kilodalton protein of spinach oxygen-evolving complexes: kinetic studies of folding and disulfide reduction. *Biochemistry* **28**: 7188–7193. doi: 10.1021/bi00444a009

The Arabidopsis Genome Initiative (**2000**) Analysis of the genome sequence of the flowering plant Arabidopsis thaliana. *Nature* **408**: 796.

Thornton L.E., Ohkawa H., Roose J.L., Kashino Y., Keren N., Pakrasi H.B. (**2004**) Homologs of Plant PsbP and PsbQ Proteins Are Necessary for Regulation of Photosystem II Activity in the Cyanobacterium Synechocystis 6803. *The Plant Cell Online* **16**: 2164–2175. doi: 10.1105/tpc.104.023515

Tokano T., Kato Y., Sugiyama S., Uchihashi T., Noguchi T. (**2020**) Structural Dynamics of a Protein Domain Relevant to the Water-Oxidizing Complex in Photosystem II as Visualized by High-Speed Atomic Force Microscopy. *The Journal of Physical Chemistry B* **124**: 5847–5857. doi: 10.1021/acs.jpcb.0c03892

Tyanova S., Temu T., Sinitcyn P., Carlson A., Hein M.Y., Geiger T., Mann M., Cox J. (**2016**) The Perseus computational platform for comprehensive analysis of (prote)omics data. *Nature Methods* **13**: 731–740. doi: 10.1038/nmeth.3901

Umena Y., Kawakami K., Shen J.-R., Kamiya N. (**2011**) Crystal structure of oxygen-evolving photosystem II at a resolution of 1.9 Å. *Nature* **473**: 55–60. doi: 10.1038/nature09913

Vassiliev S., Comte P., Mahboob A., Bruce D. (**2010**) Tracking the Flow of Water through Photosystem II Using Molecular Dynamics and Streamline Tracing. *Biochemistry* **49**: 1873–1881. doi: 10.1021/bi901900s

Wang S., Blumwald E. (**2014**) Stress-Induced Chloroplast Degradation in Arabidopsis Is Regulated via a Process Independent of Autophagy and Senescence-Associated Vacuoles[W]. *The Plant Cell* **26**: 4875–4888. doi: 10.1105/tpc.114.133116

Wang S., Li Q.-P., Wang J., Yan Y., Zhang G.-L., Yan Y., Zhang H., Wu J., Chen F., Wang X., Kang Z., Dubcovsky J., Gou J.-Y. (**2019**) YR36/WKS1-Mediated Phosphorylation of PsbO, an Extrinsic Member of Photosystem II, Inhibits Photosynthesis and Confers Stripe Rust Resistance in Wheat. *Molecular Plant* **12**: 1639–1650. doi: 10.1016/j.molp.2019.10.005

Wang Y., Zeng L., Xing D. (**2015**) ROS-mediated enhanced transcription of CYP38 promotes the plant tolerance to high light stress by suppressing GTPase activation of PsbO2. *Frontiers in Plant Science* **6**. doi: 10.3389/fpls.2015.00777

Wei X., Su X., Cao P., Liu X., Chang W., Li M., Zhang X., Liu Z. (**2016**) Structure of spinach photosystem II–LHCII supercomplex at 3.2 Å resolution. *Nature* **534**: 69–74. doi: 10.1038/nature18020

Wyman A., Yocum C. (**2005**) Structure and Activity of the Photosystem II Manganese-Stabilizing Protein: Role of the Conserved Disulfide Bond. *Photosynthesis Research* **85**: 359–372. doi: 10.1007/s11120-005-7385-9

Xue W., Ruprecht C., Street N., Hematy K., Chang C., Frommer W.B., Persson S., Niittylä T. (**2012**) Paramutation-Like Interaction of T-DNA Loci in Arabidopsis. *PLOS ONE* **7**: e51651. doi: 10.1371/journal.pone.0051651

Yadav N.S., Khadka J., Domb K., Zemach A., Grafi G. (**2018**) CMT3 and SUVH4/KYP silence the exonic Evelknievel retroelement to allow for reconstitution of CMT1 mRNA. *Epigenetics & Chromatin* **11**: 69. doi: 10.1186/s13072-018-0240-y

Yi X., McChargue M., Laborde S., Frankel L.K., Bricker T.M. (**2005**) The Manganese-stabilizing Protein Is Required for Photosystem II Assembly/Stability and Photoautotrophy in Higher Plants. *Journal of Biological Chemistry* **280**: 16170–16174. doi: 10.1074/jbc.M501550200

Yuan J., Henry R., McCaffery M., Cline K. (**1994**) SecA Homolog in Protein Transport Within Chloroplasts: Evidence for Endosymbiont-Derived Sorting. *Science* **266**: 796–798.

Zhang B., Sun L. (**2019**) Artificial photosynthesis: opportunities and challenges of molecular catalysts. *Chemical Society Reviews* **48**: 2216–2264. doi: 10.1039/C8CS00897C

Zouni A., Witt H.-T., Kern J., Fromme P., Kraub N., Saenger W., Orth P. (**2001**) Crystal structure of photosystem II from Synechococcus elongatus at 3.8 A resolution. *Nature* **409**: 739.

Zubrzycki I.Z., Frankel L.K., Russo P.S., Bricker T.M. (**1998**) Hydrodynamic Studies on the Manganese-Stabilizing Protein of Photosystem II. *Biochemistry* **37**: 13553–13558. doi: 10.1021/bi981469y

9 Attachments

9.1 Electronic attachment

Table 9.1: Table of proteins identified and quantified by mass spectrometry analysis. The details about quantification and annotation of proteins are described in Materials and methods.

Table is attached in electronic form on enclosed CD.

9.2 PUBLICATION 1

20 pages (80 – 99)

Additional file 1 (List of analysed *psbO* genes) is available in electronic attachment or online:

https://static-content.springer.com/esm/art%3A10.1186%2Fs12870-015-0523-4/MediaObjects/12870_2015_523_MOESM1_ESM.xls

Duchoslav and Fischer *BMC Plant Biology* (2015) 15:133
DOI 10.1186/s12870-015-0523-4

BMC Plant Biology

RESEARCH ARTICLE Open Access

Parallel subfunctionalisation of PsbO protein isoforms in angiosperms revealed by phylogenetic analysis and mapping of sequence variability onto protein structure

Miloš Duchoslav and Lukáš Fischer*

Abstract

Background: PsbO, the manganese-stabilising protein, is an indispensable extrinsic subunit of photosystem II. It plays a crucial role in the stabilisation of the water-splitting Mn_4CaO_5 cluster, which catalyses the oxidation of water to molecular oxygen by using light energy. PsbO was also demonstrated to have a weak GTPase activity that could be involved in regulation of D1 protein turnover. Our analysis of *psbO* sequences showed that many angiosperm species express two *psbO* paralogs, but the pairs of isoforms in one species were not orthologous to pairs of isoforms in distant species.

Results: Phylogenetic analysis of 91 *psbO* sequences from 49 land plant species revealed that *psbO* duplication occurred many times independently, generally at the roots of modern angiosperm families. In spite of this, the level of isoform divergence was similar in different species. Moreover, mapping of the differences on the protein tertiary structure showed that the isoforms in individual species differ from each other on similar positions, mostly on the luminally exposed end of the β-barrel structure. Comparison of these differences with the location of differences between PsbOs from diverse angiosperm families indicated various selection pressures in PsbO evolution and potential interaction surfaces on the PsbO structure.

Conclusions: The analyses suggest that similar subfunctionalisation of PsbO isoforms occurred parallelly in various lineages. We speculate that the presence of two PsbO isoforms helps the plants to finely adjust the photosynthetic apparatus in response to variable conditions. This might be mediated by diverse GTPase activity, since the isoform differences predominate near the predicted GTP-binding site.

Keywords: Gene duplication, GTPase, Homology modelling, Manganese-stabilizing protein (MSP), Oxygen evolving complex, Parallel evolution, Protein structure, PsbO

Background

Photosynthetic conversion of light into chemical energy in oxygenic phototrophs is accompanied with evolution of molecular oxygen released from water molecules. This process is realized in the oxygen evolving complex of photosystem II present in thylakoid membranes. Photosystem II (PSII) is a multisubunit protein–cofactor complex that uses light energy to oxidize water and to reduce plastoquinone. PsbO, also known as the manganese-stabilising protein, is one of the extrinsic subunits of photosystem II, located on the luminal side of the thylakoid membrane. PsbO is present in all known oxygenic photosynthetic organisms [1]. Despite the ability of the cyanobacterium *Synechocystis* sp. PCC 6803 mutant to grow photoautotrophically with deleted *psbO* gene [2], PsbO seems to be crucial for PSII function. Neither the mutant of green alga *Chlamydomonas reinhardtii* lacking PsbO, nor *Arabidopsis thaliana* (*A. thaliana*) with silenced expression of both *psbO* paralogs were able to grow photoautotrophically or even assemble PSII [3, 4].

* Correspondence: lukasf@natur.cuni.cz
Department of Experimental Plant Biology, Faculty of Science, Charles University in Prague, Viničná 5, 128 44 Praha 2, Czech Republic

Three-dimensional structure of PsbO from cyanobacterium *Thermosynechococcus* was resolved as a part of PSII by X-ray crystallography with a resolution down to 1.9 Å [5]. The crystal structure of PSII or PsbO alone from plants or other eukaryotes is not available. Some information about the structure of the whole PSII dimer surrounded by antenna complexes (the PSII-LHCII supercomplex) from higher plants was obtained by single particle cryo-electron microscopy and cryo-electron tomography [6–8]. Unfortunately, the resolution is insufficient to provide any plant-specific knowledge about the PsbO structure. Still, relatively high pairwise identity between PsbO sequences of *Thermosynechococcus* and higher plants (around 45 %) allows construction of homologous models for plant PsbOs [9, 10].

The X-ray crystallography of cyanobacterial PSII revealed that PsbO is a β-barrel protein (structural features of PsbOs are discussed in connection with our results and PsbO functions in chapter Discussion). It is located in the vicinity of the water splitting Mn_4CaO_5 cluster, but it is not directly involved in binding of the cluster [9]. The main function of the PsbO is to stabilise the Mn_4CaO_5 cluster, in particular to modulate the calcium and chloride requirements for efficient water splitting (for review see [11]). Besides this "basic" function, PsbO seems to be involved also in other processes (for review see [12, 13]). Spinach PsbO was shown to be able to bind GTP [14] and also to hydrolyse it, although very slowly [10]. It was proposed that the GTPase activity of PsbO in plants might be involved in D1 repair cycle [10].

In plants and algae, the PsbO protein is encoded by a nuclear *psbO* gene [1]. Transport to chloroplasts and thylakoids is ensured by two consecutive N-terminal transit peptides, that are cleaved to produce the mature PsbO [15]. *A. thaliana* expresses two *psbO* genes, *psbO1* [TAIR:At5g66570] and *psbO2* [TAIR:At3g50820], encoding for PsbO1 and PsbO2 proteins [16, 17]. The two isoforms differ in only 11 amino acids [18]; nevertheless, their function seems to be slightly different. Murakami *et al.* [18] reported that *A. thaliana* PsbO2 recovered oxygen evolution of PsbO-depleted spinach PSII particles less efficiently than PsbO1. The activity with PsbO2 reached only 80 % of that with PsbO1, while the binding efficiency of the isoforms was very similar. In contrast, the oxygen evolution of PSII membranes isolated from *A. thaliana* mutants lacking PsbO1 or PsbO2 was similar when corrected for the amount of PSII [19].

The amount of PsbO1 in wild-type *A. thaliana* plants is higher than that of PsbO2 [18–20]. The expression of the isoforms stays similar during plant development and during various short time stresses [21]. Only after 40 days of cold stress, noticeable change in relative abundance of isoforms was observed in favour of PsbO2 [22].

In *A. thaliana* mutants with an impaired *psbO1* or *psbO2* gene, the compensatory upregulation of the remaining isoform was observed. The expression level of PsbO2 in *psbo1* mutant was increased several times, reaching 75 % of the total amount of PsbO in wild-type. The expression level of PsbO1 in *psbo2* mutant was 125 % of the total PsbO in wild-type. The amount of other PSII proteins was affected similarly, leading to the same stoichiometry of PsbO per PSII as in wild type [19].

The *psbo1* mutant plants have pale green leaves, reduced rosette size and slower growth rate as compared to wild-type plants [17, 19, 23]. Descriptions of the *psbo2* mutant phenotype slightly differ from each other, probably because of different growth conditions and age of used plants [23]. Lundin *et al.* [19] observed growth rate slower than in wild-type and the leaf weight was even lower than that of *psbo1*, while Allahverdiyeva *et al.* [23] reported a phenotype very similar to that of wild-type.

Under growth light (120 μmol photons m^{-2} s^{-1}), the *psbo2* mutant had characteristics of electron transport chain very similar to wild-type, whereas investigation of the *psbo1* mutant showed malfunction of both the donor and acceptor sides of PSII and high sensitivity of PSII centres to photodamage [23]. Bricker and Frankel [24] reported that many of the defects of *psbo1* photosystems are reverted by higher concentration of $CaCl_2$, but Allahverdiyeva *et al.* [23] did not observe similar effect. Nevertheless, the importance of the PsbO2 seems to be exhibited under high light conditions. For example, the maximum quantum efficiency (F_V/F_M) values of wild-type and mutant plants became similar after 3 weeks of moderate light (500 μmol photons m^{-2} s^{-1}) [23]. Lundin *et al.* [19] reported that after 15 days of high light (1000 μmol photons m^{-2} s^{-1}), the *psbo1* mutant did not have significantly reduced leaf weight, whereas the leaf weight of *psbo2* mutant was reduced drastically.

Lundin *et al.* [19] also showed that *psbo2* mutant has lower level of phosphorylation of D1 and D2 subunits and that the degradation of photo-damaged D1 protein is impaired in this mutant. This, together with a finding that PSII membranes with PsbO2 have higher GTPase activity than PSII membranes with PsbO1 [21], led to a conclusion, that PsbO1 has a main function in the stabilisation of Mn_4CaO_5 cluster and the facilitation of the water oxidation reaction, whereas PsbO2 regulates the turnover of D1 subunit [19, 21, 23].

The presence of two PsbO isoforms is not unique for *A. thaliana*. Our previous study focused on the analysis of a spontaneously tuberising potato mutant revealed that potato plants also express two PsbO isoforms, one of which is missing in the mutant [25]. A comparison of the two characterised *A. thaliana* and two potato PsbO isoforms showed that sequences of the two paralogs in each species are more related than isoforms coming

from different species. It indicated independent duplication of *psbO* gene in these two species. To understand this unexpected phylogeny and evolution of PsbO isoforms, we did a detailed analysis of *psbO* sequences from a number of land plant species. Mapping the sequence differences between PsbO proteins from various species and families and between PsbO isoforms in individual species on their tertiary structure, we found that the evolution of the two isoforms was parallel in numerous angiosperm lineages. Based on the location of isoform-specific differences and literature data about *A. thaliana* and spinach PsbOs, we hypothesise that the pairs of isoforms present in many species differ in GTPase activity and that the presence of proteins diversified in this way helps to improve photosynthetic performance under varying conditions.

Materials and methods

Retrieval and analysis of psbO sequences

Sequences of expressed *psbO* genes were retrieved as ESTs (expressed sequence tags) and assembled ESTs (PUTs, PlantGDB-assembled unique transcripts) in public sequence databases NCBI GenBank [26] and PlantGDB (Plant Genome Database) [27], respectively. The database searches were performed using tBLASTn [28, 29] with potato PsbO protein sequence (sequence "Solanum tuberosum 2", translation of [PlantGDB:PUT-157a-Solanum_tuberosum-55973153]) as a query. ESTs were aligned into contigs for each species using "De Novo Assemble" tool of Geneious R6 [30]. Formation of consensus sequences from multiple overlapping ESTs strongly increased reliability of analysed sequences compared to individually submitted annotated cDNAs, some of which contain evident errors. All retrieved sequences were aligned using MAFFT v7.017 [31] and incomplete and unreliable sequences were excluded from further analyses (see analysed sequences in Additional file 1). Spinach *psbO* sequence was retrieved as cDNA [GenBank:X05548.1] because of the lack of ESTs and included in alignment for comparison (Additional file 2). Indexing of isoforms in each family was random and does not reflect relation to *A. thaliana* isoforms.

Phylogenetic trees were built from *psbO* coding sequences by maximum likelihood (ML) method using CIPRES Science Gateway [32]. ML analysis was implemented in tool RAxML v7.6.6 [33] using GTRGAMMA approximation with 1000 bootstrap replicates.

The presence and position of introns was analysed by comparing *psbO* cDNAs (Additional file 1) and corresponding genomic sequences, obtained using BLASTn [28, 29] searches in Phytozome database [34] for the following representative species with easily available genomic sequence: *Arabidopsis lyrata*, *Arabidopsis thaliana*, *Brassica rapa*, and *Thellungiella halophila* from Brassicaceae family and *Oryza sativa*, *Physcomitrella patens*, *Populus trichocarpa*, *Solanum lycopersicum*, and *Vitis vinifera* from other families.

Evaluation of PsbO sequence variability

The frequency of differences between isoforms, between species and between families were calculated for each position in the alignment independently using scripts written in R language [35] and partially using SeqinR package [36]. Plant families represented with just a single PsbO sequence were not included in the calculation. Only two most divergent isoforms were considered in case of species expressing more than two isoforms. All sequences excluded from calculation are marked with an asterisk in Additional file 2. To estimate the between-isoform and between-species variability across all angiosperms, both types of differences were first calculated for every family independently and afterwards the values were averaged, in order to avoid bias caused by different numbers of analysed species within each family.

The frequency of between-isoform differences within a family was calculated as follows; first, each position in the alignment was assigned 0 or 1 (for the same or different amino acids in the two compared isoforms, respectively) for each species and then the values were averaged within a family. To get the frequency of between-species differences, all species within a family were compared pair wise with each other, giving the values 0, 0.5 or 1 (for amino acids in both isoforms identical, amino acid in one isoform identical or no identical amino acid) for each position and each comparison. Values for each position were averaged within a family. As the dependency of this average variability value on the proportion of species that have certain amino acid different from the consensus is not linear, it was linearised using the equation

$$\Delta_{species\ linear} = \frac{(2n-1)-\sqrt{4\left(1-\Delta_{species}\right)n\left(n-1\right)+1}}{2\left(n-1\right)}$$

where n is the number of compared species, $\Delta_{species}$ is the non-linear average value of between-species variability (the mean from pair wise comparisons) and $\Delta_{species\ linear}$ is the linearised value of the between-species variability.

To estimate the between-family variability, the above mentioned method for the calculation of the between-species differences was applied on sets containing sequences from just one species from each family. A mean values obtained from all such combinations of species (53,760 in total) included both between-species and between-family differences, so the values of between-species differences were subtracted from it, giving the net between-family differences.

Homology modelling and mapping of variability on the protein structure

Homology model of potato PsbO (sequence "Solanum tuberosum 2") was built using Swiss-Model server [37, 38] based on PsbO from cyanobacterium *Thermosynechococcus vulcanus* [PDB:3ARC] (chain O) [5]. Extra 13 amino acids present on the N-terminus of potato PsbO were pasted to the model manually using Swiss-PdbViewer v4.1.0 [39] without attempt to show any folding.

Homology model of potato PsbO was coloured according to the frequency of the respective type of variability using Swiss-PdbViewer v4.1.0 [39] and scripts written in R language [35]. The images were rendered using POV-Ray v3.6 [40].

Determination of spatial centres of differences

Spatial centres of the differences were calculated using coordinates of α-carbon atoms of amino acids in the PsbO homology model using scripts written in R language [35]. The arithmetic mean of the coordinates was weighed by frequency of the respective difference on each position. The 13 N-terminal amino acids with unknown folding were excluded from the calculation. Overall spatial centres of the differences between isoforms and the differences between species in angiosperms were calculated as an arithmetic mean of spatial centres calculated for all families. The statistical significance of the divergence in the location of the spatial centres of the between-isoform and the between-species differences was assessed using a randomisation test. Variable positions in the alignment were randomly shuffled and the spatial centres for the between-isoform and the between-species variability were calculated. Difference between means of the two types of spatial centres projected on the axis of highest variability was compared with the value obtained for real alignment. The *p*-value was calculated from 50,000 randomisations.

Results

The majority of angiosperm species express two *psbO* genes

Searching public databases for expressed sequences of *psbO* genes from land plants (Embryophyta) we obtained 91 sequences from 49 species and 36 genera. Analysis of these sequences showed that the majority of the analysed angiosperm species express more than one, in most cases two *psbO* isoforms (Additional file 3). In contrast, all analysed representatives of gymnosperms (from both Cycadophyta and Coniferophyta groups) seem to express only one *psbO* isoform.

In monocots, *psbO* sequences were available from only two families: Zingiberaceae species have two *psbO* isoforms, whereas most Poaceae species with available ESTs express only one *psbO* gene. A single *psbO* gene was found also in the genomic sequence of *Oryza sativa*. *Zea mays*, a recent tetraploid, expresses two isoforms with little divergence (Additional file 3).

Among dicots, Malvaceae, Myrtaceae, Phrymaceae and Rutaceae seem to express only one *psbO* gene. Asteraceae, Euphorbiaceae, Fabaceae, Salicaceae, Solanaceae and Vitaceae seem to express two *psbO* genes (or four in the case of recent tetraploids such as *Glycine max* or *Nicotiana tabacum*). Brassicaceae have various numbers of *psbO* isoforms; however, most of them can be sorted into two groups. While *Arabidospsis thaliana* expresses just two isoforms (*psbO1*, *psbO2*), each from one group, genus *Brassica* expresses three to five genes - one gene corresponds to *psbO2* of *A. thaliana*, while the gene orthologous to *psbO1* of *A. thaliana* is present in several very similar sub-isoforms (4 in *B. napus*, 3 in *B. rapa* and 2 in *B. oleracea*; Additional files 3 and 4). *Thellungiella halophila* expresses three *psbO* genes, two of which correspond to *psbO1* and *psbO2* of *A. thaliana*, the third one is most similar to pseudogenes that can be found in genomic sequences of *A. thaliana* [TAIR:At4g37230], *Arabidopsis lyrata* [GenBank:XM_002866937] and *Brassica rapa* [Phytozome:Bra017790] (data not shown).

Pairs of PsbO isoforms evolved in every angiosperm family independently

The majority of analysed angiosperm species have just two PsbO isoforms (Additional file 3). Such situation could likely results from a gene duplication event in a common ancestor followed by functional divergence of the paralogs. The paralogous genes encoding the functionally divergent isoforms can be inherited by descendants or potentially lost. However, the phylogenetic tree derived from coding sequences of *psbOs* indicates a different evolutionary scenario (Fig. 1).

The basic topology of the phylogenetic tree does not contain dichotomous branching to two groups of functionally diverged orthologs at the tree base, but it reflects basic phylogeny of land plant families. The branching to two isoforms is also absent at the base of angiosperms. Instead, the branching events are clearly present at the bases of several families (for example Solanaceae, Fabaceae, Brassicaceae, Zingiberaceae; Fig. 1). This unexpected topology indicates that duplications of *psbO* gene occurred independently in each plant family that contains species with multiple PsbO isoforms. Moreover, these families do not form any cluster in the phylogenetic tree of *psbO* or in the consensual phylogeny of angiosperms.

To further confirm the independent duplication of *psbO* genes in ancestor of each angiosperm family, the presence and position of introns was analysed in available genomic sequences of *psbO* genes. According to this analysis, all land plants have an intron at a conserved site, 12 nucleotides upstream the boundary between sequences

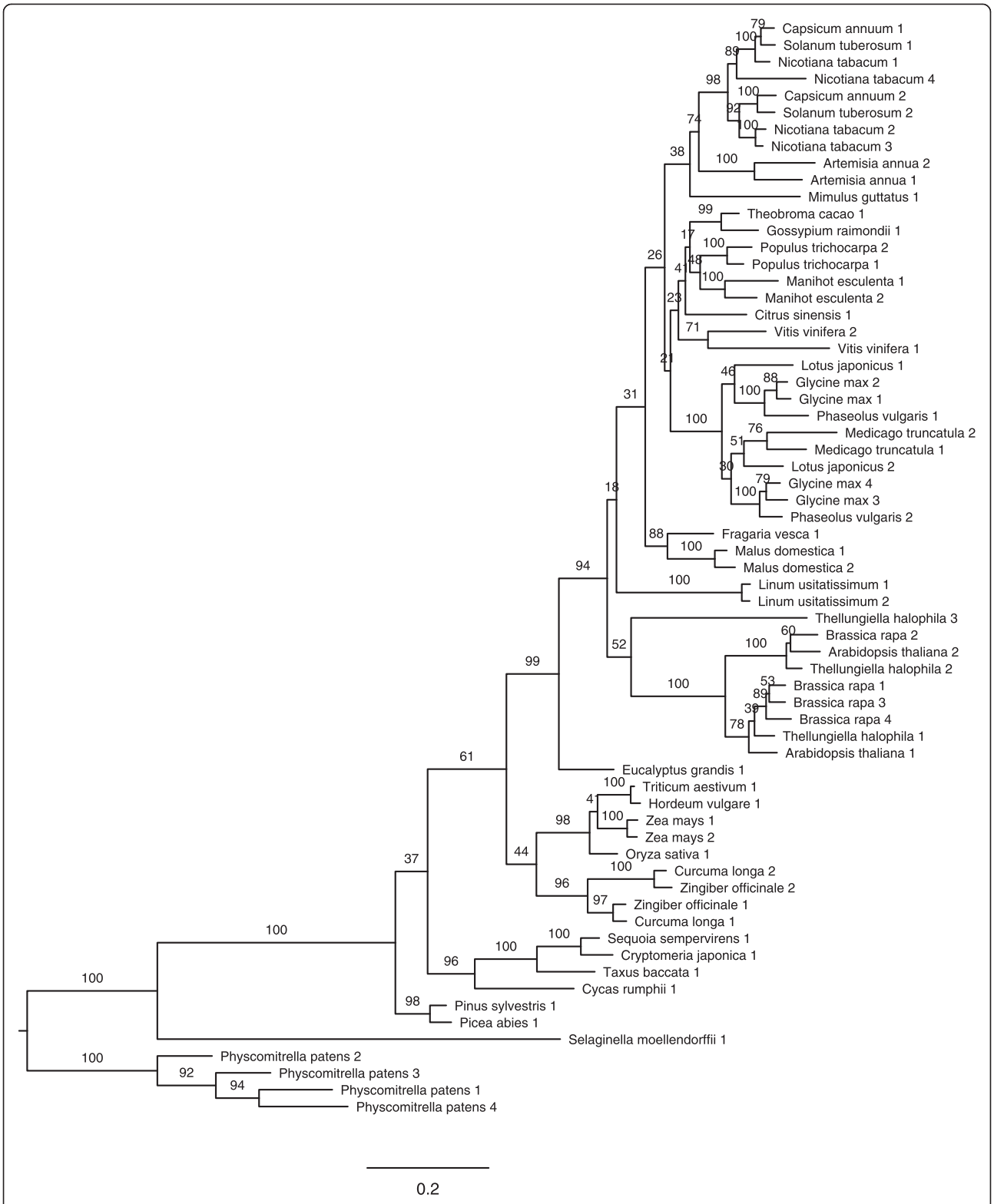

Fig. 1 A phylogenetic tree from coding sequences of *psbO* genes from 36 genera of land plants. Each genus is represented by sequences from only one species for the sake of simplicity. Sequences from different species belonging to the same genus are very similar and their inclusion does not change the phylogenetic tree topology (see the full phylogenetic tree in Additional file 4). The tree was constructed by the maximum likelihood method, numbers at branches denote bootstrap percentages

encoding the transit peptide and the mature protein. In addition, all *psbO* genes from Brassicaceae family contain an additional intron, 282 nucleotides downstream the boundary between the transit peptide and the mature protein. The intron is present at a conserved site in all *psbO* genes in this family, including the most divergent isoform of *Thellungiella halophila*. This indicates that all these *psbO* genes evolved from one common Brassicaceae-specific ancestor gene containing the additional intron, absent in *psbOs* in other families.

Extent of divergence of PsbO isoforms is similar in all species

The extent of differences between protein sequences of PsbO isoforms in every species is in the same range, even though the duplication seems to have occurred in each family independently. The numbers of different amino acid residues range from six in a recent tetraploid *Zea mays* to 23 in *Populus deltoides* and *Populus x canadensis* (2–9 % of total residues; Additional file 3). Interestingly, similar divergence between isoforms can be found also in the moss *Physcomitrella patens* (24 different amino acid residues between two most divergent isoforms).

The level of differences between PsbO isoforms is kept within this range even if the duplication events of *psbO* occurred at different times in evolutionary history. For instance, pairwise identity of nucleotide sequences encoding mature PsbOs of *V. vinifera* (80 %) is much lower than that of *Populus trichocarpa* (92 %). This indicates that the duplication of the *Vitis psbO* gene probably occurred earlier compared to that of the *Populus* gene. However, pairwise identity of the protein sequences of PsbO isoforms of *V. vinifera* (93 %) is similar to that of *P. trichocarpa* (92 %).

Three classes of PsbO sequence variability

Considering that many angiosperm species express two isoforms of *psbO*, we asked whether the differences between the isoforms are similar in multiple families despite the independent duplications of *psbO* genes. Detailed analysis of the sequence alignment failed to identify any compact region in the primary sequence that would be specific for one or the other isoform across the analysed plant families. Also, single positions with similar differences between isoforms in the majority of species were rare (see the alignment in Additional file 2).

To analyse the character of the differences in PsbO sequences in detail, we assorted the variability into three classes: i) variability between isoforms (within a species), ii) variability between species (within a family) and iii) variability between families (Fig. 2). Frequencies of these three classes of variability were calculated for each position of the primary sequence (Additional file 2; see Materials and methods section for details). In the alignment of mature PsbO sequences from angiosperms (Additional file 2), 59 % of positions are fully identical, 77 % of positions can be described as conserved (with low level of variability below 10 %). The variability in the remaining 23 % of positions could stem from either selection pressure favouring a specific substitution (positive selection), or, on the contrary, from the lack of strong selection pressure to keep the position invariable (negative selection). The lack of selection pressure should result in frequent random changes and a high level of variability in all three classes. When analysing the PsbO sequences, it was obvious that a certain class of variability predominated at many positions and that the overlap between the classes at a given position was only partial (Additional file 5).

Amino acid residues varying between isoforms differ predominantly in the length of side chains

Analyses of substitutions at positions variable between isoforms showed that some substitutions were more frequent than others. The most frequent differences between

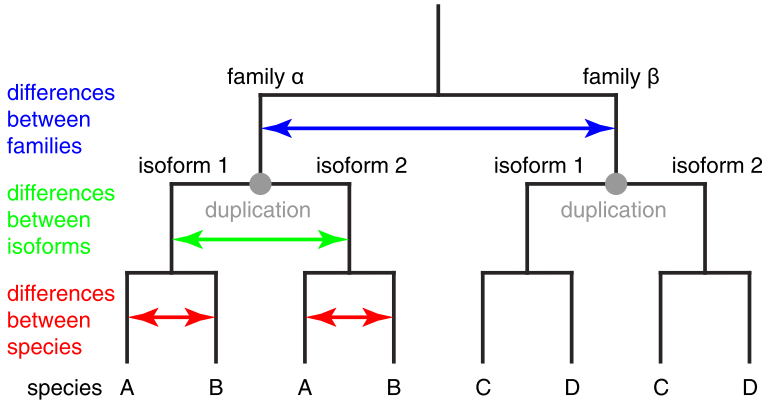

Fig. 2 A scheme of the *psbO* phyllogeny showing three classes of PsbO sequence variability. Differences between families are in blue, differences between isoforms in green and differences between species in red

isoforms resided in mutual exchanges of glutamic (E) and aspartic (D) acid residues (more than 20 % of all substitutions; Fig. 3). Distribution of these two residues within the isoform pairs was usually unequal. In PsbO pair in certain species, glutamic acid often predominated in most of variable positions in one isoform, whereas aspartic acid in the other (Additional file 6). The total number of these two residues was more or less constant. According to this distribution and the residue present on position 140 (E139 in spinach), almost each pair of isoforms could be divided into the E-type isoform (with predominating longer glutamate) and the D-type isoform (with prevailing shorter aspartate). According to this, *A. thaliana* PsbO1 clustered into D-type isoforms, whereas PsbO2 into E-type, though the divergence in D/E ratio between isoforms was not as strong as in many other species. PsbOs in the analysed species with single isoform were either closer to the E-type or to the D-type isoforms or were in the mid-way, e.g. PsbOs from Poaceae species or *Linum usitatissimum* clustered with E-type isoforms, whereas PsbOs from non-herbaceous Rutaceae or Myrthaceae species were close to D-type isoforms (Additional file 6). The D-type isoforms were also often prolonged at C-terminus with an additional amino acid residue.

Exchanges in other amino acid residues were less conserved among various families. But generally, substitutions between residues, which differed only in the length of the side chain and had similar physicochemical properties, predominated over substitutions between residues with more variable character. The three most frequent amino acid substitutions (D-E, I-V and S-T; Fig. 3) match these criteria and comprise together almost 50 % of all exchanges. Though seemingly synonymous, these substitutions are strongly conserved in orthologous isoforms within families and in some cases even shared across more families (see the alignment in Additional file 2).

Residues varying between isoforms cluster together on the tertiary structure of PsbO

The positions with amino acids varying predominantly between isoforms did not cluster together in the primary sequence. As protein function is tightly connected with tertiary structure, we decided to analyse spatial location of amino acid substitutions between PsbO isoforms on the protein structure. Because no crystal structure of eukaryote PsbO is available, we constructed homologous model of PsbO2 from *Solanum tuberosum* using PsbO structure from *Thermosynechococcus vulcanus* [5] as a template (identity of the protein sequences is 47 %). All PsbO sequences of angiosperms are well comparable on a single model of structure thanks to a very high conservation of both the amino acid sequence and the length

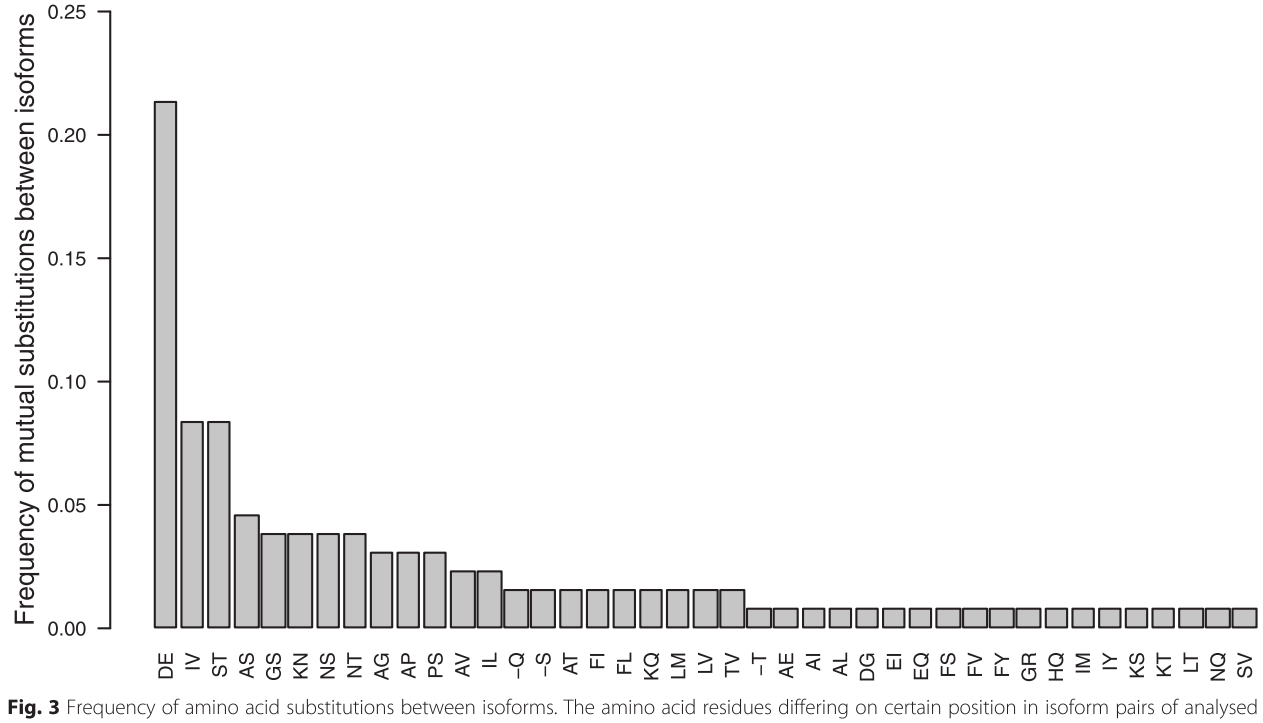

Fig. 3 Frequency of amino acid substitutions between isoforms. The amino acid residues differing on certain position in isoform pairs of analysed species are given below the bars, the hyphen (–) represents a gap. For the analysis, one representative species with two isoforms was chosen from each family in order to avoid the bias caused by various numbers of species with available data in each family (analysed species: *Arabidopsis thaliana*, *Artemisia annua*, *Lotus japonicus*, *Malus domestica*, *Manihot esculenta*, *Populus trichocarpa*, *Solanum tuberosum*, *Vitis vinifera*, *Zea mays*, *Zingiber officinale*)

of the chain. In the alignment of 78 protein sequences of PsbOs from angiosperms, 59 % of positions are fully identical and the length of the chain of mature proteins varies mostly between 247 and 248 amino acid residues (Additional file 2).

The isoforms diverged independently in every family, so we first mapped the isoform differences on the model in each family separately. Fig. 4a shows the model of PsbO coloured according to the frequency of differences between isoforms in species of the Solanaceae family. The differences are situated mostly on the luminal end of the β-barrel structure and some differences can be found also on the β1-β2 loop. Comparing this location with positions of differences between isoforms averaged across all angiosperm families, we can see that the general pattern is shared (Fig. 4b). Interestingly, the same pattern is exhibited also in the recently diverged isoforms of maize with only 6 different amino acids and in the moss *Physcomitrella patens* with four PsbO isoforms (Additional file 7).

Before drawing any conclusions, we had to prove that this spatial location is specific for differences between isoforms and does not reflect a high level of general variability in these regions. We compared the position of isoform differences with between-species differences in all families (Fig. 4c). We found that differences between species (red-coloured in the figure) are more dispersed over the PsbO structure. To allow statistical analysis, we calculated spatial centres of between-isoform differences and between-species differences (green and red spheres in Fig. 4c, respectively) for each family. The spatial centres of isoform differences are shifted towards the luminal end of the β-barrel (with one exception, the Salicaceae family, which has the centre of differences between isoforms shifted towards the β1-β2 loop due to high frequency of differences in this part of the structure). The

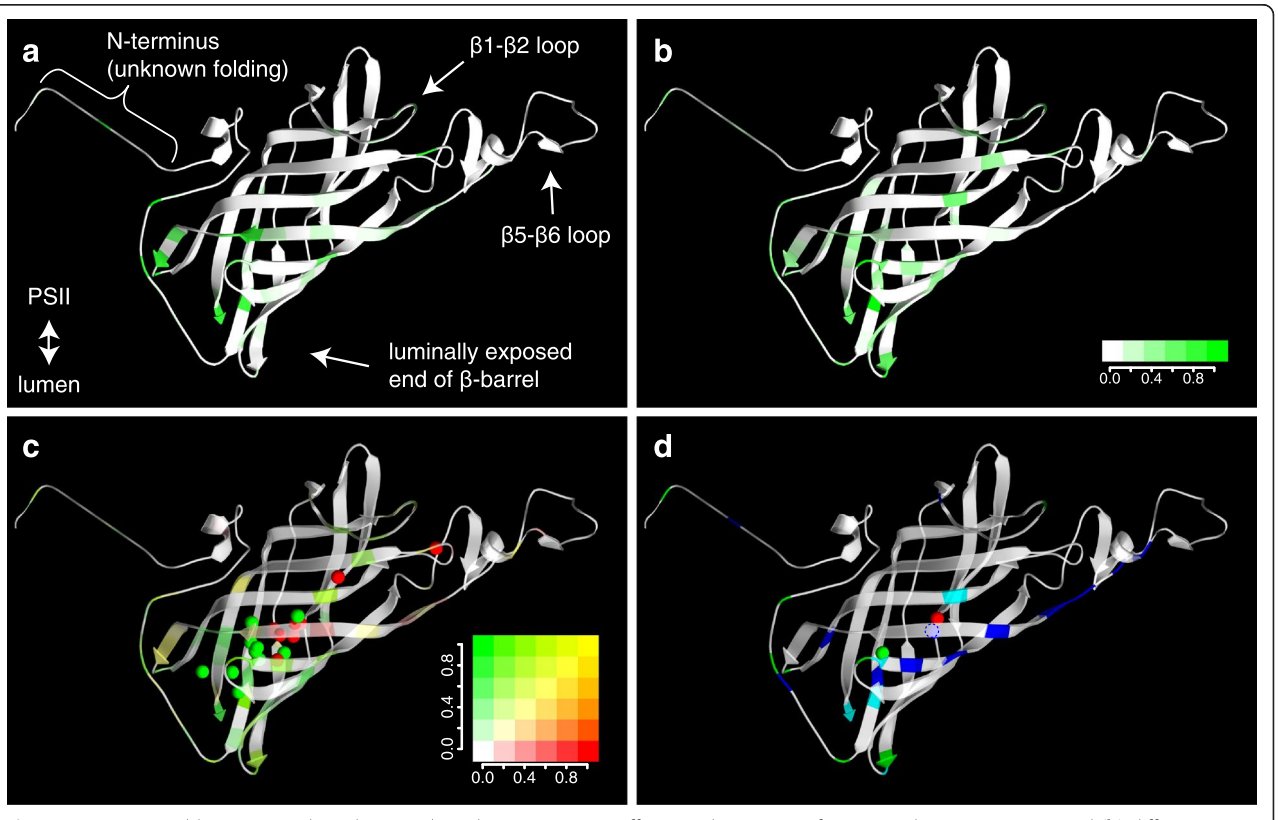

Fig. 4 Mapping variable amino acid residues on the PsbO structure. **a** Differences between isoforms in Solanaceae species and (**b**) differences between isoforms averaged across all angiosperm families. The varying positions are green-coloured depending on frequency of differences among the analysed pairs of isoforms. **c** Merged differences between isoforms (in green) and between species (in red) with equally coloured spheres indicating spatial centres of these differences calculated separately for each angiosperm family, the frequency of particular differences on each position is indicated by colour gradient. **d** Merged averaged differences between isoforms (in green), between plant families (in blue) or both types (in cyan); only positions with a value of variability above a given threshold (0.24) are shown together with overall spatial centres of differences between isoforms, species (within families) and families (green, red and blue spheres, respectively). The homology model of the *Solanum tuberosum* PsbO2 based on the X-ray structure of cyanobacterial PsbO [PDB:3ARC] [5] was constructed using Swiss-Model program [38]; the first 13 N-terminal amino acids were not present in the template structure, so they were pasted in the model without attempts to show any folding and they were not included in calculation of the spatial centres

shift of spatial centres of isoform differences compared with the centres of between-species differences is significant according to a randomization test ($p = 0.002$).

PSII-exposed surface is conserved, while differences between families are mainly on the luminal side of the β5-β6 loop

Mapping of all variable positions on the model of PsbO structure also showed that the PsbO surface interacting with PSII core proteins is fully conserved in angiosperms with the exception of the β1-β2 loop (see Fig. 5). β1-β2 loop interacts with CP47 protein from the other monomer of PSII [5, 9].

Differences between families are the most frequent class of differences among PsbO sequences (Additional files 2 and 5). Fig. 4d depicts differences between families merged with the differences between isoforms and overall spatial centres of the three classes of differences (represented with green, red and blue spheres). The differences between families are more spread over the PsbO structure compared to the differences between isoforms, similarly to the differences between species within families. The highest frequency of differences between families is in the part of β5-β6 loop that is not interacting with PSII core proteins (the amino acid side chains are pointing towards thylakoid lumen) and the adjoining part of the β6 strand.

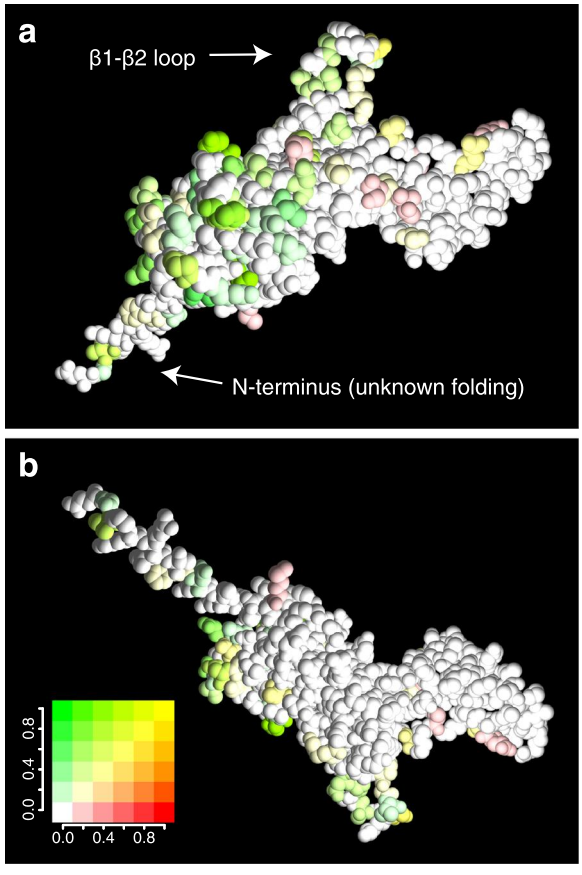

Fig. 5 Mapping variable amino acid residues on the PsbO structure. **a** View from thylakoid lumen, (**b**) view from PSII. Differences between isoforms (in green) are merged with differences between species (in red); the frequency of particular differences on each position is indicated by colour gradient. The homology model of the *Solanum tuberosum* PsbO2 based on the X-ray structure of cyanobacterial PsbO [PDB:3ARC] [5] was constructed using Swiss-Model program [38]; the first 13 N-terminal amino acids were not present in the template structure, so they were pasted in the model without attempts to show any folding

Discussion

Mechanism of duplication and subfunctionalisation of *psbO*

Several studies demonstrated that *A. thaliana* expresses two *psbO* paralogs [17–19, 21]. Here we show that *A. thaliana* is not an exception and that species from 9 out of 15 investigated angiosperm families also express two distinct *psbO* genes (Additional file 3). Unexpectedly, the phylogenetic analysis revealed that the *psbO* gene was not duplicated in the common ancestor of angiosperms, but the duplication occurred many times independently in individual families (Fig. 1).

There are various mechanisms by which gene duplication can occur. In terms of its extent, duplication can involve single genes, larger segments, chromosomes or entire genomes [41]. In *A. thaliana* and *Populus trichocarpa* we found that chromosomal segments containing *psbO* paralogs are collinear (i.e. contain homologous genes in a similar order; Duchoslav, Vosolsobě, and Fischer, unpublished results), which suggests that *psbO* was duplicated within the context of a larger-scale duplication.

The phylogenetic tree topology indicates that the duplication event occurred in ancestors of numerous families prior to extensive species radiation. The radiation that involved many extant plant lineages in Paleogene, was likely facilitated by the whole genome duplications (WGD) dated to the last global extinction period at the Cretaceous–Paleogene boundary about 66 million years ago [42, 43]. Based on this indirect evidence, we suggest that the *psbO* duplication was not gene specific, but rather that the paralogs were in many cases retained after WGD events that occurred independently in ancestors of many successful angiosperm families.

After WGD, most duplicated genes gradually accumulate deleterious mutations and vanish from the genome (within millions of years). More rarely the duplication leads to neo- or subfunctionalisation of the paralogs if these changes improve fitness [41]. Currently, one of the best models explaining stabilisation of duplicated genes is the EAC model of subfunctionalisation (escape from adaptive conflict) [44] based on the fact that a single protein can perform multiple catalytic or structural functions. In such case, the selective optimization of one function may lead to a decline in another function,

creating an adaptive conflict that preserves the single copy gene/protein in an intermediate state. Casual gene duplication can provide a solution – escape from the adaptive conflict *via* functional specialisation of the resulting paralogs [41].

Multiple angiosperm species contain just two *psbO* paralogs with similar extent of diversification, so we assume that the presence of two different PsbO proteins gives an advantage to these species. Although many plants prosper with a single PsbO gene, in species with two isoforms, the loss of one isoform negatively affects growth and photosynthesis, e.g. in *A. thaliana* [18, 19, 23, 45] or potato [25]. It indicates that functions of current diversified PsbO isoforms are no more equivalent due to subfunctionalisation after the duplication.

Structural aspects in PsbO diversification

Protein functions are connected with protein structure. Therefore, identification of common structural differences between isoforms in multiple species can indicate common functional adaptation. If various plants used duplicated *psbOs* to solve the same adaptive conflict, the structural and functional differentiation of PsbO isoforms would be similar or identical irrespective of independent duplication in individual families.

To evaluate the between-isoform differences, we first divided the overall variability of PsbO sequences on each position of the primary structure into three classes. The variability in current PsbO sequences reflects both differences present already in the ancestor species before *psbO* duplication (*between-families variability*) and differences obtained after the duplication, including specific diversification of isoforms (*between-isoforms variability*) and species-specific changes (*between-species variability*; Fig. 2; see quantification bellow the alignment in Additional file 2). The frequency of each variability class on specific positions was mapped on the homology model of PsbO (Fig. 4). The model corresponded to other published homology models of higher plants' PsbO [9, 10]. The mapping showed that occupancy of the differences on the PsbO surface was unequal and the locations of the three classes of variability significantly differ.

There are practically no differences between isoforms on the PSII-binding surface of PsbO (Fig. 5). However, Murakami *et al.* [18] reported that PsbO2 of *A. thaliana* is less efficient in reconstitution of oxygen evolution *in vitro* compared to PsbO1. Our analysis showed that the PSII-binding surface is highly conserved in all angiosperms. It indicates that the differences in water oxidation observed by Murakami *et al.* [18] were not caused by direct modulation of water oxidation on Mn_4CaO_5 cluster, but rather by some indirect effect.

The biggest contrast in localisation of between-isoform differences and other types of differences (between-family and between-species) is in the part of β5-β6 loop that is not interacting with PSII core proteins (the amino acid side chains are pointing towards lumen) and the adjoining part of the β6 strand. In this part of PsbO, there is a very high frequency of between-family differences and a high frequency of between-species differences, whereas between-isoform differences are nearly absent. This suggests that this part of the PsbO surface might be involved in binding of some other protein, whose interaction surface can differ in individual species or families. As isoforms do not differ in this region, it seems that both isoforms need to retain this interaction identical. The presence of a hypothetical interactor is further supported by the fact that an unassigned density was detected in this part of PSII supercomplex structure by cryo-electron tomography [8].

The between-isoform differences were located mostly at the end of the β-barrel protruding into the lumen and on the β1-β2 loop. This pattern was similar in all analysed families and even in the moss *Physcomitrella* and the relatively recently duplicated *psbO* in maize (Fig. 4, Additional file 7). This indicates that the differences between isoforms probably enabled the same or similar functional adaptation of PsbOs in all analysed families. Since the *psbO* duplications were independent, the functional divergence of PsbO isoforms likely represents a parallel evolution, further supporting the impact of observed diversification of PsbO isoforms.

Functional differences between PsbO isoforms

We found that the location of the differences between PsbO isoforms of *A. thaliana* fits the pattern found in other angiosperms. Nine out of 11 different amino acids are located at the luminal base of β-barrel and one is located on the β1-β2 loop (Additional file 7). Both PsbO isoforms of *A. thaliana* are able to stabilise the manganese-calcium cluster and enable water splitting [18, 19]. PsbO1 was demonstrated to provide more efficient water splitting [18], whereas PsbO2 was reported to have higher GTPase activity and was proposed to participate in D1 repair cycle [19, 21, 23].

The highest frequency of between-isoform differences is located just around the hypothetic GTP-binding site predicted by Lundin *et al.* [10], which is situated inside the luminal end of the β-barrel. Lundin *et al.* found hypothetic non-canonical GTP-binding domains in spinach [10] and *A. thaliana* PsbO sequence [21]. G1 domain, binding α-phosphate, was predicted in β1 sheet, G2-G3 domain, binding γ-phosphate, in β2 sheet and G4 domain, binding guanine ring, in β4-β5 loop (marked in the alignment in Additional file 2). Regions surrounding the G2-G3 domain, i.e. β1-β2 and β2-β3 loops, were predicted to be Switches I and II, respectively. These switches could have different conformations in GDP- and GTP-bound state.

The proposed G2-G3 domain is rather conserved in angiosperms, whereas G1 and G4 domains and Switches I and II have high frequency of differences between isoforms. The position with the most frequent differences between isoforms (T46 in spinach PsbO) is located in G1 domain, the position with the second most frequent differences between isoforms (E139 in spinach PsbO) is in G4 domain (see positions 47 and 140 in alignment in Additional file 2).

Since PsbO isoforms in *A. thaliana* were found to differ in GTPase activity [21] and the location of differences between them corresponds to the situation in other species, we propose that, in general, the differences between isoforms might modulate the GTPase activity of PsbO.

It is important to mention that the amino acids varying between isoforms have side chains mostly pointing outside of the β-barrel and not inside towards the predicted GTP-binding site. However, these amino acids might not only change the binding of GTP, but also modulate accessibility of the binding site for GTP or binding of some regulatory protein. Consistently with this assumption, we found that amino acid residues with longer side chains often predominated in one isoform, whereas residues with shorter chains in the other (mainly in the case of chains with interaction-competent carboxylic groups). Though the substitution between glutamic and aspartic acid is often regarded to be nearly synonymous, these residues alternate within isoform pairs very regularly on some positions. Their strong conservation in orthologous isoforms within families (and in some cases even across more families) indicates that they can affect the PsbO function. The simple increase in the length of amino acid side chain can allow the protein to keep the structure, isoelectric point and other important properties unchanged, whereas it can strongly facilitate (affect) the interactions with other proteins, e.g. PsbP, another extrinsic protein of PSII. Interestingly, PsbP was reported to have a crystal structure similar to the GTPase Ran regulatory protein [21, 46]. The importance of certain carboxylic amino acid residue in PsbO can be demonstrated on spontaneously tuberising potato mutant, where the absence of one PsbO isoform could not be complemented with another allele with a point mutation substituting glutamic acid for aspartic acid (Fischer and Duchoslav, unpublished results; [25]).

Based on the situation in *A. thaliana* and suggested isoform evolution by the "escape from adaptive conflict" scenario, we can hypothesise that the amino acid substitutions adapt the isoform to its specific function, which is obviously connected with losing in the other of the two functions. Murakami et al. [18] tested efficiency of *in vitro* oxygen evolution with native PsbO isoforms and their chimers that combined fragments (or selected amino acids) from both *A. thaliana* isoforms. They found that the weaker performance of PsbO2 was connected mainly with the C-terminal third of the protein, namely with two substitutions, V186S (in β5-β6 loop) and L246I (with side chain pointing towards the hypothetical GTP-binding site). On the contrary, substitution V204I (also with side chain pointing towards the hypothetical GTP-binding site) improved the activity and obviously compensated for the decrease in oxygen evolution caused by substitutions on the positions 186 and 246. Unfortunately, the GTPase activity of PsbO was proposed later, so the activity was not determined in these chimeric proteins to test the trade-off hypothesis. The importance of the C-terminal part (often differing between isoforms) was also demonstrated in spinach PsbO. The last three amino acid residues, including leucin at position 246 (245 in spinach), were shown to be critical for binding to PSII and for restoration of oxygen evolving activity [47].

Besides the modulation of the GTPase activity, there are some other presumptive interactions of PsbO that can be affected by the observed differences between isoforms. An obvious possibility is modulation of interaction with PsbP (mentioned above) or PsbQ, the other extrinsic proteins of PSII. The extrinsic proteins of PSII were suggested to be involved in the interaction between the thylakoid membranes across the lumen [12, 48]. Thus, the changes on the luminal end of the β-barrel of PsbO might modulate this interaction regardless whether the interaction is direct (PsbO-PsbO) or via other extrinsic proteins. Another possibility is that PsbO is interacting with some protein bound to the same membrane through the luminal end of the β-barrel, which is protruding not only to the lumen but also slightly over the outer rim of PSII towards the strongly bound (S) LHCII trimer [49]. This speculation is supported by the evidence that removal of PsbO has an effect on the position of LHCII in PSII-LHCII supercomplex [50] and that there is an unassigned density on the luminal side of the LHCII trimers in cryo-electron tomography structure of the supercomplex [8]. The N-terminus of PsbO might also be involved in such interaction, because angiosperm PsbOs are longer by usually 13 amino acids compared to the cyanobacterial protein analysed by Umena *et al.* [5]. Numerous biochemical studies were focused on site-directed mutagenesis of PsbO (reviewed in ref. [51] and [11]). However, these studies cannot be used for interpretation of our results, since the mutated residues were mostly the highly conserved ones.

Speculative model on the role of PsbO isoforms

Our findings together with literature data led us to formulate a speculative model explaining the functional specialisation of PsbO isoforms. Hong *et al.* [52] showed that the oxidation state of the Mn_4CaO_5 cluster influences

the structure of PsbO. We suggest that when the D1 protein and Mn_4CaO_5 cluster get damaged, PsbO shifts in the GTPase cycle. This induces a change in conformation of the β1-β2 loop. As the β1-β2 loop is interacting with the other monomer of PSII in the PSII dimer [9], such change might induce monomerisation of PSII [10] and its release from the semi-stabile organization in grana that allows diffusion to stroma lamellae. In stroma lamellae, PsbO released from PSII changes the GTPase state and D1 is degraded [53]. After reassembly of PSII, PsbO binds back.

We propose that the PsbO1 isoform is adapted for low light conditions. It has lower GTPase activity [21] (or lower affinity to GTP) and thus it does not induce as rapid monomerisation of PSII and exchange of damaged D1 subunit as the PsbO2 isoform. It was shown that under low irradiance, a part of PSII-LHCII supercomplexes form ordered crystalline arrays [54] and the grana are tightly stacked [55]. Thus, PsbO1 might prevent premature disturbance of the effectively working crystalline arrays of PSII-LHCII supercomplexes and support tight stacking of thylakoid membranes. We also suggest that PsbO2 is, on the other hand, optimized for high light conditions, when efficient light harvesting is not important due to the excess of energy, but the repair of damaged D1 subunits must be very fast to prevent further damage of photosynthetic complexes. Correspondingly, Herbstová *et al.* [56] demonstrated that high light treatment leads to an increase of protein mobility in grana thylakoids. Moreover, the proportion of PSII in PSII-LHCII supercomplexes in *A. thaliana* is high in *psbo2* mutant and low in *psbo1* mutant compared to wild-type plants [21]. Thus, the fast GTPase activity (or high affinity to GTP) of PsbO2 might facilitate rapid disorganisation of PSII-LHCII supercomplexes and crystalline arrays allowing rapid diffusion of damaged PSII out of the grana and their redeployment after D1 replacement. Modulation of the ratio of PsbO1 and PsbO2 bound to PSII can help to adjust and optimise the photosynthetic performance in response to light conditions. An increase in the amount of PsbO2 in *A. thaliana* after long-term cold stress [22], which is in many features similar to high light stress [57], supports our speculation. It suggests that the PsbO1/2 availability is regulated transcriptionally in the long term. The momentary binding of isoforms might be regulated, for example, by different dynamics of the GTPase cycle.

In the species with single PsbO isoform, the function of the PsbO is likely in the mid-way between the two specialised isoforms present in other species and supports both of the specialised functions, at least at the basic level. Depending on the growth strategy and habitat, the single isoform could be principally closer to *A. thaliana* PsbO1 (shade plants), to PsbO2 (sunny plants) or intermediate. For example, PsbO protein sequences of Poaceae species are closer to PsbO2 than to PsbO1 of *A. thaliana*, especially regarding the positions with alternating glutamic and aspartic acid residues (Additional files 2 and 6), which is consistent with the typical sunny habitat of these species. However, the species with single isoform that cluster to *A. thaliana* PsbO1 cannot be considered as shade plants. Consequently, the isoform sequence cannot be simply related to the actual habitat certain species, but it is obviously also affected by other factors such as evolutionary history or life strategy. Nevertheless, we can conclude from these considerations that *A. thaliana* PsbO1 and its functional analogs cannot be simply assumed as the main isoforms, because the importance of certain isoform depends on the habitat or even on actual growth conditions.

Conclusions

Our study showed that the pairs of PsbO isoforms evolved in numerous angiosperm lineages independently. Yet, the pairs of PsbO isoforms differ at similar regions in the protein structure, mostly on the luminally exposed end of the β-barrel structure near the predicted GTP-binding site. Mapping of conserved and variable positions on PsbO surface also indicated new potential interaction regions. Observed analogy in divergence between isoforms in various species indicates that structural diversification and subfunctionalisation of PsbO isoforms represents an example of parallel evolution. Features evolved in parallel likely bring a significant advantage, so we assume that diversification of PsbO isoforms improve photosynthetic performance under variable conditions. However, the predicted subfunctionalisation related to diverse GTPase activity will require further experimental confirmation.

Availability of supporting data

The phylogenetic data used in this study have been deposited in TreeBASE database (http://purl.org/phylo/treebase/phylows/study/TB2:S17601).

Additional files

Additional file 1: List of analyzed *psbO* genes. The dataset includes gene names used in the study, accession numbers, source databases and cDNA sequences.

Additional file 2: Alignment of the protein sequences of mature PsbOs from analyzed angiosperm species. The calculated values of the differences between isoforms, the differences between species and the differences between families are shown below the alignment. The sequences that were not included in the calculation are marked with an asterisk. Hypothetic GTP-binding domains (G motifs) predicted by Lundin *et al.* [10], conserved regions identified in wide range of photosynthetic organisms by De Las Rivas and Barber [9] and β-sheets forming the β-barrel structure are indicated below the alignment. Horizontal lines separate sequences from species belonging to the same angiosperm family.

Additional file 3: Number and divergence of expressed PsbO isoforms in the analysed land plant species. Number of distinct *psbO* cDNA sequences found in EST databases and maximal number of different amino acid residues in mature proteins derived from these sequences.

Additional file 4: A phylogenetic tree from coding sequences of *psbO* genes from 49 land plant species. The tree was constructed by the maximum likelihood method, numbers at branches denote bootstrap percentages.

Additional file 5: Venn diagrams of amino acid positions clustered according to the predominant class of variability. Threshold values of each type of variability to include an amino acid position in the diagrams are indicated.

Additional file 6: Numbers of glutamic and aspartic acid residues in PsbO protein sequences. Each point represents one PsbO; isoforms from one species are connected with a line, filled circles represent PsbOs from species with only one isoform. Points with the same coordinates are slightly shifted in order to make them visible. One representative species with two isoforms is shown from each family. Plotted species: *Arabidopsis thaliana* (Ath), *Artemisia annua* (Aan), *Citrus sinensis* (Csi), *Eucalyptus grandis* (Egr), *Fragaria vesca* (Fve), *Gossypium raimondii* (Gra), *Hordeum vulgare* (Hvu), *Linum usitatissimum* (Lus), *Lotus japonicus* (Lja), *Malus domestica* (Mdo), *Manihot esculenta* (Mes), *Mimulus guttatus* (Mgu), *Oryza sativa* (Osa), *Populus trichocarpa* (Ptr), *Solanum tuberosum* (Stu), *Spinacia oleracea* (spinach, Sol), *Theobroma cacao* (Tca), *Triticum aestivum* (Tae), *Vitis vinifera* (Vvi), *Zea mays* (Zma), *Zingiber officinale* (Zof).

Additional file 7: Mapping differences between isoforms on PsbO structure in selected species. Differences between isoforms of (A) *A. thaliana*, (B) *Zea mays* and (C) *Physcomitrella patens* are shown in green. The homologous model of the *Solanum tuberosum* PsbO2 based on the X-ray structure of cyanobacterial PsbO [PDB:3ARC] [5] was constructed using Swiss-Model program [38]; the first 13 N-terminal amino acids were not present in the template structure, so they were pasted in the model without attempts to show any folding.

Competing interests
The authors declare that they have no competing interests.

Authors' contributions
MD carried out all of the *in silico* experiments. MD and LF designed the study and wrote the manuscript. Both authors read and approved the final manuscript.

Acknowledgements
We thank Göran Samuelsson and Marek Romášek for their helpful comments and language corrections, Petr Janšta and Stanislav Vosolsobě for assistance with phylogenetic analysis, and Martin Weiser for helpful discussion about statistical tests. This work was supported by Charles University in Prague (projects GA UK No. 362211 and No. 1472314) and by Ministry of Education, Youth and Sports of Czech Republic (project No. LO1417).

Received: 12 February 2015 Accepted: 11 May 2015
Published online: 09 June 2015

References
1. De Las RJ, Balsera M, Barber J. Evolution of oxygenic photosynthesis: genome-wide analysis of the OEC extrinsic proteins. Trends Plant Sci. 2004;9:18–25.
2. Burnap RL, Sherman LA. Deletion mutagenesis in Synechocystis sp. PCC6803 indicates that the manganese-stabilizing protein of photosystem II is not essential for oxygen evolution. Biochemistry. 1991;30:440–6.
3. Mayfield SP, Bennoun P, Rochaix JD. Expression of the nuclear encoded OEE1 protein is required for oxygen evolution and stability of photosystem II particles in Chlamydomonas reinhardtii. EMBO J. 1987;6:313–8.
4. Yi X, McChargue M, Laborde S, Frankel LK, Bricker TM. The Manganese-stabilizing Protein Is Required for Photosystem II Assembly/Stability and Photoautotrophy in Higher Plants. J Biol Chem. 2005;280:16170–4.
5. Umena Y, Kawakami K, Shen J-R, Kamiya N. Crystal structure of oxygen-evolving photosystem II at a resolution of 1.9 Å. Nature. 2011;473:55–60.
6. Nield J, Balsera M, Rivas JDL, Barber J. Three-dimensional Electron Cryo-microscopy Study of the Extrinsic Domains of the Oxygen-evolving Complex of Spinach ASSIGNMENT OF THE PsbO PROTEIN. J Biol Chem. 2002;277:15006–12.
7. Caffarri S, Kouřil R, Kereïche S, Boekema EJ, Croce R. Functional architecture of higher plant photosystem II supercomplexes. EMBO J. 2009;28:3052–63.
8. Kouřil R, Oostergetel GT, Boekema EJ. Fine structure of granal thylakoid membrane organization using cryo electron tomography. Biochim Biophys Acta BBA - Bioenerg. 1807;2011:368–74.
9. De Las RJ, Barber J. Analysis of the Structure of the PsbO Protein and its Implications. Photosynth Res. 2004;81:329–43.
10. Lundin B, Thuswaldner S, Shutova T, Eshaghi S, Samuelsson G, Barber J, et al. Subsequent events to GTP binding by the plant PsbO protein: Structural changes, GTP hydrolysis and dissociation from the photosystem II complex. Biochim Biophys Acta BBA - Bioenerg. 2007;1767:500–8.
11. Bricker TM, Roose JL, Fagerlund RD, Frankel LK, Eaton-Rye JJ. The extrinsic proteins of Photosystem II. Biochim Biophys Acta BBA - Bioenerg. 1817;2012:121–42.
12. Suorsa M, Aro E-M. Expression, assembly and auxiliary functions of photosystem II oxygen-evolving proteins in higher plants. Photosynth Res. 2007;93:89–100.
13. Bricker TM, Frankel LK. Auxiliary functions of the PsbO, PsbP and PsbQ proteins of higher plant Photosystem II: A critical analysis. J Photochem Photobiol B. 2011;104:165–78.
14. Spetea C, Hundal T, Lundin B, Heddad M, Adamska I, Andersson B. Multiple evidence for nucleotide metabolism in the chloroplast thylakoid lumen. Proc Natl Acad Sci U S A. 2004;101:1409–14.
15. Seidler A. The extrinsic polypeptides of Photosystem II. Biochim Biophys Acta BBA - Bioenerg. 1996;1277:35–60.
16. The Arabidopsis Genome Initiative. Analysis of the genome sequence of the flowering plant Arabidopsis thaliana. Nature. 2000;408:796.
17. Murakami R, Ifuku K, Takabayashi A, Shikanai T, Endo T, Sato F. Characterization of an Arabidopsis thaliana mutant with impaired psbO, one of two genes encoding extrinsic 33-kDa proteins in photosystem II. FEBS Lett. 2002;523:138–42.
18. Murakami R, Ifuku K, Takabayashi A, Shikanai T, Endo T, Sato F. Functional dissection of two Arabidopsis PsbO proteins. FEBS J. 2005;272:2165–75.
19. Lundin B, Hansson M, Schoefs B, Vener AV, Spetea C. The Arabidopsis PsbO2 protein regulates dephosphorylation and turnover of the photosystem II reaction centre D1 protein. Plant J. 2007;49:528–39.
20. Dwyer SA, Chow WS, Yamori W, Evans JR, Kaines S, Badger MR, et al. Antisense reductions in the PsbO protein of photosystem II leads to decreased quantum yield but similar maximal photosynthetic rates. J Exp Bot. 2012;63:4781–95.
21. Lundin B, Nurmi M, Rojas-Stuetz M, Aro E-M, Adamska I, Spetea C. Towards understanding the functional difference between the two PsbO isoforms in Arabidopsis thaliana—insights from phenotypic analyses of psbo knockout mutants. Photosynth Res. 2008;98:405–14.
22. Goulas E, Schubert M, Kieselbach T, Kleczkowski LA, Gardeström P, Schröder W, et al. The chloroplast lumen and stromal proteomes of Arabidopsis thaliana show differential sensitivity to short- and long-term exposure to low temperature. Plant J. 2006;47:720–34.
23. Allahverdiyeva Y, Mamedov F, Holmström M, Nurmi M, Lundin B, Styring S, et al. Comparison of the electron transport properties of the psbo1 and psbo2 mutants of Arabidopsis thaliana. Biochim Biophys Acta BBA - Bioenerg. 2009;1787:1230–7.
24. Bricker TM, Frankel LK. The psbo1 Mutant of Arabidopsis Cannot Efficiently Use Calcium in Support of Oxygen Evolution by Photosystem II. J Biol Chem. 2008;283:29022–7.
25. Fischer L, Lipavska H, Hausman J-F, Opatrny Z. Morphological and molecular characterization of a spontaneously tuberizing potato mutant: an insight into the regulatory mechanisms of tuber induction. BMC Plant Biol. 2008;8:117.
26. Database of Expressed Sequence Tags, NCBI GenBank [http://www.ncbi.nlm.nih.gov/nucest]
27. Plant Genome Database [http://www.plantgdb.org/]
28. Altschul SF, Madden TL, Schäffer AA, Zhang J, Zhang Z, Miller W, et al. Gapped BLAST and PSI-BLAST: a new generation of protein database search programs. Nucleic Acids Res. 1997;25:3389–402.
29. Altschul SF, Wootton JC, Gertz EM, Agarwala R, Morgulis A, Schäffer AA, et al. Protein database searches using compositionally adjusted substitution matrices. FEBS J. 2005;272:5101–9.

30. Kearse M, Moir R, Wilson A, Stones-Havas S, Cheung M, Sturrock S, et al. Geneious Basic: An integrated and extendable desktop software platform for the organization and analysis of sequence data. Bioinformatics. 2012;28:1647–9.
31. Katoh K, Misawa K, Kuma K, Miyata T. MAFFT: a novel method for rapid multiple sequence alignment based on fast Fourier transform. Nucleic Acids Res. 2002;30:3059–66.
32. Miller MA, Pfeiffer W, Schwartz T. Creating the CIPRES Science Gateway for inference of large phylogenetic trees. In: Gateway Computing Environments Workshop (GCE), 2010. 2010. p. 1–8.
33. Stamatakis A. RAxML-VI-HPC: maximum likelihood-based phylogenetic analyses with thousands of taxa and mixed models. Bioinformatics. 2006;22:2688–90.
34. Goodstein DM, Shu S, Howson R, Neupane R, Hayes RD, Fazo J, et al. Phytozome: a comparative platform for green plant genomics. Nucleic Acids Res. 2012;40:D1178–86.
35. The R Project for Statistical Computing [http://www.r-project.org/]
36. Charif D, Lobry JR: SeqinR 1.0-2: A Contributed Package to the R Project for Statistical Computing Devoted to Biological Sequences Retrieval and Analysis. In *Structural Approaches to Sequence Evolution*. Edited by Bastolla U, Porto M, Roman HE, Vendruscolo M. Springer Berlin Heidelberg; 2007:207–232. [*Biological and Medical Physics, Biomedical Engineering*]
37. Schwede T, Kopp J, Guex N, Peitsch MC. SWISS-MODEL: an automated protein homology-modeling server. Nucleic Acids Res. 2003;31:3381–5.
38. Arnold K, Bordoli L, Kopp J, Schwede T. The SWISS-MODEL workspace: a web-based environment for protein structure homology modelling. Bioinformatics. 2006;22:195–201.
39. Guex N, Peitsch MC. SWISS-MODEL and the Swiss-Pdb Viewer: An environment for comparative protein modeling. Electrophoresis. 1997;18:2714–23.
40. POV-Ray - The Persistence of Vision Raytracer [http://www.povray.org/]
41. Flagel LE, Wendel JF. Gene duplication and evolutionary novelty in plants. New Phytol. 2009;183:557–64.
42. Fawcett JA, Maere S, de Peer YV. Plants with double genomes might have had a better chance to survive the Cretaceous–Tertiary extinction event. Proc Natl Acad Sci. 2009;106:5737–42.
43. Vanneste K, Baele G, Maere S, Peer YV de: Analysis of 41 plant genomes supports a wave of successful genome duplications in association with the Cretaceous-Paleogene boundary. *Genome Res* 2014;24:1334–47.
44. Hittinger CT, Carroll SB. Gene duplication and the adaptive evolution of a classic genetic switch. Nature. 2007;449:677–81.
45. Liu H, Frankel LK, Bricker TM. Functional Analysis of Photosystem II in a PsbO-1-Deficient Mutant in Arabidopsis thaliana. Biochemistry. 2007;46:7607–13.
46. Ifuku K, Nakatsu T, Kato H, Sato F. Crystal structure of the PsbP protein of photosystem II from Nicotiana tabacum. EMBO Rep. 2004;5:362–7.
47. Betts SD, Lydakis-Simantiris N, Ross JR, Yocum CF. The Carboxyl-Terminal Tripeptide of the Manganese-Stabilizing Protein Is Required for Quantitative Assembly into Photosystem II and for High Rates of Oxygen Evolution Activity†. Biochemistry. 1998;37:14230–6.
48. De Las RJ, Heredia P, Roman A. Oxygen-evolving extrinsic proteins (PsbO, P, Q, R): Bioinformatic and functional analysis. Biochim Biophys Acta BBA - Bioenerg. 2007;1767:575–82.
49. Dekker JP, Boekema EJ. Supramolecular organization of thylakoid membrane proteins in green plants. Biochim Biophys Acta BBA - Bioenerg. 2005;1706:12–39.
50. Boekema EJ, van Breemen JFL, van Roon H, Dekker JP. Conformational Changes in Photosystem II Supercomplexes upon Removal of Extrinsic Subunits. Biochemistry. 2000;39:12907–15.
51. Williamson A. Structural and functional aspects of the MSP (PsbO) and study of its differences in thermophilic versus mesophilic organisms. Photosynth Res. 2008;98:365–89.
52. Hong SK, Pawlikowski SA, Vander Meulen KA, Yocum CF. The oxidation state of the photosystem II manganese cluster influences the structure of manganese stabilizing protein. Biochim Biophys Acta BBA - Bioenerg. 2001;1504:262–74.
53. Aro E-M, Suorsa M, Rokka A, Allahverdiyeva Y, Paakkarinen V, Saleem A, et al. Dynamics of photosystem II: a proteomic approach to thylakoid protein complexes. J Exp Bot. 2005;56:347–56.
54. Kouřil R, Wientjes E, Bultema JB, Croce R, Boekema EJ. High-light vs. low-light: Effect of light acclimation on photosystem II composition and organization in Arabidopsis thaliana. Biochim Biophys Acta BBA - Bioenerg. 1827;2013:411–9.
55. Kirchhoff H. Structural changes of the thylakoid membrane network induced by high light stress in plant chloroplasts. Philos Trans R Soc B Biol Sci. 2014;369:20130225.
56. Herbstová M, Tietz S, Kinzel C, Turkina MV, Kirchhoff H. Architectural switch in plant photosynthetic membranes induced by light stress. Proc Natl Acad Sci. 2012;109:20130–5.
57. Huner NPA, Öquist G, Sarhan F. Energy balance and acclimation to light and cold. Trends Plant Sci. 1998;3:224–30.

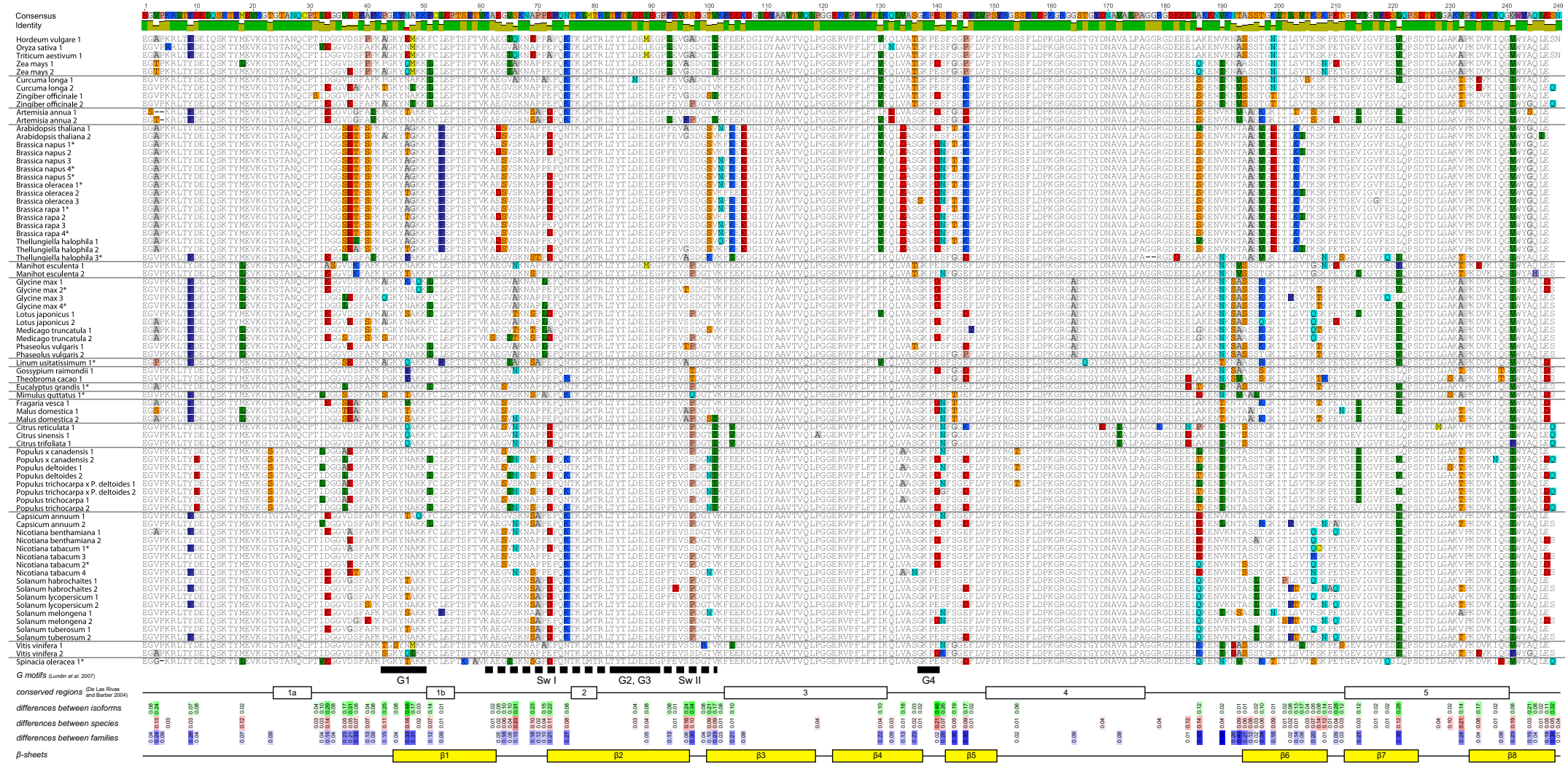

Additional file 2: Alignment of the protein sequences of mature PsbOs from analyzed angiosperm species. The calculated values of the differences between isoforms, the differences between species and the differences between families are shown below the alignment. The sequences that were not included in the calculation are marked with an asterisk. Hypothetic GTP-binding domains (G motifs) predicted by Lundin *et al.* [10], conserved regions identified in wide range of photosynthetic organisms by De Las Rivas and Barber [9] and β-sheets forming the β-barrel structure are indicated below the alignment. Horizontal lines separate sequences from species belonging to the same angiosperm family.

Additional file 3: Number and divergence of expressed PsbO isoforms in the analyzed land plant species. Number of distinct *psbO* cDNA sequences found in EST databases and maximal number of different amino acid residues in mature proteins derived from these sequences.

	Family	Species	Number of PsbO isoforms	Maximal number of different amino acid residues between any two isoforms[a]
Bryophyta	Funariaceae	*Physcomitrella patens*	4	24
Lycopodiophyta	Selaginellaceae	*Selaginella moellendorffii*	1[b]	
Cycadophyta	Cycadaceae	*Cycas rumphii*	1	
Coniferophyta	Cupressaceae	*Cryptomeria japonica*	1	
		Sequoia sempervirens	1	
	Pinaceae	*Picea abies*	1	
		Picea sitchensis	1	
		Pinus sylvestris	1	
		Pinus taeda	1	
	Taxaceae	*Taxus baccata*	1	
monocots	Poaceae	*Hordeum vulgare*	1	
		Oryza sativa	1	
		Triticum aestivum	1	
		Zea mays	2	6
	Zingiberaceae	*Curcuma longa*	2	13
		Zingiber officinale	2	12
dicots	Asteraceae	*Artemisia annua*	2	13
	Brassicaceae	*Arabidopsis thaliana*	2	11
		Brassica napus	5	7
		Brassica oleracea	3	9
		Brassica rapa	4	7
		Thellungiella halophila	3	10 (41)[c]
	Euphorbiaceae	*Manihot esculenta*	2	14
	Fabaceae	*Glycine max*	4	13
		Lotus japonicus	2	15
		Medicago truncatula	2	12
		Phaseolus vulgaris	2	7
	Linaceae	*Linum usitatissimum*	1[d]	
	Malvaceae	*Gossypium raimondii*	1	
		Theobroma cacao	1	
	Myrtaceae	*Eucalyptus grandis*	1	
	Phrymaceae	*Mimulus guttatus*	1	
	Rosaceae	*Fragaria vesca*	1	
		Malus domestica	2	11
	Rutaceae	*Citrus reticulata*	1	
		Citrus sinensis	1	
		Citrus trifoliata	1	
	Salicaceae	*Populus x canadensis*	2	23
		Populus deltoides	2	23
		Populus trichocarpa x Populus deltoides	2	22
		Populus trichocarpa	2	20
	Solanaceae	*Capsicum annuum*	2	18
		Nicotiana benthamiana	2	12
		Nicotiana tabacum	4	14
		Solanum habrochaites	2	15
		Solanum lycopersicum	2	13
		Solanum melongena	2	21
		Solanum tuberosum	2	12
	Vitaceae	*Vitis vinifera*	2	17

[a] in mature form (without a transite peptide)

[b] Two psbO sequences of *S. moellendorffii* can be found in EST databases. One of them (PlantGDB: PUT-165a-Selaginella_moellendorffii-12671) has far different mutation rate and seems to be a slightly expressed pseudogene, thus was omitted from analyses.

[c] Two isoforms of *T. halophila* that are most similar to isoforms of *A. thaliana* have only 10 different amino acid residues, another, the most diverged isoform, is orthologous to a truncated pseudogene of *A. thaliana*.

[d] *L. usitatissimum* expresses two psbO genes, but the corresponding mature proteins have the same amino acid sequence.

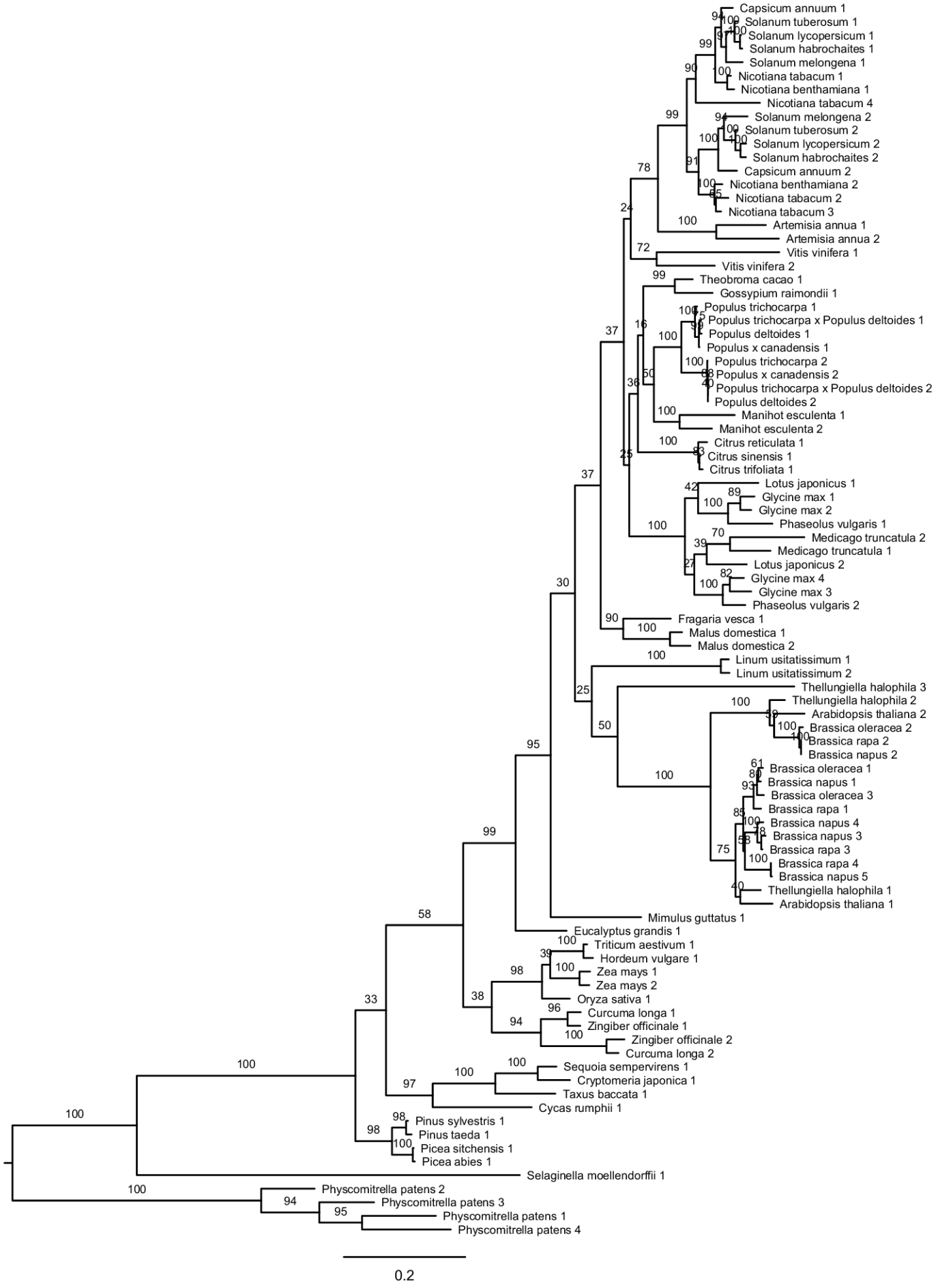

Additional file 4: A phylogenetic tree from coding sequences of *psbO* genes from 49 land plant species. The tree was constructed by the maximum likelihood method, numbers at branches denote bootstrap percentages.

A: threshold 0.10

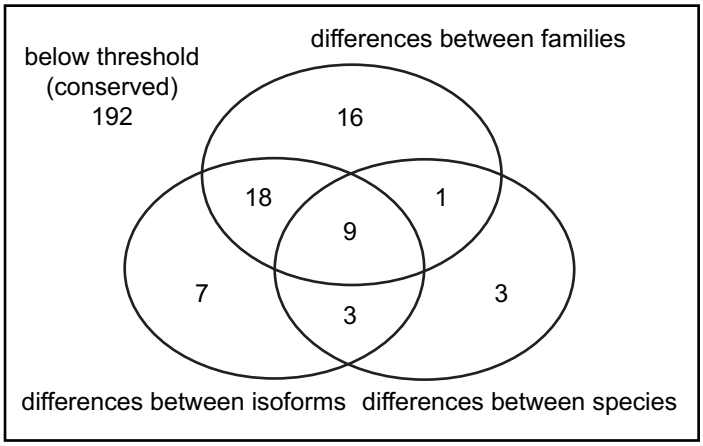

B: threshold 0.24

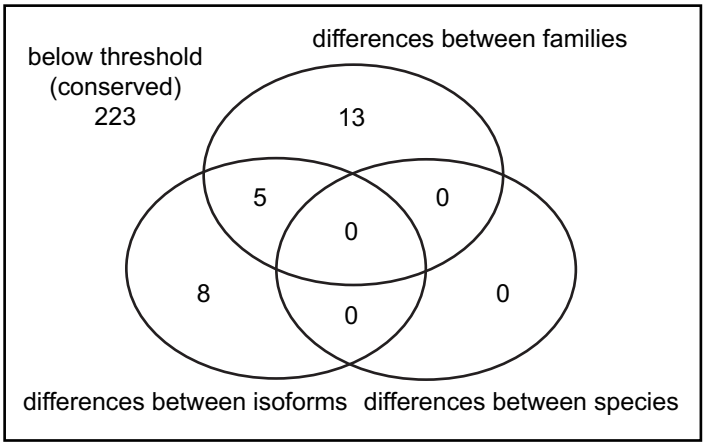

Additional file 5: Venn diagrams of amino acid positions clustered according to the predominant class of variability. Threshold values of each type of variability to include an amino acid position in the diagrams are indicated.

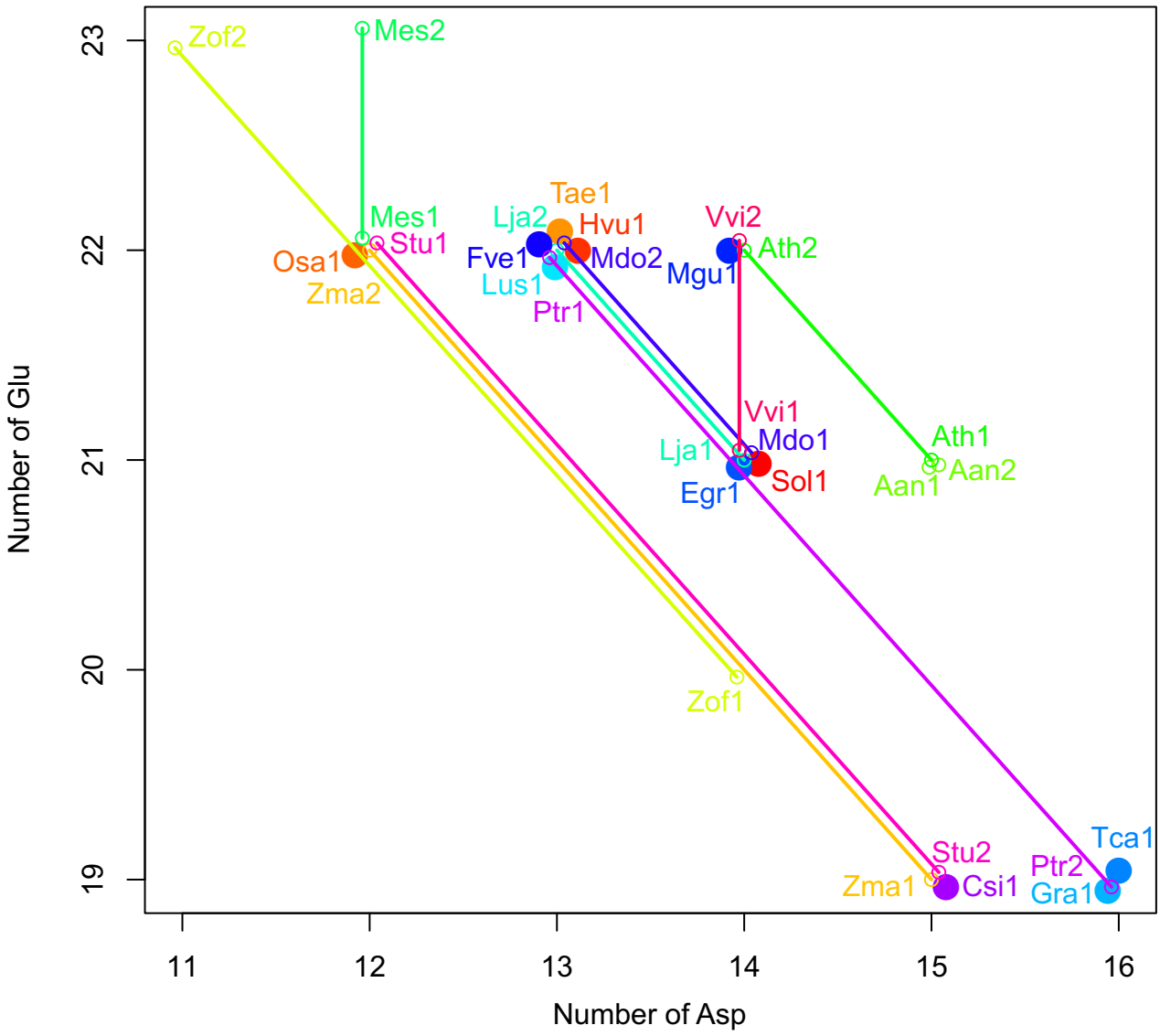

Additional file 6: Numbers of glutamic and aspartic acid residues in PsbO protein sequences. Each point represents one PsbO; isoforms from one species are connected with a line, filled circles represent PsbOs from species with only one isoform. Points with the same coordinates are slightly shifted in order to make them visible. One representative species with two isoforms is shown from each family. Plotted species: *Arabidopsis thaliana* (Ath), *Artemisia annua* (Aan), *Citrus sinensis* (Csi), *Eucalyptus grandis* (Egr), *Fragaria vesca* (Fve), *Gossypium raimondii* (Gra), *Hordeum vulgare* (Hvu), *Linum usitatissimum* (Lus), *Lotus japonicus* (Lja), *Malus domestica* (Mdo), *Manihot esculenta* (Mes), *Mimulus guttatus* (Mgu), *Oryza sativa* (Osa), *Populus trichocarpa* (Ptr), *Solanum tuberosum* (Stu), *Spinacia oleracea* (spinach, Sol), *Theobroma cacao* (Tca), *Triticum aestivum* (Tae), *Vitis vinifera* (Vvi), *Zea mays* (Zma), *Zingiber officinale* (Zof).

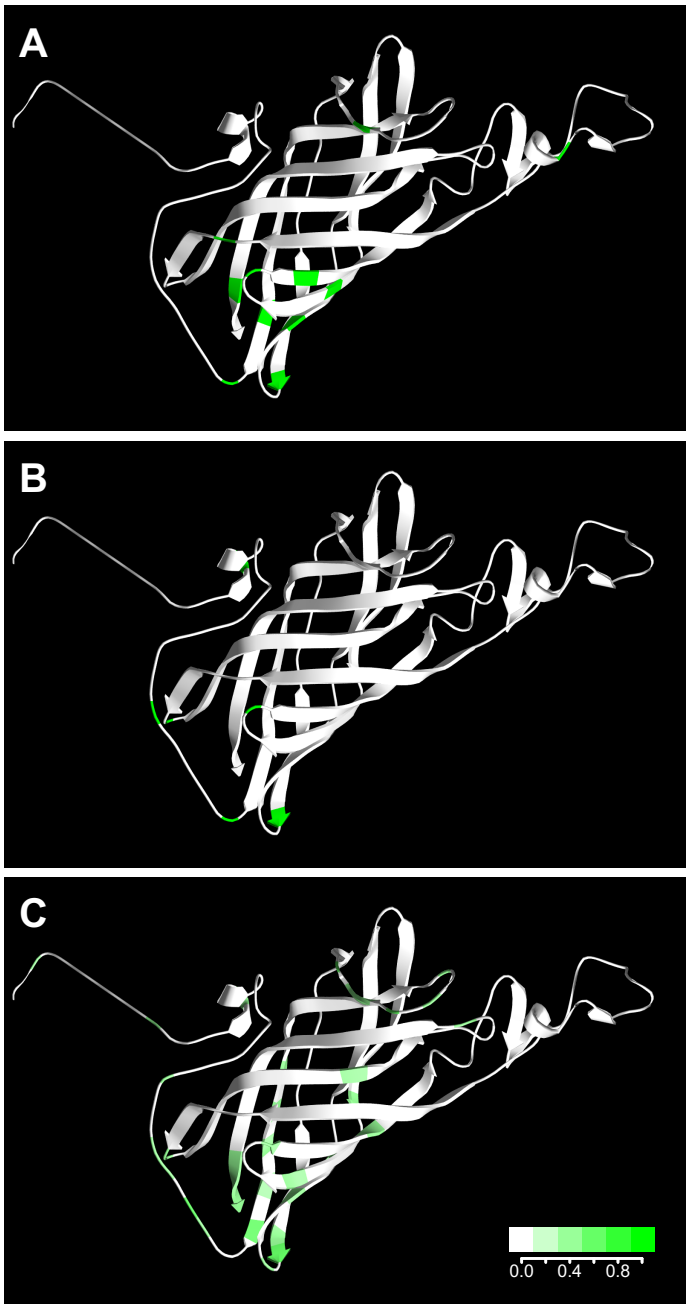

Additional file 7: Mapping differences between isoforms on PsbO structure in selected species. Differences between isoforms of (A) *A. thaliana*, (B) *Zea mays* and (C) *Physcomitrella patens* are shown in green. The homologous model of the Solanum tuberosum PsbO2 based on the X-ray structure of cyanobacterial PsbO [PDB:3ARC] [5] was constructed using Swiss-Model program [38]; the first 13 N-terminal amino acids were not present in the template structure, so they were pasted in the model without attempts to show any folding.

9.3 PUBLICATION 2

14 pages (101–114)

Physiologia Plantarum
An International Journal for Plant Biology

Physiologia Plantarum 166: 288–299. 2019

Dynamic pH-induced conformational changes of the PsbO protein in the fluctuating acidity of the thylakoid lumen

Anke B. Carius[a,*], Per Rogne[b], Miloš Duchoslav[c], Magnus Wolf-Watz[b], Göran Samuelsson[a] and Tatyana Shutova[a,*]

[a]Department of Plant Physiology, Umeå University, Umeå SE-907 36, Sweden
[b]Department of Chemistry, Umeå University, Umeå SE-901 87, Sweden
[c]Department of Experimental Plant Biology, Faculty of Science, Charles University, Prague, Czech Republic

Correspondence
*Corresponding authors,
e-mail: anke.carius@umu.se;
tatyana.shutova@umu.se

Received 15 November 2018;
revised 14 February 2019

doi:10.1111/ppl.12948

The PsbO protein is an essential extrinsic subunit of photosystem II, the pigment–protein complex responsible for light-driven water splitting. Water oxidation in photosystem II supplies electrons to the photosynthetic electron transfer chain and is accompanied by proton release and oxygen evolution. While the electron transfer steps in this process are well defined and characterized, the driving forces acting on the liberated protons, their dynamics and their destiny are all largely unknown. It was suggested that PsbO undergoes proton-induced conformational changes and forms hydrogen bond networks that ensure prompt proton removal from the catalytic site of water oxidation, i.e. the Mn_4CaO_5 cluster. This work reports the purification and characterization of heterologously expressed PsbO from green algae *Chlamydomonas reinhardtii* and two isoforms from the higher plant *Solanum tuberosum* (PsbO1 and PsbO2). A comparison to the spinach PsbO reveals striking similarities in intrinsic protein fluorescence and CD spectra, reflecting the near-identical secondary structure of the proteins from algae and higher plants. Titration experiments using the hydrophobic fluorescence probe ANS revealed that eukaryotic PsbO proteins exhibit acid–base hysteresis. This hysteresis is a dynamic effect accompanied by changes in the accessibility of the protein's hydrophobic core and is not due to reversible oligomerization or unfolding of the PsbO protein. These results confirm the hypothesis that pH-dependent dynamic behavior at physiological pH ranges is a common feature of PsbO proteins and causes reversible opening and closing of their β-barrel domain in response to the fluctuating acidity of the thylakoid lumen.

Introduction

Photosystem II (PSII) uses captured solar energy to split water into reducing equivalents and oxygen gas; it is the main source of the oxygen in the Earth's atmosphere. The structure and function of the PSII pigment protein complex have been studied extensively because of its importance to all organisms that depend on oxidative metabolism. The structure of PSII has been determined using X-ray crystallography, revealing key features including the water-oxidizing site (i.e. the Mn_4CaO_5 cluster) and several cofactors of the electron transfer chain (Ferreira et al. 2004, Umena et al. 2011, Kern et al. 2018). Although the general process of photosynthetic electron transfer at PSII is well-characterized (Nelson and Junge 2015, Junge 2019), the specific roles of many of the involved proteins (most of which are essential) remain unclear (Bricker et al. 2012). PsbO

Abbreviations – PSII, photosystem II; rH, hydrodynamic radius; rG, gyration.

is among the most prominent of these proteins. It has been given several different names, including OEE1, or oxygen evolving enhancer protein 1 (Mayfield et al. 1987); MSP, or manganese-stabilizing protein – a name that describes its role in PSII (Kuwabara et al. 1987, Burnap et al. 1996); and the 33 kDa protein, based on its apparent molecular mass in SDS PAGE experiments (although the real mass of the spinach PsbO is 27 kDa). Today it is generally referred to as PsbO protein because it is encoded by the nuclear *psbO* gene. Among the extrinsic subunits of PSII, PsbO is the only one present in all organisms capable of water splitting and oxygen evolution. The other extrinsic proteins of PSII differ between classes – in cyanobacteria they are PsbU, PsbV, CyanoQ and CyanoP (Shen and Inoue 1993, Kashino et al. 2002, Thornton et al. 2004), while in green algae and higher plants they are PsbP and PsbQ (Su et al. 2017). In red algae and diatoms, PsbQ' (a homolog of CyanoQ) is bound to PSII (Ohta et al. 2003). Diatoms also have a specific extrinsic subunit, Psb31, which may be a homolog of PsbQ (Nagao et al. 2013). For more information about the extrinsic proteins of PSII, see the works of Roose et al. (2007), Enami et al. (2008), Bricker and Frankel (2011), Ifuku (2014), Ifuku et al. (2008, 2011), Bricker et al. (2012).

The current structural model of PsbO is based on X-ray and cryo-electron microscopy data for the intact PSII complex (De Las Rivas and Barber 2004, Umena et al. 2011, Young et al. 2016, Su et al. 2017). Several attempts to crystallize PsbO in isolated form failed to yield crystals amenable to X-ray analysis (Anati and Adir 2000, Nowaczyk et al. 2004). However, the crystal structure of the isolated barrel domain of a cyanobacterial PsbO protein, PsbO-β, has been successfully resolved (Bommer et al. 2016). The PSII crystal structures reveal that PsbO is positioned on the lumenal side of the thylakoid membrane with its β-barrel projecting out into the lumen such that both the N- and C-termini are exposed while the flexible top loops are integrated into PSII, interacting with several transmembrane PSII subunits including another PSII monomer in the PSII dimer (De Las Rivas and Barber 2004, Bricker et al. 2012).

The PsbO protein has two major domains (De Las Rivas and Barber 2004). Domain I consist of highly structured antiparallel β-strands forming an elongated barrel in which the first strand is hydrogen bonded to the last one to form a typical β-barrel fold; for a review on β-barrel proteins, see Schulz (2000). The β-barrel is stabilized by intramolecular hydrophobic interactions between the lipophilic amino acid residues inside the barrel that constitute the protein's hydrophobic core. The single tryptophan residue of PsbO (W241 in the spinach sequence) is located inside this hydrophobic core and is responsible for the protein's fluorescence properties (Shutova et al. 2001). Domain II consists mostly of flexible, unstructured loops together with some turns and short α-helices. Unlike Domain I, Domain II has a relatively high content of hydrophilic amino acids. Its loops are stabilized by interactions with the other PSII proteins and are therefore quite flexible in solution. An NMR study on heterologically expressed cyanobacterial PsbO confirmed that it consists of two well-defined parts, rigid together with approximately 40% being flexible and corresponding to Domain II (Nowaczyk et al. 2004). The N-terminus of PsbO forms a tail-like structure containing a small α-helix that is attached to the β-barrel by a conserved disulfide bond (De Las Rivas and Barber 2004, Nikitina et al. 2008). This disulfide bond is involved in redox regulation of chloroplast proteins (Buchanan et al. 2002) via processes such as oxidative folding in the lumen (Kieselbach 2013) and thioredoxin-dependent degradation of PsbO (Roberts et al. 2012).

PsbO therefore has both rigid and fluid parts, giving it both stability and high flexibility. This allows PsbO to respond dynamically to changes in the abundance of redox-active thioredoxin (Roberts et al. 2012), pH (Shutova et al. 1997, 2005, 2007, Bommer et al. 2016), GTP (Lundin et al. 2007) and the calcium ions (Heredia and De Las Rivas 2003, Shutova et al. 2005, Murray and Barber 2006). The structural dynamics of PsbO have been analyzed and related to its functional role in photosynthetic water oxidation based on experiments using intra-molecular cross-linking (Enami et al. 1998) and FTIR spectroscopy (Hutchison et al. 1999, Sachs et al. 2003, Offenbacher et al. 2013). The substrate water exchange in PSII depends on the presence of the extrinsic proteins and the removal of PsbO has slightly different effect in prokaryotic and eukaryotic organisms (Hillier et al. 2001). PsbO stabilizes the Mn_4CaO_5 cluster, but the mechanism by which it does this remains unclear. The new evidences regarding the role of PsbO protein in the maintaining the functional active manganese cluster and long-distance hydrogen-bond network around it were obtained using molecular dynamic simulations (Guerra et al. 2018). PsbO also helps regulate PSII degradation during the PSII repair cycle (Lundin et al. 2007) and calcium and chloride binding in PSII (Loll et al. 2005, Popelkova et al. 2011, Roose et al. 2016). The binding of divalent manganese ions to PsbO proteins from higher plants and cyanobacteria in solution has also been reported (Shutova et al. 2005, Bommer et al. 2016). It has been suggested that PsbO contributes to the transport of protons from the water oxidation site to the thylakoid lumen via a chain of carboxylic amino acids

thereby forming the proton binding antenna (Shutova et al. 1997, 2007).

Many plants, including *Arabidopsis thaliana* (*A. thaliana*), express two *psbO* genes. Although their duplication was independent in each plant family, the differences between isoforms usually occur in similar parts of the PsbO structure, mainly at the end of the β-barrel projecting into the lumen and the β1-β2 loop. Consequently, if there are consistent functional differences between the isoforms in various plant families, one would expect those differences to have arisen via parallel evolution (Duchoslav and Fischer 2015). A detailed functional analysis of *A. thaliana* mutants lacking one PsbO isoform or the other (Allahverdieva et al. 2009) revealed that the absence of PsbO2 had no detectable phenotypic consequences, but plants lacking PsbO1 exhibited impaired PSII functionality and an increased susceptibility to photodamage. The function of PsbO2 is therefore unclear.

Only a few studies have examined PsbO proteins from algae. However, FUD44, a Δ-psbO strain of *Chlamydomonas reinhardtii*, was characterized over 30 years ago (Mayfield et al. 1987). *C. reinhardtii* can survive as an organo-heterotroph or a photo-organoheterotroph solely with functional photosystem I. It has a single copy of the *psbO* gene that can be easily modified or replaced. For example, Suzuki et al. (2005) reported the cross-reconstitution of the extrinsic proteins and PSII from *C. reinhardtii* and spinach; functional exchange allowed the PSII complex from *C. reinhardtii* to produce oxygen when bound to PsbO proteins from spinach and vice-versa. Chemical cross-linking experiments have corroborated these results (Nagao et al. 2010).

Here we report the efficient heterologous expression and structural characterization of two members of the PsbO family: PsbO from the green alga *C. reinhardtii* and PsbO1/PsbO2 isoforms from the higher plant *Solanum tuberosum* (potato). We address the pH dependent dynamics in the wild-type and truncated versions of PsbO protein produced and tested for correct folding and for hysteresis in pH responses by ANS fluorescence and acid titration and an NMR and CD spectrometry.

Materials and methods

Cloning

The amino acid sequences of the PsbO protein from *C. reinhardtii* and *S. tuberosum* were used without the transit peptide for location in the lumen of chloroplast because this peptide is removed during translocation in vivo (amino acid sequences of proteins used in this study are presented in Fig. S1). The sequence of *C. reinhardtii* PsbO (same as Uniprot: A8J0E4) was converted to a new DNA sequence with *Escherichia coli* codon usage and synthesized by Eurofins Genomics including NcoI and Acc65I restriction sites for cloning. The *psbO* gene was excised (NcoI/Acc65I) and transferred into the pET_zz_1a expression vector.

For the truncated version of the PsbO protein, the synthesis vector was amplified by inverse PCR. Primers (5′-GCGCTGAAAGGCAGCGCGGTGTTTA-3′ and 5′-GCCCGGCACCAGAAAATCGCCTTTAATGT-3′) were chosen so that the truncation area would be left out of the *psbO* gene. For all PCR reactions high fidelity polymerase KAPA HiFi™ Hot Start ready mix (Kapa Biosystems) was used. After PCR amplification, the plasmid was recirculated by blunt end ligation. The truncated gene was excised (NcoI/Acc65I) and transferred into the pET_zz_1a expression vector. The sequence was confirmed using sequencing (Eurofins).

The *S. tuberosum psbO1* and *psbO2* genes were isolated by PCR from cDNA from potato (*Solanum tuberosum* L.) cv. Lada (breeder Selekta Pacov, Czech Republic). Primer pairs used for isolation were 5′-TTG TCTACTCTCTCCATAGTCC-3′ and 5′-CGAGCTTGATAA TATACAGCAAG-3′ (*psbO1*) and 5′-ACCATCCAACTGTC ACACTTGT-3′ and 5′-CCAAACACAGACAGATTCAACG-3′ (*psbO2*). Sequences (checked by sequencing) were the same as in Duchoslav and Fischer (2015). After addition of NcoI and KpnI restriction sites by successive PCR with primers 5′-GCTTCCATGGAAGGAGTTCCAAA ACGTTT-3′ and 5′-GCTTGGTACCTTATTCAAGTTGGG CATACCAGA-3′ (*psbO1*) and 5′-GCTTCCATGGAAGG AGTTCCAAAACGTCTA-3′ and 5′-GCTTGGTACCTTATG ATTCAAGCTGGGCATAC-3′ for the *psbO2*, *psbO* genes were excised and transferred into the pET_DsbAin_1b expression vector.

Protein expression and purification

E. coli Bl21 (DE3) pLysS was used as the expression host. Several pET vectors designed for fusion of protein of interest with various carrier proteins, provided by the Umeå Protein Expertise Platform, Sweden, were tested. The highest expression levels in the soluble fraction were achieved with the pET_zz_1a (*C. reinhardtii*) and pET_DsbAin_1b (*S. tuberosum*) vectors. These vectors include sequences for His-tag, ZZ/DsbAin carrier protein and TEV protease cleavage site located at the N-terminal end of the PsbO protein. *C. reinhardtii* PsbO expression was achieved using autoinduction media (Grabski 2005, Studier 2005), *S. tuberosum* PsbO was expressed at 22°C using LB media with 0.5 mM IPTG. The cells were harvested by centrifugation for 30 min at 5000 *g* and the pellets were frozen and stored at −20°C until use. For protein purification, the pellets

were resuspended in 10 ml lysis buffer per gram of wet cell weight (lysis buffer composition: 20 mM Tris, 10 mM imidazole, 150 mM NaCl, 0.2% Igepal CA-630, 1 mg ml^{-1} Lysozyme, 5 μg ml^{-1} DNAse I, 1 μM PEFABLOC, pH 8).

Purification was achieved by NiNTA ligand affinity chromatography using the following Tris-based buffers: Wash 1: lysis buffer w/o lysozyme and DNAse; Wash 2: wash 1 w/o Igepal; Wash 3: wash 2 with 1 M NaCl; elution: 20 mM Tris, 150 mM NaCl, 330 mM imidazole. The resin (Macherey-Nagel, Düren, Germany) was washed with 20 vol. of deionized water and then equilibrated with 20 vol. of Wash 1. A spin protocol for 50 ml Falcon tubes was used throughout the procedure except during the elution step, which was performed with a column. The eluted protein was digested with TEV protease 1:50 w/w for 1–2 days, depending on the accessibility of the recognition site (Tropea et al. 2009). The sample was then desalted in a Millipore 10 kDa falcon centrifuge filter unit until the imidazole concentration was below 10 mM (as in the Wash 2 buffer) in preparation for a second NiNTA step.

The second purification was performed to remove residual uncleaved protein and the TEV protease. Excess NiNTA material was used to maximize the protein's purity. Because the protein of interest was contained in the flowthrough rather than the eluate in this case, the column's dead volume was estimated, collected separately, and later checked for protein content. The flow through was also collected and reloaded onto the column 3 times. An amount of Wash buffer 2 equal to the estimated dead volume was added. Samples of all fractions were loaded on an acrylamide gel for SDS-PAGE (Laemmli 1970). All SDS-PAGE separations were performed using Bio-Rad precast gels and hot Coomassie stain. The separated proteins were aliquoted and stored at −80°C. The sequence aliment of proteins used in the study is shown in Fig. S1. Compared to native mature protein, the proteins used here are 3–4 amino acid residues longer in the N-terminus (GAM/GAMA) due to introduction of restriction site and TEV protease digestion site.

Protein structure analysis

All analytical procedures were performed in 10 mM $KHPO_4$ buffer (pH 7.2) containing 10 mM NaCl. Buffer exchange was performed using Microcon 10 microcentrifuge filter units (Merck Millipore). Protein concentrations were measured using a NanoDrop 1000 spectrometer (Thermo Scientific). Secondary structure was monitored by circular dichroism spectroscopy. The protein concentration was set to 20 μmol ml^{-1} and a spectrum was recorded in a quartz cuvette with a path length of 0.5 mm (Starna scientific) with a JASCO J-810 spectrophotometer.

Fluorescence

The proteins' intrinsic fluorescence spectra were measured at 25°C in quartz cuvettes with a path length of 0.5 mm (Starna Cells 20-O/Q/0.5, Starna Scientific) using a Cary Eclipse Fluorimeter (Varian/Agilent Technologies). The bandwidth of the excitation and emission beams was 5 nm. Protein fluorescence was recorded using excitation wavelengths of 280 or 295 nm to excite tryptophan and tyrosine or tryptophan alone, respectively. Emission was recorded between 300 and 400 nm. All fluorimetry experiments were performed using 10 mM protein solutions in a pH 8.0 buffer containing 10 mM $KHPO_4$ and 10 mM NaCl. For ANS (8-anilino-1-naphthalenesulfonic acid) fluorescence, the excitation wavelength was 395 nm and emission was recorded between 400 and 600 nm. Titration assays were performed using four similar 2 ml glass fluorescence cuvettes (Starna 3/G/10, Starna Scientific) with a 10 mm path length supplied with a 5 mm magnetic stirrer. ANS titrations were performed with sample solutions containing the protein under investigation (5 mM) and ANS (20 mM) in 10 mM $KHPO_4$ with 10 mM NaCl and an initial pH of 8.0. The pH was lowered in steps of approximately 0.5 pH units by adding 0.1 M HCl until the pH reached 3.80, at which point the pH was increased stepwise to its original value by adding 0.1 M NaOH. A fluorescence spectrum was recorded after each addition of HCl or NaOH.

NMR

For the NMR spectroscopy the proteins were expressed in M9 minimal medium including 1 g ^{15}N NH_4Cl for ^{15}N enrichment, pH 7 to prevent precipitation, sterile filtered with 0.2 μM filter. NMR spectra were recorded in a Bruker™ 850 spectrometer using 178 mm long high precision tubes with a diameter of 5 mm. The hydrodynamic radius (rH) was determined by performing NMR-based diffusion experiments and using the Stokes–Einstein relationship. In addition, predicted rH values were obtained based on the calculated radius of gyration (rG), which was determined from the crystal structure of PSII (Pdb:3ARC) using HYDROPRO (Ortega et al. 2011). The relationship between rG and rH was taken to be $rG^2 = (3/5)\ rH^2$ (Burchard et al. 1980).

Structural protein modeling

Models of WT and ΔS145K187 PsbO proteins from *C. reinhardtii* were generated based on the reported

crystal structure of the PSII from *Thermosynechococcus elongatus* (3ARC.pdb) using MODBASE (Pieper et al. 2011).

Results

Secondary structure composition of PsbO protein from different species

To characterize the PsbO protein from *C. reinhardtii*, its folding and behavior in comparison with higher plants PsbO the heterologously expressed protein was purified and characterized. Moreover, we created a mutant lacking 43 amino acids from the large top loop of Domain II (Ser145 to Lys187) to be able to distinguish between effects in different areas of PsbO, the β-barrel and the flexible loops. Structural models of the WT and ΔS145K187 proteins are presented in Fig. 1. In addition, the circular dichroism spectrum of the heterologously expressed PsbO protein from *C. reinhardtii* was recorded and used to elucidate the protein's secondary structure in solution. Fig. 2 compares the far-UV regions of the CD spectra of the WT PsbO protein and the truncated version. Removing the large hydrophilic loop did not greatly alter the CD spectrum, indicating that the WT and mutant proteins have very similar secondary structures. We therefore conclude that the mutant folds correctly. The CD spectra of the two PsbO isoforms from *S. tuberosum* both closely resembled that of the algal protein (Fig. S2). The CD spectra of the WT PsbO protein at pH 7.5 and 3.8 appeared almost identical, as previously reported for the spinach PsbO protein (Shutova et al. 1997). The PsbO protein from the green alga thus folded similarly to that from a higher plant (Fig. 2).

Calculations performed using the program CDPRO (Sreerama and Woody 2004) based on the CD spectrum of the WT PsbO protein from *C. reinhardtii* revealed that α-helices comprised 8% of its secondary structural elements, β-strands comprised 32%, turns comprised 15% and the remaining 43% consisted of random coils. Table 1 compares the relative abundances of α-helices and β-strands calculated from the CD spectra of PsbO in solution to the corresponding values observed in the structure of the protein attached to the thylakoid membrane and the crystal structure of PSII. The data summarized in this Table 1 include results for cyanobacterial and algal PsbO proteins as well as those from higher plants. The results obtained in this work and the literature data indicate that the secondary structure composition of PsbO in solution is virtually identical to that seen in the PSII supercomplex; the means and standard deviations for the relative abundances of α-helices and β-strands over the entire dataset shown in Table 1

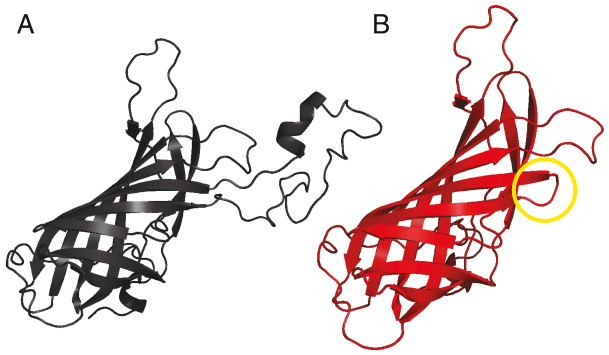

Fig. 1. Structural model of WT (A) and ΔS145K187 (B) truncated version of the PsbO protein from *Chlamydomonas reinhardtii*. The crystal structure of PsbO protein from *Thermosynechococcus elongatus* 3ARC pdb was used as a template in homology-based calculations MODBASE (Piper et al. 2011).

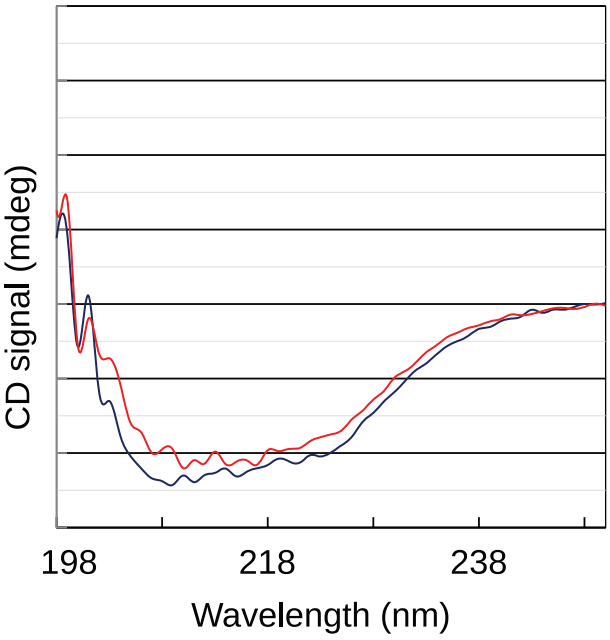

Fig. 2. Far-UV circular dichroism spectra of the WT PsbO protein from *Chlamydomonas reinhardtii* at pH 7.5, red line and ΔS145K187 truncated version, blue line. Protein concentration was 30 μM in a medium containing 10 mM phosphate buffer and 20 mM NaCl.

are 7 ± 2 and 40 ± 5%, respectively. These values are consistent with those computed for spinach PsbO based on its CD spectrum (Xu et al. 1994) and are typical of β-type proteins in general (Schulz 2000). Moreover, the secondary structure of the cyanobacterial PsbO protein closely resembles that of the PsbO proteins from higher plants: its contents of α-helices and β-strands are 5.5 ± 2 and 44 ± 2%, respectively, compared to 6.7 ± 2 and 38 ± 4% for the higher plants. The proportions of α-helical structure in the algal (8 ± 2%) and higher plant

Table 1. The secondary structure content (%) in the native PsbO protein from different species.

PDB	Organism	α-helix	β-strand	Location	Comment
Cyanobacteria					
5GTH	*Thermosynechococcus vulcanus*	5	47	PSII bound	Dark state
3WU2	*Thermosynechococcus vulcanus*	5	45	PSII bound	3ARC
5KAF	*Thermosynechococcus elongatus*	4	41	PSII bound	Dark state
5G39	*Thermosynechococcus elongatus*	-	45	In solution	100 K
PsbO	*Thermosynechococcus elongatus*	8	43	In solution	Loll et al. 2005
	Average	5.5 ± 1.5	44.2 ± 2		
Algae					
4YUU	*Cyanidium caldarium*	8.5	42	PSII bound	O1
PsbO	*C. reinhardtii*	8	32	In solution	CD
	Average	8.3 ± 0.3	37 ± 5.1		
Plants					
5XNM	*Pisum sativum*	5	41	PSII bound	Unstacked
5XNL	*Pisum sativum*	9	44	PSII bound	Stacked
PsbO	*Spinacia oleracea*	9	38	In solution	Xu et al. 1994
PsbO	*Spinacia oleracea*	8	33	In solution	Shutova et al. 1997
PsbO2	*S. tuberosum*	6	36	In solution	CD
PsbO1	*S. tuberosum*	3	37	In solution	CD
	Average	6.7 ± 2	38.2 ± 3.5		

(7 ± 2%) PsbO proteins appeared to be slightly higher than that in the cyanobacterial protein (5.5 ± 2%); this probably reflects the presence of a small α-helical extension on the N-terminal domain of the higher plant proteins (De las Rivas and Barber 2004). In conclusion, our results suggest that PsbO proteins from cyanobacteria, algae and higher plants have similar secondary structures, both when bound to PSII and in solution (i.e. both in vitro and in situ).

Fluorescence of PsbO protein from *C. reinhardtii* and *S. tuberosum*

Fluorescence spectroscopy is a sensitive tool for studying conformational changes in proteins. The intrinsic fluorescence of proteins containing tryptophan and/or tyrosine residues can provide important information about conformation changes because the fluorescence of these residues is highly sensitive to their microenvironment (for a review, see Callis and Liu 2004). In addition, proteins may bind to various extrinsic fluorescent dyes via hydrophobic or electrostatic interactions, providing additional ways to use fluorescence spectroscopy for protein characterization. Fig. 3A shows the room temperature fluorescence spectra of the green algal PsbO protein in a pH 7.5 buffer solution. The spectra were acquired using excitation at wavelengths of 275 nm (solid line) and 295 nm (dashed line). The spectrum obtained by 275 nm excitation has a strong emission peak centered at around 310 nm. Conversely, excitation at 295 nm (which excites only tryptophan residues) produced a broad and weak emission peak, with a maximum at approximately 323 nm. The PsbO protein from *C. reinhardtii* has only one tryptophan residue, W235, which corresponds to residue W241 in the spinach protein based on sequence aliment. The spectrum shown using the dashed line in Panel A of Fig. 3 can be ascribed to emission originating from residue W235. This spectrum exhibits a pronounced blue shift of more than 20 nm relative to free tryptophan in solution, which is indicative of a tryptophan residue in a hydrophobic environment. This is consistent with the known location of the W235 residue inside the hydrophobic β-barrel of the PsbO protein, and thus indicates that the β-barrel remained intact when the protein was expressed heterologously and stored in solution.

The spectrum obtained by excitation at 275 nm was analyzed by curve fitting based on a log-normal function (Fig. 3B). The de-convolution suggested the presence of two major components in the fluorescence spectrum obtained by 275 nm excitation: a 310 nm band due to tyrosine residues and a 325 nm band due to the W235 residue, which appears to be buried in the β-barrel in a similar fashion to the corresponding residue in PsbO proteins from higher plants (Shutova et al. 2001). The overall fluorescence spectrum of PsbO in solution thus contains contributions originating from two different emitters: a peak at around 310 nm due to tyrosine, and a long-wavelength band due to the lone tryptophan residue in the PsbO sequence (W235 in *C. reinhardtii*). The tryptophan fluorescence has low quantum yield because the emission is strongly quenched, probably by the neighboring fully conserved disulfide and/or the nearby tyrosine residue, which is present in all eukaryotic

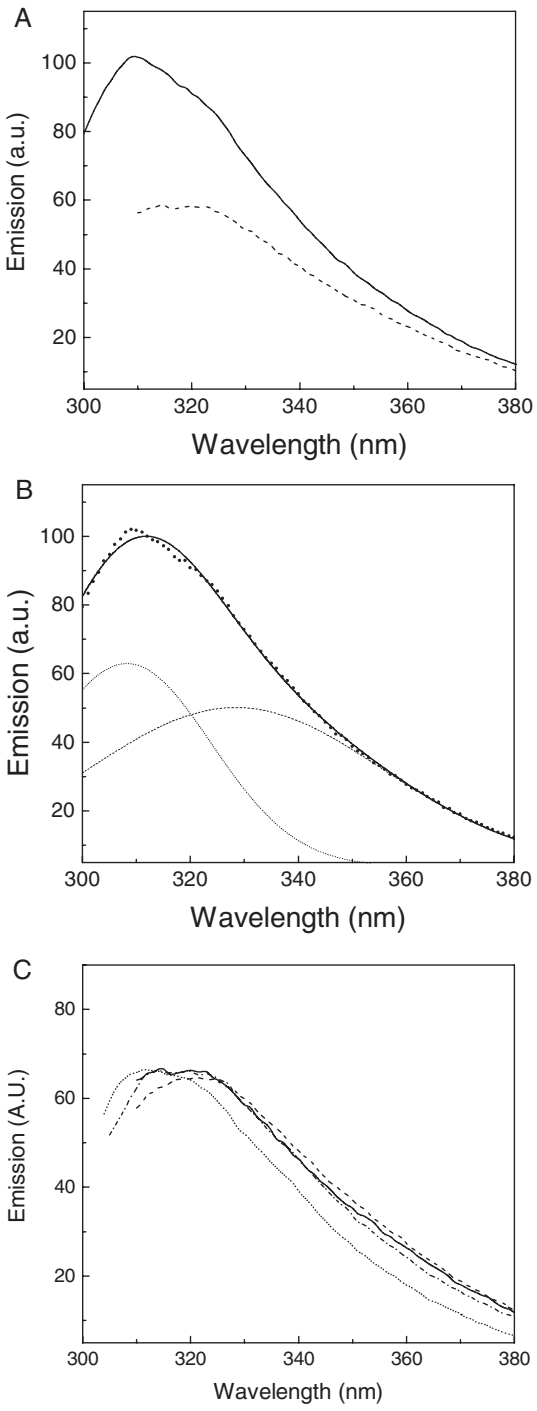

Fig. 3. Room temperature fluorescence spectra of the PsbO protein from *Chlamydomonas reinhardtii* in buffer solution at pH 7.5. (A) The excitation wavelength was 275 nm, solid line and 295 nm, dashed line. (B) Deconvolution of the spectra excited at 275 nm. (C) Room temperature emission spectra recorded with 295 nm excitation light of WT *C. reinhardtii* PsbO, solid line; its truncated version ΔS145K187, dashed line; PsbO1 from *Solanum tuberosum*, dash/dotted line and PsbO2, short dashed line.

PsbO proteins (Shutova et al. 2001). To compare the folding of PsbO proteins from different species, the PsbO proteins from *C. reinhardtii* and *S. tuberosum* were isolated using the described purification protocol and their tryptophan fluorescence emission spectra were studied under the described measurement conditions. As shown in Fig. 3C, all spectra acquired with excitation at 295 nm are very similar, with a peak centered around 320 nm.

The titration of PsbO protein from *C. reinhardtii* and its truncated version in the presence of hydrophobic fluorescent probe ANS

The fluorescence of the hydrophobic probe ANS is a useful tool for the monitoring conformational changes in proteins (Semisotnov et al. 1991) because it depends on the water-soluble fluorophore's access to hydrophobic patches within the protein molecule (Hawe et al. 2008). The intensity of ANS emission in the presence of the WT and mutant PsbO proteins from *C. reinhardtii* is shown in Fig. 4 as a function of pH. Interestingly, the intensity of ANS fluorescence increased dramatically as the protein solution was made more acidic. Subsequent titration towards neutrality by the addition of KOH caused a progressive decrease in the ANS emission. The results plotted in Fig. 4A,B show that titration from pH 7.5 to pH 3.8 was accompanied by a pronounced reversible increase in ANS emission both for the WT and the ΔS145K187 mutant PsbO proteins. This indicates that the protein's hydrophobic core responds to pH changes by becoming more accessible under acidic conditions and less accessible closer to neutral pH, as was also observed for PsbO proteins from higher plants (Shutova et al. 1997).

As shown by Figs 1 and 4, the deletion of the large extrinsic loop does not affect the folding of PsbO of its dynamics in response to changes in pH. Indeed, conformational changes related to the protonation/deprotonation of amino acid residues with varying pH appear to occur exclusively in the β-barrel of PsbO. The pH-dependence of ANS fluorescence is monotonic, reflecting the protein's transition from an open to a closed state as the pH rises. The titration curve shows that the most pronounced change occurs between pH 5.5 and 4. Moreover, the acid and base titration curves do not coincide but exhibit a reproducible discrepancy and form a loop. This behavior is known as hysteresis and appears to be characteristic of PsbO because it has also been observed in PsbO proteins from higher plants protein but is not seen during titration of other extrinsic PSII proteins (Shutova et al. 1997). Because the lumenal pH decreases upon illumination (Kramer et al. 2003), the response of PsbO to changes in pH suggests that it may

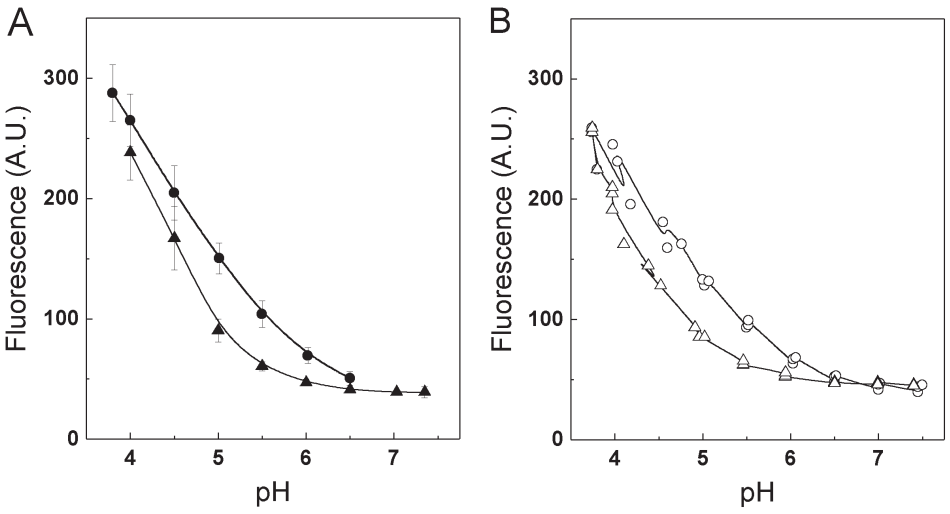

Fig. 4. pH titration of the PsbO protein monitored by the hydrophobic fluorescent probe ANS. Titration curves were measured by adding either HCl to the protein kept at pH 7.5 (triangles), or NaOH to protein kept at pH 3.8 (open circles). Each point represents the area under emission spectra of the ANS added to the PsbO protein in three independent experiments for each pH values. (A) WT PsbO and (B) ΔS145K187 truncated version of the PsbO protein from *Chlamydomonas reinhardtii*.

contribute to the regulation of photosynthetic electron flow from the water oxidation site. The characteristic hysteresis of PsbO under acid–base titration is thus associated with a reversible increase in the accessibility of the hydrophobic core of the *β*-barrel at low pH.

NMR spectroscopy of PsbO protein from *C. reinhardtii* and its truncated version ΔS145K187

The proton-induced conformational changes of the green algal PsbO protein were further analyzed by diffusion NMR spectroscopy. The hydrodynamic radius calculated for *C. reinhardtii* PsbO based on its NMR spectra yielded a correct estimate of the protein's molecular mass (Fig. 5). The hydrodynamic radius of the truncated PsbO protein, ΔS145K187, is significantly smaller, in keeping with its lower molecular mass. As shown in Fig. 5, the PsbO protein is stable over a broad pH range (pH: 3–8), clearly demonstrating that it does not undergo pH-induced unfolding or reversible dimerization/multimerization in this pH range. PsbO diffused more slowly at pH above 8.5, suggesting that it does partially unfold at higher pH values (see also fluorescence study of the spinach PsbO, Shutova et al. 2001).

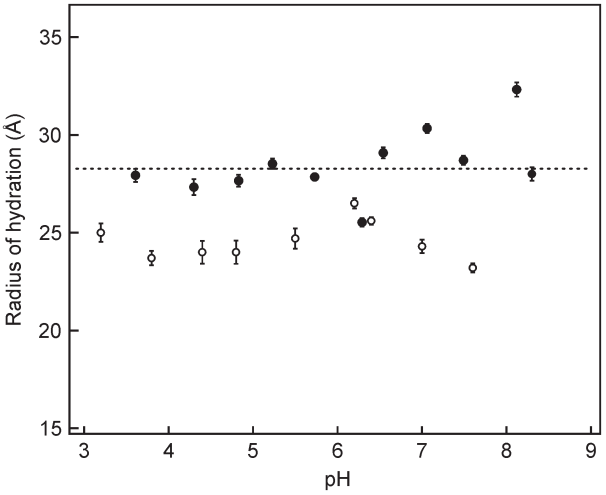

Fig. 5. Radius of hydration (rH) of PsbO, wild-type (filled circles) and ΔS145K187 (open circles), as a function of the pH. The rH was determined from NMR based diffusion experiments and the Stokes–Einstein relationship. The dotted line represents the calculated rH for the homolog PsbO from *Thermosynechococcus elongatus* (Pdb 3ARC). The calculated rH was determined from the radius of gyration (rG) calculated using HYDROPRO (Ortega et al. 2011). The relationship between rG and rH is estimated to: $rG^2 = (3/5)\ rH^2$ (Burchard et al.1980).

Discussion

The light-induced acidification of the thylakoid lumen by protons liberated during water oxidation in the Mn_4CaO_5 cluster generates the ΔpH across the thylakoid membrane that drives ATP synthesis. The acidification of the lumen upon illumination is also an important regulatory factor in many processes in chloroplast (Jarvi et al. 2013). The catalytic site of water oxidation, the Mn_4CaO_5 cluster, is bound to the PSII intrinsic subunits approximately 30 Å apart from the bulk phase of the lumen. The surrounding protein matrix of the Mn_4CaO_5 cluster in PSII is enriched in negatively charged amino acid residues capable of proton binding at this physiologically acidic pH range (del Val and Bondar 2017).

In solution, protonation of PsbO protein increased the fluorescence intensity of a hydrophobic fluorescent probe (ANS) bound to the PsbO and showed that the protein's tertiary structure changes at pH values below 5.7. At neutral pH, the hydrophobic core of the *β*-barrel is closed, and lipophilic amino acid residues

are inaccessible to the water-soluble fluorescent probe. When the protein is placed in an acidic solution, the hydrophobic patches of the protein become exposed to the surrounding medium, enabling them to bind ANS. Remarkably, the sigmoidal curves for acid and base titration had common saturation points but were otherwise non-coincident, forming a hysteresis loop. Hysteresis in protein chemistry is indicative of cooperativity and non-equilibrium states. The protonation/deprotonation hysteresis did not disappear or become less pronounced after multiple cycles of titration and was sufficiently persistent to be considered a permanent aspect of the light/pH-induced conformational behavior of PsbO in PS II. Hysteresis was also observed during the titration of the spinach PsbO protein in the presence and in the absence of ANS (Shutova et al. 1997), allowing us to omit the possibility that it is due to reversible binding of ANS to the protein.

The protonation points of the titration curves differ, so they cannot be directly compared to the known pKa values of amino acid residues. However, the two sides of a given hysteresis loop limit the range of the corresponding pK value. The pK values of the amino acid residues involved in the acid-induced conformational changes of PsbO appear to be shifted relative to their previously values depending on titration direction (Shutova et al. 1997). The amino acid with an ionizable side chain found in PsbO is tyrosine. As shown previously (Shutova et al. 2001), the titration of the Tyr fluorescence is described by a titration curve with a pK of 11.7 that was attributed to deprotonation of tyrosine residues in PsbO. Because the PsbO protein from *C. reinhardtii* lacks histidine side chains, the hysteresis described here presumably originates from the reversible protonation of carboxylic amino acid residues, i.e. aspartic acid and glutamic acid side chains. The large hydrophilic loop of Domain II is enriched in aspartic and glutamic residues, but its removal in the truncated PsbO, ΔS145K187, does not alter the protein's acid–base titration hysteresis (Fig. 4). We therefore conclude that the pH-induced conformational changes of PsbO occur within the properly folded β barrel of Domain I (Figs 4 and 5). The results from crystallography in combination with MD simulations of cyanobacterial PsbO (Bommer et al. 2016) show reversible opening of the hydrogen bond between two carboxyl residues, E97 and D102. They form strong hydrogen bonds resulting in local structural change with apparent pK in the functional relevant pH range. The carboxyl side chains involved in hysteresis of the PsbO protein also exhibit high pK (Shutova et al. 1997, 2005 and this study).

The conformational changes of PsbO could substantially affect the dynamic processes it performs in vivo, which include removing protons from the site of water oxidation (Shutova et al. 1997, 2005, 2007) and substrate water supply (Shutova et al. 1997, Hillier et al. 2001). Although the distance between the Mn_4CaO_5 cluster and the PsbO protein is at least 17 Å, the phenomena described herein may help explain the function of PsbO. Moreover, PsbO proteins from evolutionary distant organisms including cyanobacteria, algae and higher plants are very similar in terms of basic structure and functionality and pH-induced conformational changes. Consequently, the conclusions presented herein are generally valid for almost any PsbO protein. Including our findings, our hypothesis is that PsbO is not directly regulated by light, but via light-induced pH-changes in the lumen. Protons released during water oxidation protonate the carboxyl side-chains of PsbO. This leads to reversible conformational changes that open the hydrophobic core of Domain I to partially expose its hydrophobic patches. In its protonated, open conformation a hydrogen-bond network (proton binding antenna) is formed, enhancing the speed of proton transport to the lumen. Essentially, we are suggesting a Grotthuss mechanism for proton transport, involving the PsbO carboxylic groups at low pH. When the pH increases, for example in darkness, the PsbO protein closes and the proton-binding antenna are retracted; the hydrogen bond network dissolves.

To conclude, the biochemical observations presented in this work reveal that PsbO proteins exhibit pH-dependent dynamics and hysteresis over the range of pH values encountered in the thylakoid lumen. This dynamic behavior results in the reversible opening and closing of the protein's β-barrel (Domain I) in response to changes in the acidity of the thylakoid lumen.

Author contributions

A.C., P.R., M.D. carried out the experiments, A.C. and T.S. wrote the manuscript with input from all coauthors. G.S. and M.W-W. planned the project and guided the work along all stages. All authors provided critical feedback and shaped the experiments and manuscript.

Acknowledgements – We thank the Protein Expertise Platform (PEP) at Umeå University for providing materials for molecular cloning and expression of the PsbO proteins. A.C., T.S. and G.S. gratefully acknowledge the financial support from the Kempestiftelsena and K. and A. Wallenberg Foundation, Artificial Leaf project Umeå (KAW 2011.0055). M. D. was supported by Charles University (project no. 1472314) and by Czech Ministry of Education, Youth

and Sports (project no. NPUI LO1417). We also thank Prof. Elisabeth Sauer-Eriksson for inspiration and expertise on protein structures and Prof. Stefan Jansson for encouragement and support in writing this manuscript.

References

Allahverdieva Y, Mamedov F, Holmström M, Numi M, Lundin B, Styring S, Spetea C, Aro EM (2009) Comparison of the electrontransport properties of the psbo1 and psbo2 mutants of Arabidopsis thaliana. Biochim Biophys Acta 1787: 1230–1237

Anati R, Adir N (2000) Crystallization of dimers of the manganese-stabilizing protein of Photosystem II. Photosynth Res 64: 167–177

Bommer M, Bondar AN, Zouni A, Dobbek H, Dau H (2016) Crystallographic and computational analysis of the barrel part of the PsbO protein of photosystem II: carboxylate-water clusters as putative proton transfer relays and structural switches. Biochemistry 55: 4626–4635

Bricker TM, Frankel LK (2011) Auxiliary functions of the PsbO, PsbP and PsbQ proteins of higher plant photosystem II: a critical analysis. J Photochem Photobiol 104: 165–178

Bricker TM, Roose JL, Fagerlund RD, Frankel LK, Eaton-Rye J-J (2012) The extrinsic proteins of photosystem II. Biochim Biophys Acta 1817: 121–142

Buchanan BB, Schurmann P, Wolosiuk RA, Jacquot JP (2002) The ferredoxin/thioredoxin system: from discovery to molecular structures and beyond. Photosynth Res 73: 215–222

Burchard W, Schmidt M, Stockmayer WH (1980) Information on polydispersity and branching from combined quasi-elastic and intergrated scattering. Macromolecules 13: 1265–1272

Burnap RL, Qian M, Pierce C (1996) The manganese stabilizing protein of photosystem II modifies the in vivo deactivation and photoactivation kinetics of the H2O oxidation complex in Synechocystis sp. PCC6803. Biochemistry 35: 874–882

Callis PR, Liu TQ (2004) Quantitative prediction of fluorescence quantum yields for tryptophan in proteins. J Phys Chem 108: 4248–4259

De Las Rivas J, Barber J (2004) Analysis of the structure of the PsbO protein and its implications. Photosynth Res 81: 329–343

Del Val C, Bondar AN (2017) Charged groups at binding interfaces of the PsbO subunit of photosystem II: A combined bioinformatics and simulation study. Biochim Biophys Acta Bioenerg (6): 432–441

Duchoslav M, Fisher L (2015) Parallel subfunctionalisation of PsbO protein isoforms in angiosperms revealed by phylogenetic analysis and mapping of sequence variability onto protein structure. BMC Plan Biol 15: 133–147

Enami I, Kamo M, Ohta H, Takahashi S, Miura T, Kusayanagi M, Tanabe S, Kamei A, Motoki A, Hirano M, Tomo T, Satoh K (1998) Intramolecular cross-linking of the extrinsic 33-kDa protein leads to loss of oxygen evolution but not its ability of binding to photosystem II and stabilization of the manganese cluster. J Biol Chem 273: 4629–4634

Enami I, Okumura A, Nagao R, Suzuki T, Iwai M, Shen JR (2008) Structures and functions of the extrinsic proteins of photosystem II from different species. Photosynth Res 98: 349–363

Ferreira KN, Iverson TM, Maghlaoui K, Barber J, Iwata S (2004) Architecture of the photosynthetic oxygen-evolving center. Science 303: 1831–1838

Grabski AC, Mehler M, Drott D (2005) The Overnight Express Autoinduction System: High-density cell growth and protein expression while you sleep. Nature Methods 2: 233–235

Guerra F, Siemers M, Mielack C, Bondar AN (2018) Dynamics of long-distance hydrogen-bond networks in photosystem II. J Phys Chem 122: 4625–4641

Hawe A, Sutter M, Jiskoot W (2008) Extrinsic fluorescent dyes as tools for protein characterization. Pharm Res 25: 1487–1499

Heredia P, De Las RJ (2003) Calcium-dependent conformational change and thermal stability of the isolated PsbO protein detected by FTIR spectroscopy. Biochemistry 42: 11831–11838

Hillier W, Hendry G, Burnap RL, Wydrzynski T (2001) Substrate water exchange in photosystem II depends on the peripheral proteins. J Biol Chem 276: 46917–46924

Hutchison RS, Steenhuis JJ, Yocum CF, Razeghifard MR, Barry BA (1999) Deprotonation of the 33-kDa, extrinsic, manganese-stabilizing subunit accompanies photooxidation of manganese in photosystem II. J Biol Chem 274: 31987–31995

Ifuku K, Ishihara S, Shimamoto R, Ido K, Sato F (2008) Structure, function, and evolution of the PsbP protein family in higher plants. Photosynth Res 98: 427–437

Ifuku K, Ido K, Sato F (2011) Molecular functions of PsbP and PsbQ proteins in the photosystem II supercomplex. J Photochem Photobiol 104: 158–164

Ifuku K (2014) The PsbP and PsbQ family proteins in the photosynthetic machinery of chloroplasts. Plant Physiol Biochem 81: 108–114

Jarvi S, Gollan PJ, Aro EM (2013) Understanding the roles of the thylakoid lumen in photosynthesis regulation. Front Plant Sci 4: 434

Junge W (2019) Oxygenic photosynthesis: history, status and perspective. Q Rev Biophys 52(e1): 1–17. https://doi.org/10.1017/S0033583518000112

Kashino Y, Lauber WM, Carroll JA, Wang Q, Whitmarsh J, Satoh K, Pakrasi HB (2002) Proteomic analysis of a

highly active photosystem II preparation from the cyanobacterium *Synechocystis sp*. PCC 6803 reveals the presence of novel polypeptides. Biochemistry 41: 8004–8012
Kern J, Chatterjee R, Young ID, Fuller FD, Lassalle L, Ibrahim M, Gul S, Fransson T, Brewster AS, Alonso-Mori R, Hussein R, Zhang M, Douthit L, de Lichtenberg C, Cheah MH, Shevela D, Wersig J, Seuffert I, Sokaras D, Pastor E, Weninger C, Kroll T, Sierra RG, Aller P, Butryn A, Orville AM, Liang M, Batyuk A, Koglin JE, Carbajo S, Boutet S, Moriarty NW, Holton JM, Dobbek H, Adams PD, Bergmann U, Sauter NK, Zouni A, Messinger J, Yano J, Yachandra VK (2018) Structures of the intermediates of Kok's photosynthetic water oxidation clock. Nature 563: 421–425
Kieselbach T (2013) Oxidative folding in chloroplasts. Antioxid Redox Signal 19: 72–82
Kramer DM, Cruz JA, Kanazawa A (2003) Balancing the central roles of the thylakoid proton gradient. Trends Plant Sci 8: 27–32
Kuwabara TK, Reddy J, Sherman LA (1987) Nucleotide sequence of the gene from the cyanobacterium *Anacystis nidulans* R2 encoding the Mn-stabilizing protein involved in photosystem II water oxidation. Proc Natl Acad Sci USA 84: 8230–8234
Laemmli UK (1970) Cleavage of structural proteins during assembly of head of bacteriophage T4. Nature 227: 680–687
Loll B, Gerold G, Slowik D, Voelter W, JunG C, Saenger W, Irrgang KD (2005) Thermostability and Ca2+ binding properties of wild type and heterologously expressed PsbO protein from cyanobacterial photosystem II. Biochemistry 44: 4691–4698
Lundin B, Thuswaldner S, Shutova T, Eshaghi S, Samuelsson G, Barber J, Andersson B, Spetea C (2007) Subsequent events to GTP binding by the plant PsbO protein: structural changes, GTP hydrolysis and dissociation from the photosystem II complex. Biochim Biophys Acta 1767: 500–508
Mayfield SP, Bennoun P, Rochaix JD (1987) Expression of the nuclear encoded OEE1 protein is required for oxygen evolution and stability of photosystem II particles in *Chlamydomonas reinhardtii*. EMBO J 6: 313–318
Murray JW, Barber J (2006) Identification of a calcium-binding site in the PsbO protein of photosystem II. Biochemistry 45: 4128–4130
Nagao R, Suzuki T, Okumura A, Niikura A, Iwai M, Dohmae N, Tomo T, Shen JR, Ikeuchi M, Enami I (2010) Topological analysis of the extrinsic PsbO, PsbP and PsbQ proteins in a green algal PSII complex by cross-linking with a water-soluble carbodiimide. Plant Cell Physiol 51: 718–727
Nagao R, Suga M, Niikura A, Okumura A, Koua FH, Suzuki T, Tomo T, Enami I, Shen JR (2013) Crystal structure of Psb31, a novel extrinsic protein of photosystem II from a marine centric diatom and implications for its binding and function. Biochemistry 52: 6646–6652
Nelson N, Junge W (2015) Structure and energy transfer in photosystems of oxygenic photosynthesis. Annu Rev Biochem 84: 659–683
Nikitina J, Shutova T, Melnik B, Chernyshov S, Marchenkov V, Semisotnov G, Klimov V, Samuelsson G (2008) Importance of a single disulfide bond for the PsbO protein of photosystem II: protein structure stability and soluble overexpression in *Escherichia coli*. Photosynth Res 98: 391–403
Nowaczyk M, Berghaus C, Stoll R, Rogner M (2004) Preliminary structural characterisation of the 33 kDa protein (PsbO) in solution studied by site-directed mutagenesis and NMR spectroscopy. Phys Chem Chem Phys 6: 4878–4881
Offenbacher AR, Polander BC, Barry BA (2013) An intrinsically disordered photosystem II subunit, PsbO, provides a structural template and a sensor of the hydrogen-bonding network in photosynthetic water oxidation. J Biol Chem 288: 29056–29068
Ohta H, Suzuki T, Ueno M, Okumura A, Yoshihara S, Shen JR, Enami I (2003) Extrinsic proteins of photosystem II: an intermediate member of PsbQ protein family in red algal PS II. Eur J Biochem 270: 4156–4163
Ortega A, Amorós D, García de la Torre J (2011) Prediction of hydrodynamic and other solution properties of rigid proteins from atomic- and residue-level models. Biophys J 101: 892–898
Pieper U, Webb BM, Barkan DT, Schneidman-Duhovny D, Schlessinger A, Braberg H, Yang Z, Meng EC, Pettersen EF, Huang CC, Datta RS, Sampathkumar P, Madhusudhan MS, Sjolander K, Ferrin TE, Burley SK, Sali A (2011) ModBase, a database of annotated comparative protein structure models, and associated resources. Nucleic Acids Res 39: 465–474
Pieper U, Webb BM, Dong GQ, Schneidman-Duhovny D, Fan H, Kim SJ, Khuri N, Spill YG, Weinkam P, Hammel M, Tainer JA, Nilges M, Sali A (2014) MODBASE, a database of annotated comparative protein structure models and associated resources. Nucleic Acids Research 42: 336–346
Popelkova H, Boswell N, Yocum C (2011) Probing the topography of the photosystem II oxygen evolving complex: PsbO is required for efficient calcium protection of the manganese cluster against dark-inhibition by an artificial reductant. Photosynth Res 110: 111–121
Roberts IN, Lam XT, Miranda H, Kieselbach T, Funk C (2012) Degradation of PsbO by the Deg protease HhoA is thioredoxin dependent. PLoS One 7: e45713
Roose JL, Wegener KM, Pakrasi HB (2007) The extrinsic proteins of photosystem II. Photosynth Res 92: 369–387

Roose JL, Frankel LK, Mummadisetti MP, Bricker TM (2016) The extrinsic proteins of photosystem II: update. Planta 243: 889–908
Sachs RK, Halverson KM, Barry B (2003) Specific isotopic labeling and photooxidation-linked structural changes in the manganese-stabilizing subunit of photosystem II. J Biol Chem 278: 44222–44229
Schulz GE (2000) beta-Barrel membrane proteins. Curr Opin Struct Biol 10: 443–447
Semisotnov G, Rodionova N, Razgulyaev O, Uversky V, Gripas A, Gilmanshin R (1991) Study of the molten globule intermediate state in protein folding by a hydrophobic fluorescent probe. Biopolymers 31: 119–128
Shen JR, Inoue Y (1993) Binding and functional properties of two new extrinsic components, cytochrome c-550 and a 12-kDa protein, in cyanobacterial photosystem II. Biochemistry 32: 1825–1832
Shutova T, Irrgang KD, Shubin V, Klimov VV, Renger G (1997) Analysis of pH-induced structural changes of the isolated extrinsic 33 kilodalton protein of photosystem II. Biochemistry 36: 6350–6358
Shutova T, Deikus G, Irrgang KD, Klimov VV, Renger G (2001) Origin and properties of fluorescence emission from the extrinsic 33 kDa manganese stabilizing protein of higher plant water oxidizing complex. Biochim Biophys Acta 1504: 371–378
Shutova T, Nikitina J, Deikus G, Andersson B, Klimov V, Samuelsson G (2005) Structural dynamics of the manganese-stabilizing protein-effect of pH, calcium, and manganese. Biochemistry 44: 15182–15192
Shutova T, Klimov VV, Andersson B, Samuelsson G (2007) A cluster of carboxylic groups in PsbO protein is involved in proton transfer from the water oxidizing complex of photosystem II. Biochim Biophys Acta 1767: 434–440
Sreerama N, Woody RW (2004) On the analysis of membrane protein circular dichroism spectra. Protein Sci 13: 100–112
Studier FW (2005) Protein production by auto-induction in high-density shaking cultures. Protein Expr Purif 41: 207–234
Su X, Ma J, Wei X, Cao P, Zhu D, Chang W, Liu Z, Zhang X, Li M (2017) Structure and assembly mechanism of plant C2S2M2-type PSII-LHCII supercomplex. Science 357: 815–820
Suzuki TH, Ohta K, Enami I (2005) Cross-reconstitution of the extrinsic proteins and photosystem II complexes from *Chlamydomonas reinhardtii* and *Spinacia oleracea*. Photosynth Res 84: 239–244
Thornton LE, Ohkawa H, Roose JL, Kashino Y, Keren N, Pakrasi HB (2004) Homologs of plant PsbP and PsbQ proteins are necessary for regulation of photosystem II activity in the cyanobacterium Synechocystis 6803. Plant Cell 16: 2164–2175
Tropea JE, Cherry S, Waugh DS (2009) Expression and purification of soluble His(6)-tagged TEV protease. Methods Mol Biol 498: 297–307
Umena Y, Kawakami K, Shen JR, Kamiya N (2011) Crystal structure of oxygen-evolving photosystem II at a resolution of 1.9 Å. Nature 473: 55–60
Xu Q, Nelson J, Bricker TM (1994) Secondary structure of the 33 kDa, extrinsic protein of photosystem II: a far-UV circular dichroism study. Biochim Biophys Acta 1188: 427–431
Young ID, Ibrahim M, Chatterjee R, Gul S, Fuller F, Koroidov S, Brewster AS, Tran R, Alonso-Mori R, Kroll T, Michels-Clark T, Laksmono H, Sierra RG, Stan CA, Hussein R, Zhang M, Douthit L, Kubin M, de Lichtenberg C, Long P, Vo H, Nilsson H, Cheah MH, Shevela D, Saracini C, Bean MA, Seuffert I, Sokaras D, Weng TC, Pastor R, Weninger C, Fransson T, Lassalle L, Brauer P, Aller P, Docker PT, Andi B, Orville AM, Glownia JM, Nelson S, Sikorski M, Zhu D, Hunter MS, Lane TJ, Aquila A, Koglin JE, Robinson J, Liang M, Boutet S, Lyubimov AY, Uervirojnangkoorn M, Moriarty NW, Liebschner D, Afonine PV, Waterman DG, Evans G, Wernet P, Dobbek H, Weis WI, Brunger AT, Zwart PH, Adams PD, Zouni A, Messinger J, Bergmann U, Sauter NK, Kern J, Yachandra VK, Yano J (2016) Structure of photosystem II and substrate binding at room temperature. Nature 540: 453–457

Supporting Information

Additional supporting information may be found online in the Supporting Information section at the end of the article.

Fig. S1. Sequence alignment for the proteins used in the study.

Fig. S2. Far-UV circular dichroism spectra of *Solanum tuberosum* PsbO1 and PsbO2.

Edited by C. Spetea

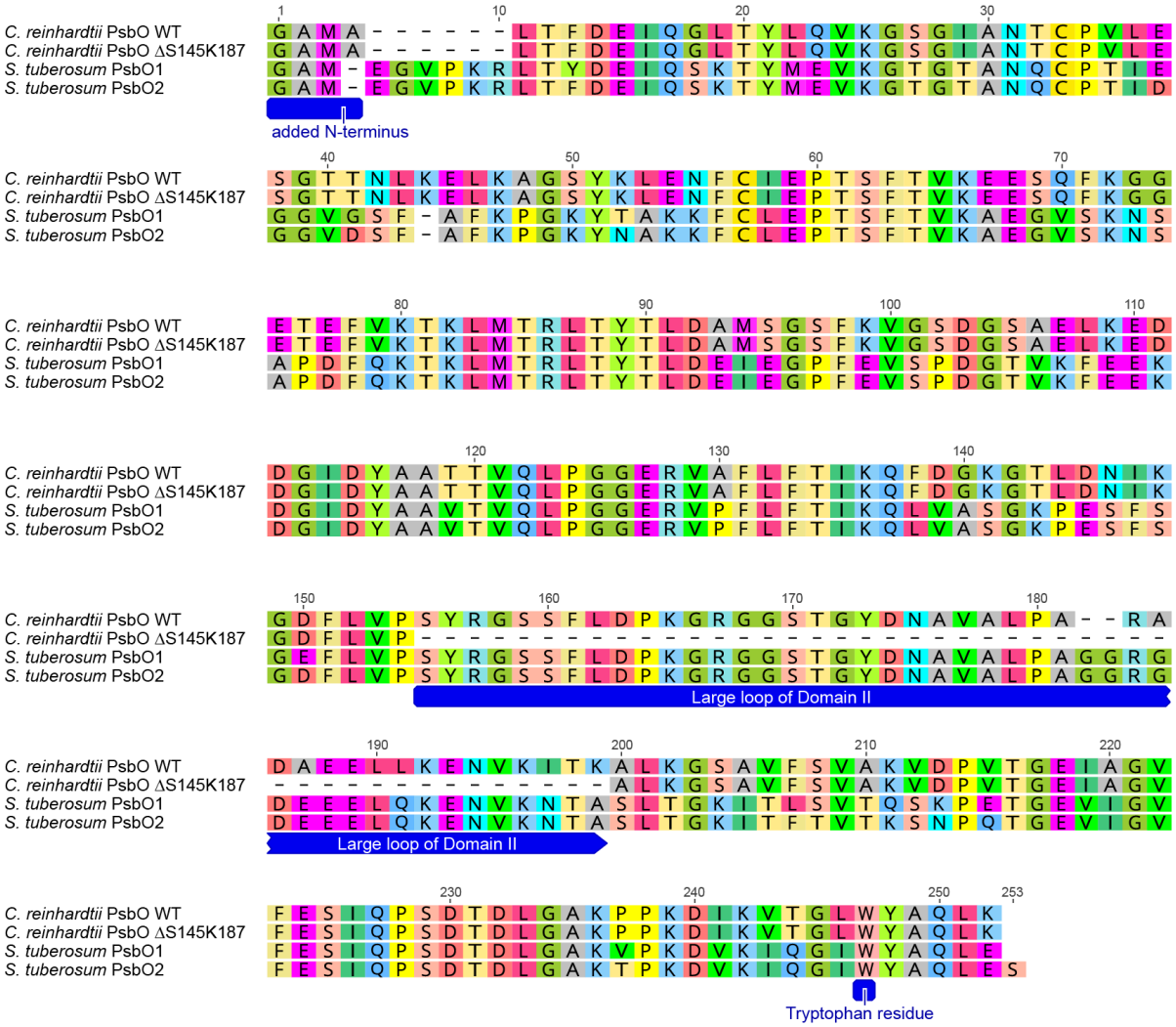

Figure S1. Sequences of proteins used in the study. Compared to native mature protein, 3-4 amino acid residues (GAM/GAMA) were added in the N-terminus because of introduction of restriction site for cloning and TEV protease digestion site. These are marked, together with the large loop of Domain II and the only tryptophan residue.

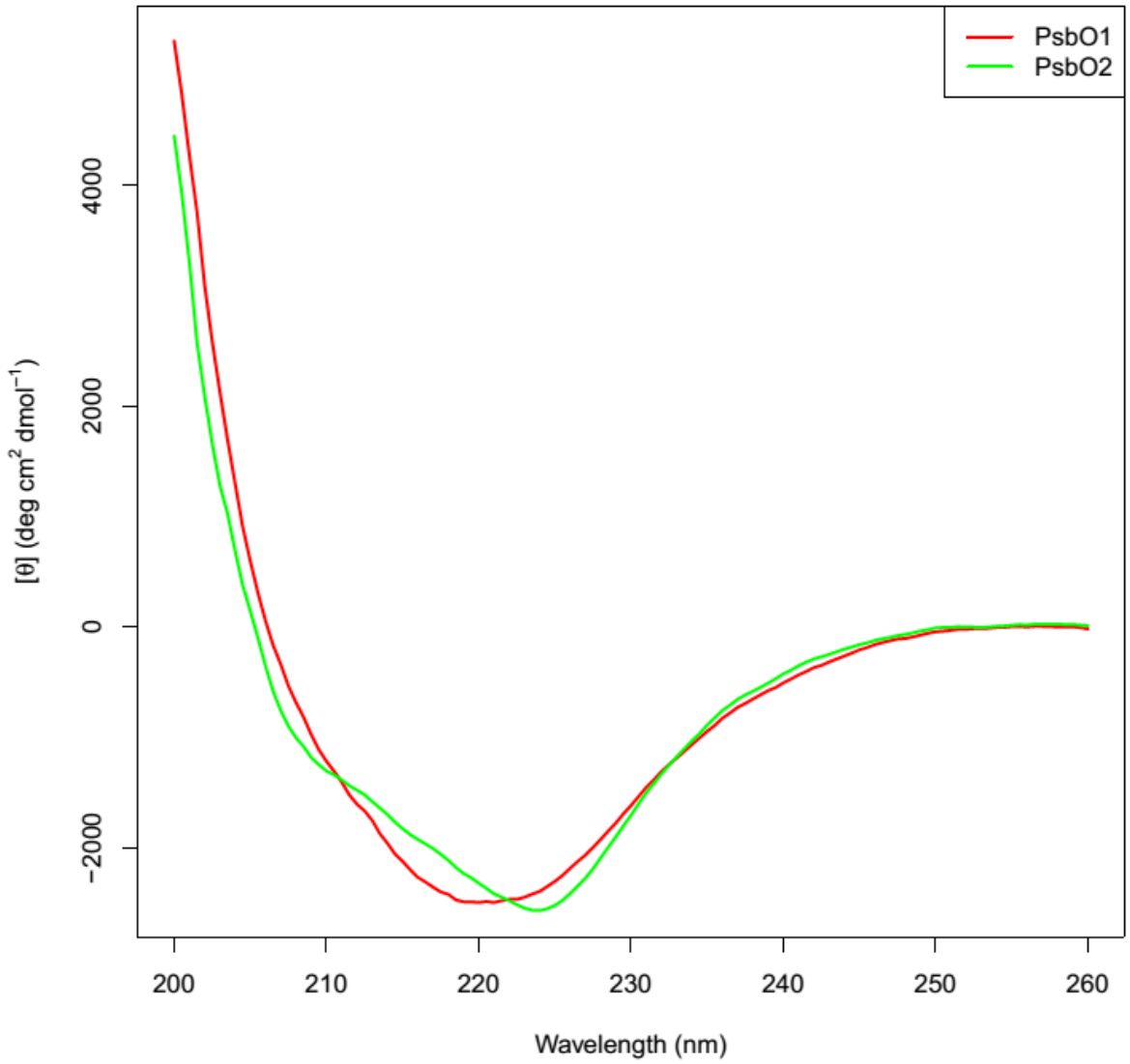

Figure S2. Far-UV circular dichroism spectra of potato PsbO1 and PsbO2. Protein (concentration 30 μ*M*) was dissolved in 10 m*M* KH_2PO_4/K_2HPO_4 buffer (pH 7.2) containing 10 m*M* NaCl. Multiple spectra were accumulated (35 for PsbO1, 30 for PsbO2).